Cardiometabolic benefits of a non-industrialized-type diet are linked to gut microbiome modulation
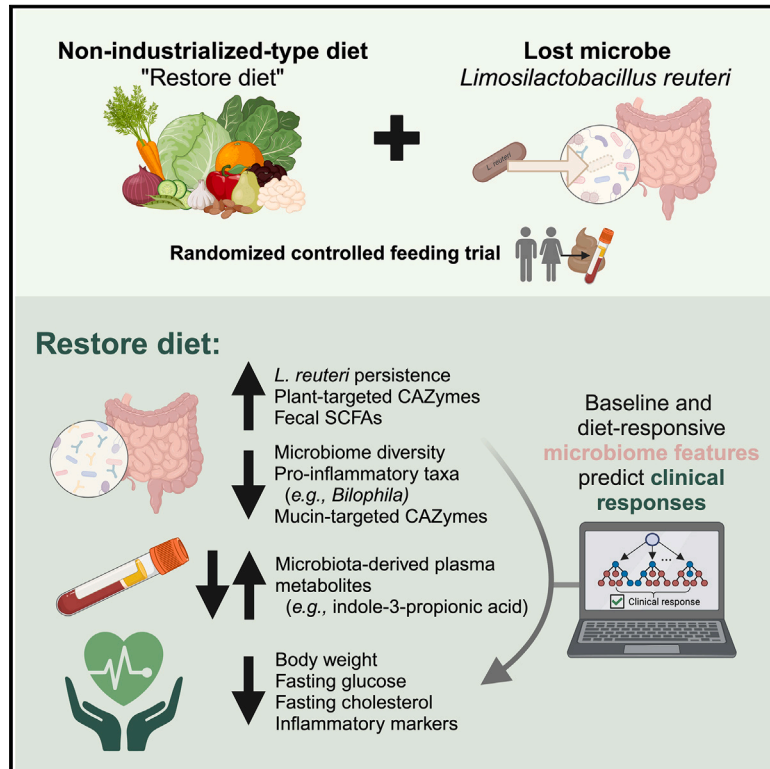
Graphical abstract

Highlights

- The restore diet reduced microbiome diversity but enhanced *L. reuteri* persistence

- The diet redressed several microbiome features altered by industrialization

- The diet induced beneficial changes to microbiota-derived plasma metabolites

- Cardiometabolic benefits of the diet were predicted by microbiome features

Authors

Fuyong Li, Anissa M. Armet,
Katri Korpela, ..., Liang Li, Carla M. Prado,
Jens Walter

Correspondence

jenswalter@ucc.ie

In brief

Is it possible to restore the human gut microbiome in industrialized settings and reintroduce microbial species that have been lost? In healthy adults, Li et al. found that consuming a diet mimicking non-industrialized dietary patterns (restore diet) together with a bacterium rarely found in industrialized human gut microbiomes (*Limosilactobacillus reuteri*) enhanced persistence of the latter. The diet also redressed several microbiome features altered by industrialization, which was linked to considerable cardiometabolic benefits.

CellPress

Cell

Article

Cardiometabolic benefits of a non-industrialized-type diet are linked to gut microbiome modulation

Fuyong Li,[1,2,22] Anissa M. Armet,[1,22] Katri Korpela,[3] Junhong Liu,[1] Rodrigo Margain Quevedo,[1] Francesco Asnicar,[4] Benjamin Seethaler,[5] Tianna B.S. Rusnak,[1] Janis L. Cole,[1] Zhihong Zhang,[1,6] Shuang Zhao,[7] Xiaohang Wang,[7] Adele Gagnon,[1] Edward C. Deehan,[1,8] João F. Mota,[9,10] Jeffrey A. Bakal,[11] Russell Greiner,[12,13] Dan Knights,[14,15] Nicola Segata,[4] Stephan C. Bischoff,[5] Laurie Mereu,[16] Andrea M. Haqq,[1,17] Catherine J. Field,[1] Liang Li,[7,18] Carla M. Prado,[1] and Jens Walter[1,9,19,20,21,23,*]

[1]Department of Agricultural, Food & Nutritional Science, University of Alberta, Edmonton, AB T6G 2E1, Canada
[2]Department of Animal Science and Technology, College of Animal Sciences, Zhejiang University, Hangzhou 310058, Zhejiang, China
[3]Department of Bacteriology and Immunology, Faculty of Medicine, University of Helsinki, Helsinki 00014, Uusimaa, Finland
[4]Department of Cellular, Computational and Integrative Biology, University of Trento, Trento 38123, Trentino, Italy
[5]Institute of Nutritional Medicine, University of Hohenheim, Stuttgart 70599, Baden-Württemberg, Germany
[6]State Key Laboratory of Food Science and Resources, Nanchang University, Nanchang 330047, Jiangxi, China
[7]The Metabolomics Innovation Centre, Edmonton, AB T6G 2E9, Canada
[8]Department of Food Science and Technology, University of Nebraska, Lincoln, NE 68588, USA
[9]APC Microbiome Ireland, University College Cork, Cork T12 YT20, Munster, Ireland
[10]Faculty of Nutrition, Federal University of Goiás, Goiânia, Goiás 74605-080, Brazil
[11]Division of General Internal Medicine, University of Alberta, Edmonton, AB T6G 2B7, Canada
[12]Department of Computing Science, University of Alberta, Edmonton, AB T6G 2R3, Canada
[13]Alberta Machine Intelligence Institute, Edmonton, AB T5J 3B1, Canada
[14]Department of Computer Science and Engineering, University of Minnesota, Minneapolis, MN 55455, USA
[15]Biotechnology Institute, University of Minnesota, Saint Paul, MN 55108, USA
[16]Department of Medicine, University of Alberta, Edmonton, AB T6G 2B7, Canada
[17]Department of Pediatrics, University of Alberta, Edmonton, AB T6G 2B7, Canada
[18]Department of Chemistry, University of Alberta, Edmonton, AB T6G 2G2, Canada
[19]School of Microbiology, University College Cork, Cork T12 YT20, Munster, Ireland
[20]Department of Medicine, University College Cork, Cork T12 YT20, Munster, Ireland
[21]Department of Biological Sciences, University of Alberta, Edmonton, AB T6G 2E1, Canada
[22]These authors contributed equally
[23]Lead contact
*Correspondence: jenswalter@ucc.ie
https://doi.org/10.1016/j.cell.2024.12.034

SUMMARY

Industrialization adversely affects the gut microbiome and predisposes individuals to chronic non-communicable diseases. We tested a microbiome restoration strategy comprising a diet that recapitulated key characteristics of non-industrialized dietary patterns (restore diet) and a bacterium rarely found in industrialized microbiomes (*Limosilactobacillus reuteri*) in a randomized controlled feeding trial in healthy Canadian adults. The restore diet, despite reducing gut microbiome diversity, enhanced the persistence of *L. reuteri* strain from rural Papua New Guinea (PB-W1) and redressed several microbiome features altered by industrialization. The diet also beneficially altered microbiota-derived plasma metabolites implicated in the etiology of chronic non-communicable diseases. Considerable cardiometabolic benefits were observed independently of *L. reuteri* administration, several of which could be accurately predicted by baseline and diet-responsive microbiome features. The findings suggest that a dietary intervention targeted toward restoring the gut microbiome can improve host-microbiome interactions that likely underpin chronic pathologies, which can guide dietary recommendations and the development of therapeutic and nutritional strategies.

Cell
Article

INTRODUCTION

Humans harbor complex microbiomes in their gastrointestinal tract that make important contributions to host fitness, development, and health.[1] This symbiosis evolved over millions of years under environmental and nutritional conditions that are substantially different from those in modern industrialized societies.[2,3] The lifestyle factors that are hallmarks of industrialization constitute either hurdles to symbiont transmission and dispersal (e.g., cesarean sections, antibiotics) or lead to an undersupply of nutrients to the gut microbiome (e.g., formula feeding, refined western diets).[4,5] Although these factors have contributed substantially to increased life expectancy through infectious disease prevention and food security,[6] they have been linked to an increased risk of developing chronic non-communicable diseases (NCDs) in epidemiological research.[7–9] These connections led to hypotheses proposing that the rise in NCDs, which have reached epidemic proportions in several socio-economically developed societies,[10] might be caused, at least in part, by lifestyle-induced disruptions of host-microbiome symbiosis.[11,12]

Investigations of the gut microbiome in non-industrialized and industrialized human populations,[13–16] over lifestyle gradients,[17–19] and across generations of immigrants,[20] as well as the reconstruction of microbial genomes from paleofeces,[21] have consistently confirmed lifestyle-induced alterations of the gut microbiome. Industrialization has resulted in decreased gut microbiome diversity,[13,15,22] loss of fiber-degrading and immunomodulatory microbes,[22–25] increased pro-inflammatory microbial taxa (e.g., Bilophila),[13,14] reduced fiber fermentation,[22] and diminished enzymatic capacity for plant-carbohydrate utilization and enrichment of mucus-degrading organisms and enzymes.[26] Mechanistic work in mice showed that "western-style" diets deprived of fiber led to starvation and subsequent extinction of commensal microbes,[27] as well as metabolic and immunological pathologies driven by increased mucus degradation and inflammation.[28,29] There is, therefore, strong rationale supported by epidemiology, anthropology, and mechanistic animal research to restore the gut microbiome and redress adverse effects of industrialization.

Proposals to restore the industrialized gut microbiome to improve health have focused on providing adequate supply of dietary fibers and lost microbes.[12] However, such research in humans is still scarce, and scientific and ethical concerns have been raised about different aspects of microbiome restoration.[30,31] For example, doubts exist on whether reversing gut microbiome features to ancestral states will provide benefits in industrialized environments and to what degree such attempts are even possible.[30] In this work, we explored the effects of a microbiome restoration strategy comprised of a bacterium (Limosilactobacillus reuteri) rarely found in industrialized gut microbiomes[32] and a diet that shared key characteristics of non-industrialized dietary patterns (Non-industrialized Microbiome Restore [NiMe] diet, referred to as restore diet throughout the publication). In a randomized controlled feeding trial in healthy Canadian adults, we characterized the effects of the restoration strategy on the persistence of L. reuteri (primary objective), gut microbiome ecology and metabolism, and host metabolism and risk markers of chronic diseases and identified microbiome and metabolome features predictive of clinical outcomes.

RESULTS

Design of a microbiome restoration strategy

The species L. reuteri was selected as it is rarely found in industrialized microbiomes,[32] and was dominant in fecal microbiomes of rural Papua New Guineans but undetectable in US control subjects.[13] The species is further generally recognized as safe and has well-established health-promoting effects.[33–36] To test the hypothesis that an L. reuteri strain originating from a non-industrialized population would display adaptations toward a non-industrialized-type diet, we compared an L. reuteri strain derived from rural Papua New Guinea ("PB-W1")[37] with the L. reuteri-type strain isolated in Germany ("DSM 20016T").[38] These two strains belong to distinct phylogenetic lineages and subspecies of L. reuteri and show an average nucleotide identity (ANI) value of only 96.2%,[39,40] indicating genetic divergence.

We designed a complementary diet (restore diet) based on foods regularly consumed in rural Papua New Guinea but available in Canada (e.g., beans, sweet potato, rice, cucumber, and cabbage)[13] and foods that contained high amounts of raffinose and stachyose (e.g., Jerusalem artichokes, peas, and onions),[41,42] which are growth substrates of L. reuteri.[43] The diet shared key characteristics with non-industrialized dietary patterns that likely mimic ancestral diets[44]: primarily plant-based, devoid of dairy and wheat, limited in highly processed foods, low glycemic index and energy density, and amounts of dietary fiber (22 g per 1,000 kcal) that exceed recommendations. The restore diet provided approximately 60% of total energy from carbohydrate, 15% from protein, and 25% from fat, which falls within the acceptable macronutrient distribution ranges.[45]

A human trial to characterize the effects of the gut microbiome restoration strategy

We conducted a randomized controlled feeding trial in healthy adults (n = 30) to test the effects of our microbiome restoration strategy on gut microbiome and host metabolism (Figure 1A). Our objective was to simultaneously determine (1) if L. reuteri could be re-established in the gut microbiome in a western cohort and the effects on the host, (2) the effects of the restore diet independent of L. reuteri supplementation, and (3) potential beneficial interactions between L. reuteri and the restore diet. Participants were randomized to consume either the restore diet for 3 weeks, which involved standardized meals based on a 4-day rotating menu (Table S1; example depicted in Figure S1) adjusted to maintain individual caloric requirements, or remain on their usual diet for 3 weeks and advised to maintain usual dietary intake, which was monitored by repeated 24-h dietary recalls (Table S2). After a 3-week washout, subjects were crossed over to the other diet period for 3 weeks, followed by a final 3-week washout. In a parallel-arm design, participants were randomized to receive a single inoculum of either $\sim 10^{10}$ viable cells of L. reuteri PB-W1 or DSM 20016T or a placebo (maltodextrin) on the fourth day of each diet period (days 4 and 46 of the trial).

From January 2019 to January 2020, 266 individuals were screened, and 42 were assessed for eligibility (see STAR Methods for inclusion and exclusion criteria). Of the latter, only one individual had detectable levels of L. reuteri in feces,
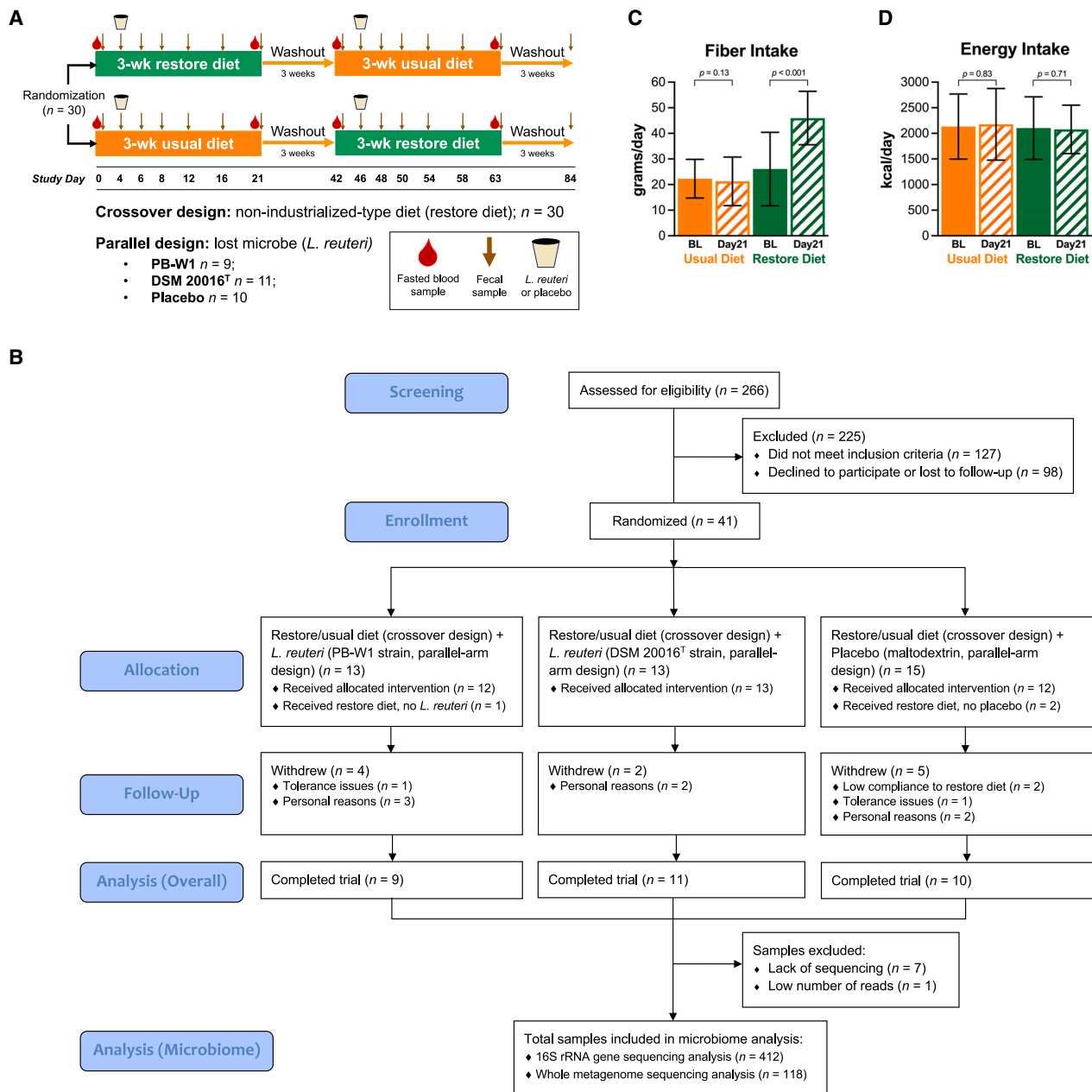
Cell
Article

Figure 1. Experimental test of microbiome restoration strategy in healthy adults
(A) Depiction of randomized controlled trial design and sample type collection.
(B) CONSORT diagram of the study flow.
(C and D) Changes in (C) fiber and (D) energy intake within each diet period are shown in bar plots, with mean ± SD; paired t tests with $p < 0.05$. See also Figure S1 and Tables S1–S4. BL, baseline of each diet period; Day21, day 21 of each diet period; DSM 20016[T], L. reuteri-type strain; PB-W1, L. reuteri strain from rural Papua New Guinea.

confirming that *L. reuteri* is rare in western cohorts.[32] The 41 individuals without detectable *L. reuteri* were randomized, and 30 participants (aged 28.2 ± 6.7 years, body mass index [BMI] 23.8 ± 2.6 kg/m² [mean ± SD]; baseline characteristics in Table S3) completed the intervention and were included in statistical analyses, while 11 subjects withdrew either for personal reasons ($n = 7$), low compliance ($n = 2$), or unwillingness to tolerate GI symptoms ($n = 2$) (Figure 1B). On average, fiber intake doubled during the restore diet compared with participants' usual diets (Figure 1C), while saturated fat was significantly reduced (Table S2), but there were no significant changes to energy intake (Figure 1D).
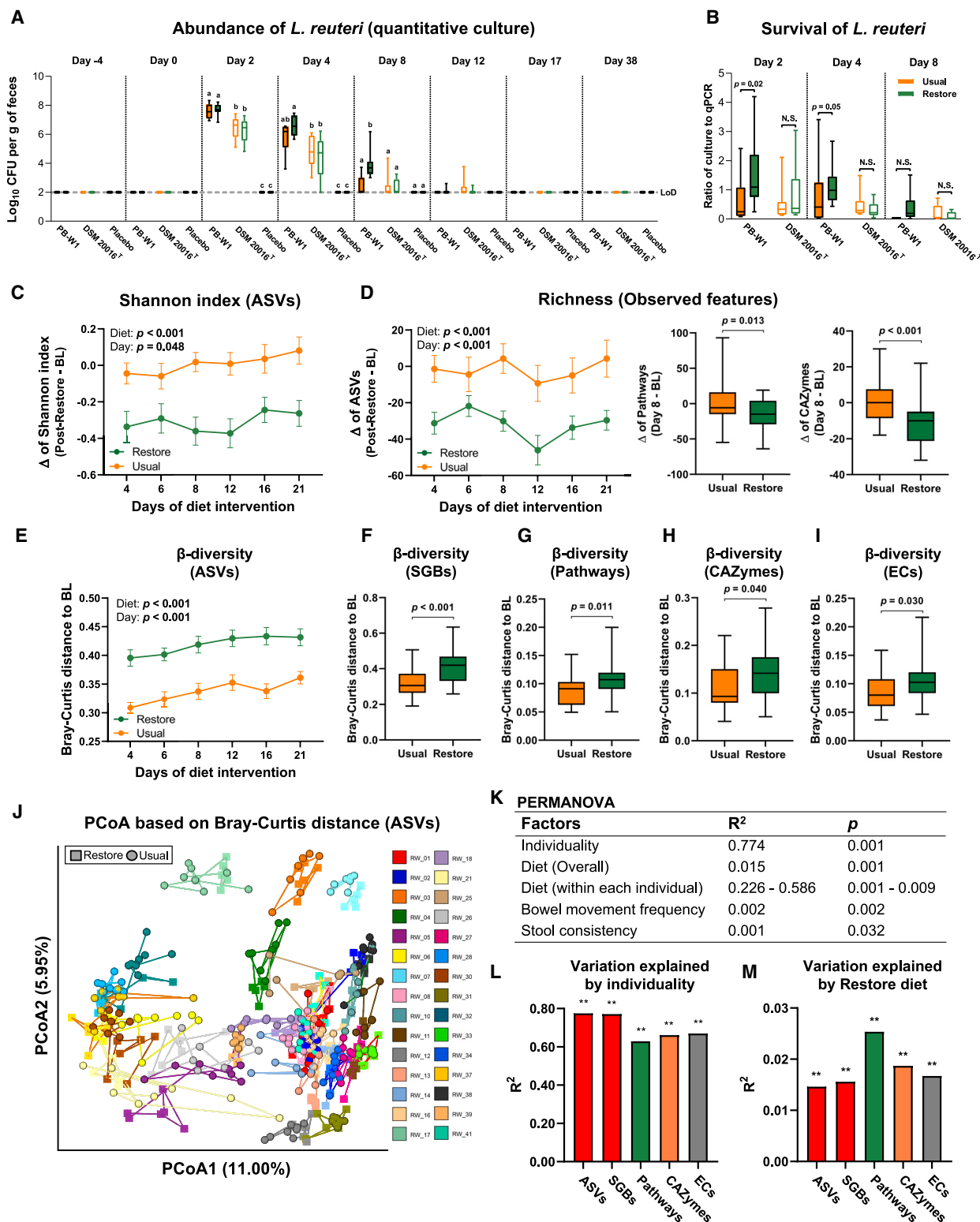
Figure 2. Effects of the restore diet on *L. reuteri* persistence and microbiome diversity indices and variation

(A) Cell numbers of *L. reuteri* in fecal samples determined by quantitative culture. Data presented as Log_{10} of cells per g of feces, and within each day of the intervention, different letters indicate significant differences based on repeated-measures two-way ANOVA with $p < 0.05$.

(legend continued on next page)

CellPress
OPEN ACCESS

Safety and tolerability of the microbiome restoration strategy

Supplementation of *L. reuteri* PB-W1 and DSM 20016[T] had no detectable effects on safety-related laboratory measures (e.g., complete blood count, electrolytes) (Table S4). Although consuming the restore diet increased creatinine from 73.0 ± 14.4 to 76.4 ± 13.6 mmol/L (false discovery rate [FDR]-adjusted $p = 0.029$, linear mixed models; see STAR Methods section statistical analyses) and reduced estimated glomerular filtration rate from 107.4 ± 16.8 to 104.0 ± 16.8 mL/min/1.73m² ($p = 0.027$), these values as well as all other safety-related laboratory measures remained within normal ranges.

Compared with the usual diet, the restore diet softened stool consistency ($p = 0.006$, generalized estimating equations [GEE] models) and increased the number of daily bowel movements ($p = 0.021$) (Figure S2A), indicating a reduction in gut transit time likely due to increased fiber intake.[46,47] The restore diet increased gastrointestinal symptoms (i.e., stomach aches, abdominal tension, and flatulence; $p < 0.01$ at all time points, GEE models; Figure S2A), which were the only intervention-related adverse events in the study. There were no detectable effects of *L. reuteri* inoculum on any of these parameters (Figure S2B). Other participant-reported outcomes, including perceived stress, mood, and physical activity, remained unchanged (data not shown). There were no serious adverse events related to the intervention.

Persistence and survival of *L. reuteri* strains

L. reuteri became detectable in feces by culture and quantitative PCR (qPCR) 2 days after consuming either PB-W1 or DSM 20016[T] but not in the placebo group (Figures 2A and S3A). PB-W1 reached higher numbers (7.64 ± 0.11 and 7.85 ± 0.15 Log₁₀ of cells/g of feces based on culture and qPCR, respectively) than DSM 20016[T] (6.36 ± 0.11 and 6.66 ± 0.20 Log₁₀ of cells/g for culture and qPCR, respectively) 2 days after administration in both diet periods ($p < 0.001$ for both culture and qPCR, paired t tests) (Figures 2A and S3A). The abundance of both *L. reuteri* strains declined and became undetectable 12–17 days post-administration in all but one participant, in whom PB-W1 stably colonized for the entirety of the trial, albeit at a low abundance (Figure S3B).

The restore diet enhanced the abundance of PB-W1 but not DSM 20016[T] 4 (6.61 ± 0.24 versus 5.78 ± 0.37, $p = 0.02$ based

on culture) and 8 (3.90 ± 0.35 versus 2.40 ± 0.24, $p = 0.02$ based on culture) days post-administration, and PB-W1 cell numbers were significantly higher than DSM 20016[T] at these time points ($p < 0.001$ for both days based on culture; $p = 0.003$ and 0.02 for 4 and 8 days after administration based on qPCR) (Figures 2A and S3A). Given that detectable effects of the diet on PB-W1 were stronger with culture (live bacteria) as compared with qPCR data (both live and dead bacteria), we hypothesized that the restore diet enhanced the survival of PB-W1. In fact, the ratio of culture versus qPCR counts was significantly higher for PB-W1 on the restore diet ($p = 0.02$ and 0.05, 2 and 4 days after administration, respectively; paired t tests) but not for DSM 20016[T] (Figure 2B). Overall, these results indicate higher ecological performance and survival of PB-W1 compared with DSM 20016[T], which is further enhanced by the restore diet, but only temporal persistence with one single exception.

We included *L. reuteri* inoculum as a fixed factor in downstream analyses of the gut microbiome using linear mixed models or repeated-measures two-way ANOVA, but these analyses did not detect any significant effects of *L. reuteri* inoculum on gut microbiome composition, diversity, or functional features (data not shown).

Impact of the restore diet on the gut microbial community

The restore diet reduced measures of gut microbiota alpha-diversity, assessed using both 16S rRNA gene amplicon sequencing (based on amplicon sequence variants [ASVs]) and whole metagenome sequencing (WMS, based on species-level genome bins [SGBs]): Shannon index ($p < 0.001$ based on ASVs, linear mixed model; $p = 0.003$ based on SGBs, repeated-measures two-way ANOVA) (Figures 2C and S3C), number of observed features ($p < 0.001$ for both ASVs and SGBs) (Figures 2D and S3D), and Pielou's evenness ($p < 0.001$ based on ASVs; $p = 0.024$ based on SGBs) (Figure S3E). The reduction in alpha diversity occurred within the first 4 days of the restore diet and was stably maintained throughout the diet period (Figures 2C, 2D, and S3E). Reductions in alpha diversity were also observed for predicted functional features derived from WMS, e.g., the number of observed pathways ($p = 0.013$, repeated-measures two-way ANOVA) and carbohydrate-active

(B) Survival of *L. reuteri*, represented as the ratio of cell numbers estimated using quantitative culture to qPCR in fecal samples collected on days 6, 8, and 12 of each diet period (i.e., 2, 4, and 8 days after *L. reuteri* administration). This timeframe was chosen because *L. reuteri* became undetectable in most samples by day 16 (12 days after *L. reuteri* administration). Within the same day, paired t tests were applied to compare the survival status between the restore diet and usual diet periods for *L. reuteri* PB-W1 and DSM 20016[T], separately; $p < 0.05$.

(C) Changes in Shannon index between each subject's microbiota at baseline and during the two diet periods, estimated based on ASVs (linear mixed model).

(D–I) (D) Changes of observed features (richness) between baseline and different days of each diet period, based on ASVs (linear mixed model), pathways (repeated-measures two-way ANOVA), and CAZymes (repeated-measures two-way ANOVA). Intra-individual (within-subject) Bray-Curtis distance (i.e., distance between different days of each diet period and subject's baseline), estimated based on (E) ASVs (linear mixed model), (F) SGBs, (G) pathways, (H) CAZymes, and (I) ECs (repeated-measures two-way ANOVA for F–I).

(J) PCoA of microbial communities using ASV-based Bray-Curtis dissimilarity matrices (each color represents a different participant).

(K–M) (K) PERMANOVA based on Bray-Curtis dissimilarity matrices was conducted with 1,000 permutations to evaluate the effects of various factors (i.e., individuality, diet, bowel movement frequency, and stool consistency) on the microbial community structure. Variation in microbial compositional profiles (ASVs and SGBs) and functions (pathways, CAZymes, and ECs) explained by (L) individuality and (M) the restore diet; ** $p \leq 0.001$, PERMANOVA. Data presented as box plots or mean ± SEM. See also Figures S2 and S3. ASVs, amplicon sequencing variants; BL, baseline of each diet period; CAZymes, carbohydrate-active enzymes; DSM 20016[T], *L. reuteri*-type strain; ECs, level-4 enzyme commission categories; LoD, limit of detection; PB-W1, *L. reuteri* strain from rural Papua New Guinea; N.S., not significant; PCoA, principal-coordinate analysis; PERMANOVA, permutational multivariate analysis of variance; SGBs, species-level genome bins.

enzymes (CAZymes) ($p < 0.001$) (Figure 2D), while Shannon index and Pielou's evenness of these functional features did not significantly change (Figures S3C and S3E). Indices of alpha diversity for level-4 enzyme commission categories (ECs) were not altered by the diet intervention (Figures S3C–S3E).

The restore diet significantly altered the overall gut microbial community, assessed by comparing beta diversity (Bray-Curtis distance) differences between treatment time points to baseline, which was detectable for both ASVs ($p < 0.001$, linear mixed model; Figure 2E) and SGBs ($p < 0.001$, repeated-measures two-way ANOVA; Figure 2F). Diet-induced differences of beta diversity between baseline and day 4 of the restore diet period were negatively correlated with baseline richness (number of observed ASVs; $r_s = -0.38$, $p = 0.04$, Spearman's rank correlation). This indicates that a more diverse baseline microbiota is more resistant to diet-induced changes, which agrees with the diversity-stability hypothesis[48] and several previous studies that assessed gut microbiota responses to diet interventions.[49–51] Temporal data derived from 16S rRNA gene amplicon sequencing revealed that microbiota community shifts occurred within the first 4 days and were stably maintained throughout the restore diet (Figure 2E). Higher beta diversity differences induced through the restore diet were also detected for functional features (pathways [$p = 0.011$, repeated-measures two-way ANOVA], CAZymes [$p = 0.040$], and ECs [$p = 0.030$]) (Figures 2G–2I). The restore diet further increased inter-subject dissimilarity (assessed as Bray-Curtis distance between individuals) of microbial compositional profiles ($p < 0.001$ for both ASVs and SGBs; Wilcoxon signed-ranks test) and some functional features ($p = 0.014$ for pathways and $p < 0.001$ for ECs) but not CAZymes (Figure S3F).

To determine the relative contribution of diet in shaping gut microbiota as compared with other relevant factors (e.g., individuality and transit time[52,53]), we generated a Bray-Curtis distance matrix and projected it in two dimensions via principal-coordinate analysis (PCoA) (Figure 2J). Permutational multivariate analysis of variance (PERMANOVA) revealed that the restore diet significantly altered global microbial community composition ($p = 0.001$, $R^2 = 0.015$), but microbiota continued to cluster by individual ($p = 0.001$, $R^2 = 0.774$), meaning that diet explained only 1.5% of microbiota variation in the overall participant cohort (Figure 2K). Therefore, diet standardization did not reduce inter-individual variation of gut microbiota, which agrees with previous research.[54,55] However, the effect of diet was at least 5 times larger than that of markers of transit time (0.2% of variation explained by bowel movement frequency and 0.1% by stool consistency; Figure 2K).

Interestingly, diet explained 22.6%–58.6% ($p = 0.001$–0.009) of microbiota variation within each individual (Figure 2K). These findings suggest a strong individualized effect of the restore diet on gut microbiota composition. In addition, the contribution of "individuality" on beta diversity variation was 62.8%–66.9% ($p = 0.001$) for microbiome functional features (Figure 2L), while the impact of "diet" was 1.7%–2.5% ($p = 0.001$; Figure 2M). This suggests that, although functional redundancy reduces the importance of individuality in explaining microbiome functional variations compared with composition, the gut microbiome remains significantly individualized even if viewed through functional lenses, and the effect of diet is comparatively small.

Impact of the restore diet on relative abundance of gut microbial taxa and encoded functions

More than half of the detectable ASVs (122 out of 205 ASVs) were significantly altered during the diet intervention (FDR-adjusted $p < 0.05$, linear mixed models) (Table S5). Hierarchical clustering revealed that average values of all samples collected during the restore diet period clustered separately from those collected during the usual diet period and the baselines of each diet period (Figure 3A). These findings suggest that despite the large individuality detected above (Figures 2J and 2K), average relative abundances of individual microbial taxa still showed significant diet-induced changes.

Several putative health-promoting species (Figure 3B) and genera (Figure 3C), including the genus *Bifidobacterium* with three *Bifidobacterium* species (*B. adolescentis* [ASV70 and ASV187], *B. longum* [ASV73 and ASV144], and *B. pseudocatenulatum* [ASV111 and ASV153]), the genus *Faecalibacterium* and the species *F. prausnitzii* (ASV6, ASV10, ASV72, and ASV95), *Roseburia hominis* (ASV49 and ASV188), and *Lachnospira* sp. (ASV23, ASV30, and ASV37) were enriched during the restore diet period (FDR-adjusted $p < 0.05$). Average relative abundances of putative pro-inflammatory bacterial taxa, such as *Bilophila wadsworthia* (ASV21), *Alistipes putredinis* (ASV127 and ASV171), *Mediterraneibacter torques* (synonym of *Ruminococcus torques*; ASV167), and *Parabacteroides merdae* (ASV9, ASV130, and ASV183), were reduced (Figure 3B). The dominant changes were confirmed through analysis of SGBs (Table S5). Although the overall effects of the restore diet on microbial taxa were statistically significant and effect sizes were often large, effects and their magnitude were highly individualized. For example, diet-induced changes of the relative abundance of *Bifidobacterium* varied from −12% to 760% when compared with baseline, enriching the genus to more than 15% relative abundance in seven subjects. In addition, although *Alistipes* and *Bacteroides* were overall significantly decreased during the restore diet period, around 30% of the participants showed increases in these genera (Figure S4). Many taxa reduced by the restore diet are considered BloSSUM taxa (bloom or selected in societies of urbanization/modernization),[14] while taxa typically associated with non-industrialized populations were not enriched by the restore diet, such as *Segatella copri* (data not shown).

The average relative abundance of 63 microbial pathways (12 increased and 51 decreased), 95 ECs (36 increased and 59 decreased), and 11 CAZymes (6 increased and 5 decreased) were altered by the restore diet (FDR-adjusted $p < 0.05$, linear mixed models) (Table S5). The restore diet increased the total abundance of CAZymes ($p = 0.029$, linear mixed model; Figure 3D), especially CAZymes targeted toward plant-carbohydrate utilization ($p = 0.021$; Figure 3E). The ratio of CAZymes targeted toward plant- versus animal-carbohydrates increased from 1.50 ± 0.28 in the usual diet to 1.64 ± 0.30 in the restore diet ($p = 0.08$; Figure 3F) while the ratio of mucin- versus plant-carbohydrates reduced from 0.53 ± 0.09 to 0.49 ± 0.06 ($p = 0.10$; Figure 3G). Four CAZyme sub-families belonging to GH43 (GH43_22, GH43_26, GH43_27, and GH43_29), which play a role in breaking down plant fibers like hemicelluloses,[56] were enriched by the restore diet (FDR-adjusted $p < 0.05$;
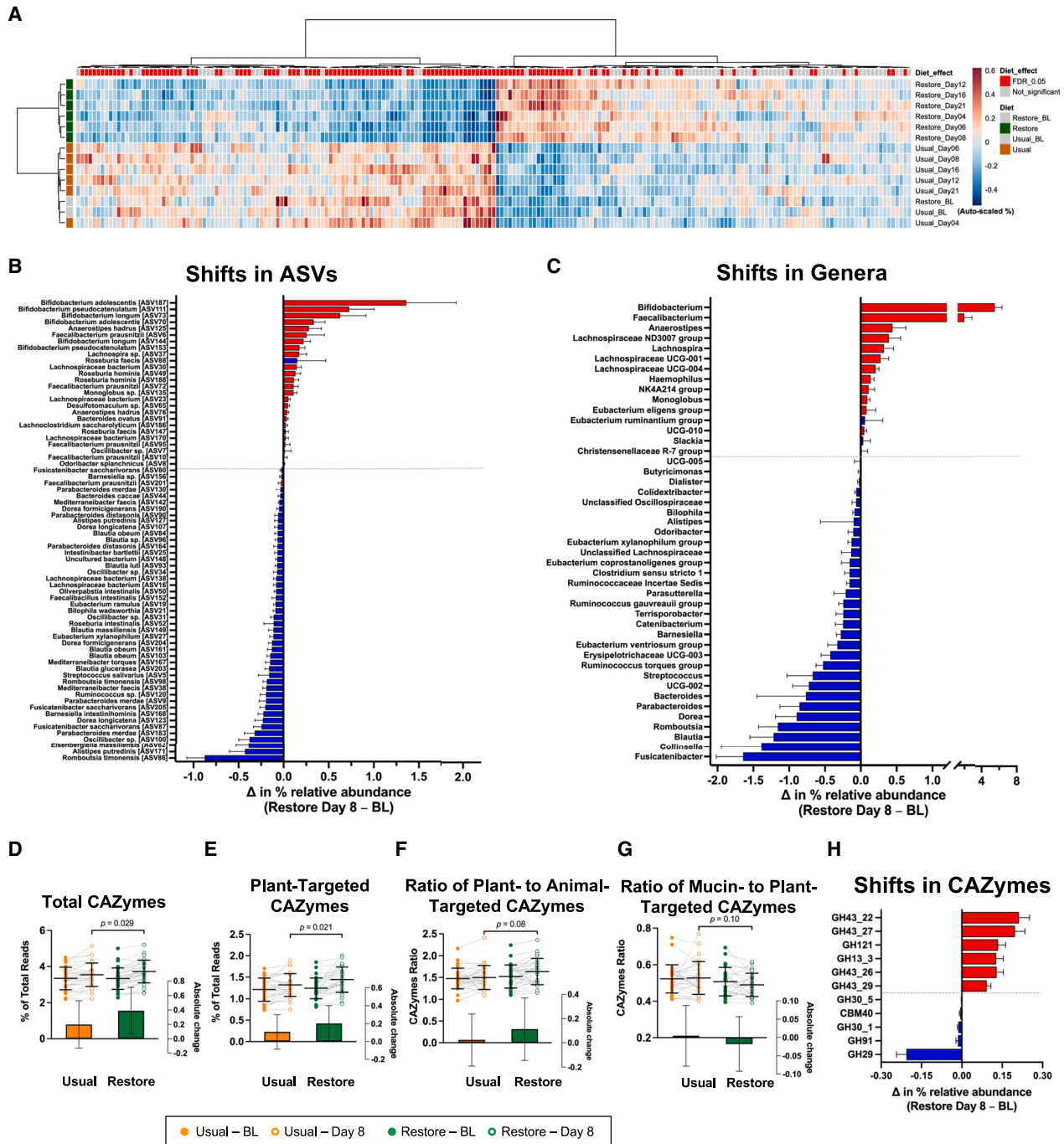
Figure 3. Gut microbial taxa and CAZymes altered by the restore diet

(A–G) (A) Heatmap showing average relative abundances of ASVs at each sampling day (based on auto-scaled relative abundances using Euclidean distance and Ward.D clustering). ASVs significantly altered by the restore diet (FDR-adjusted $p < 0.05$; linear mixed models) are identified in red, while ASVs not significantly affected are in gray. Waterfall plots show changes in relative abundances of significantly altered (B) ASVs and (C) genera (linear mixed models; FDR-adjusted $p < 0.05$). Bars colored based on coefficients—red indicates positive, and blue indicates negative. Changes to CAZymes corresponding to utilization of different carbohydrate sources during each diet period: (D) total CAZymes, (E) plant-carbohydrate, and ratios between (F) plant- to animal-carbohydrate and (G) mucin- to plant-carbohydrate (linear mixed models, FDR-adjusted $p < 0.05$). Bars (insets) represent absolute changes from baseline values within each diet period. (H) Waterfall plot showing changes in relative abundances of significantly altered CAZymes. Data presented as mean ± SD, with symbols representing individual samples. See also Figure S4 and Table S5. ASVs, amplicon sequencing variants; BL, baseline of each diet period; CAZymes, carbohydrate-active enzymes.
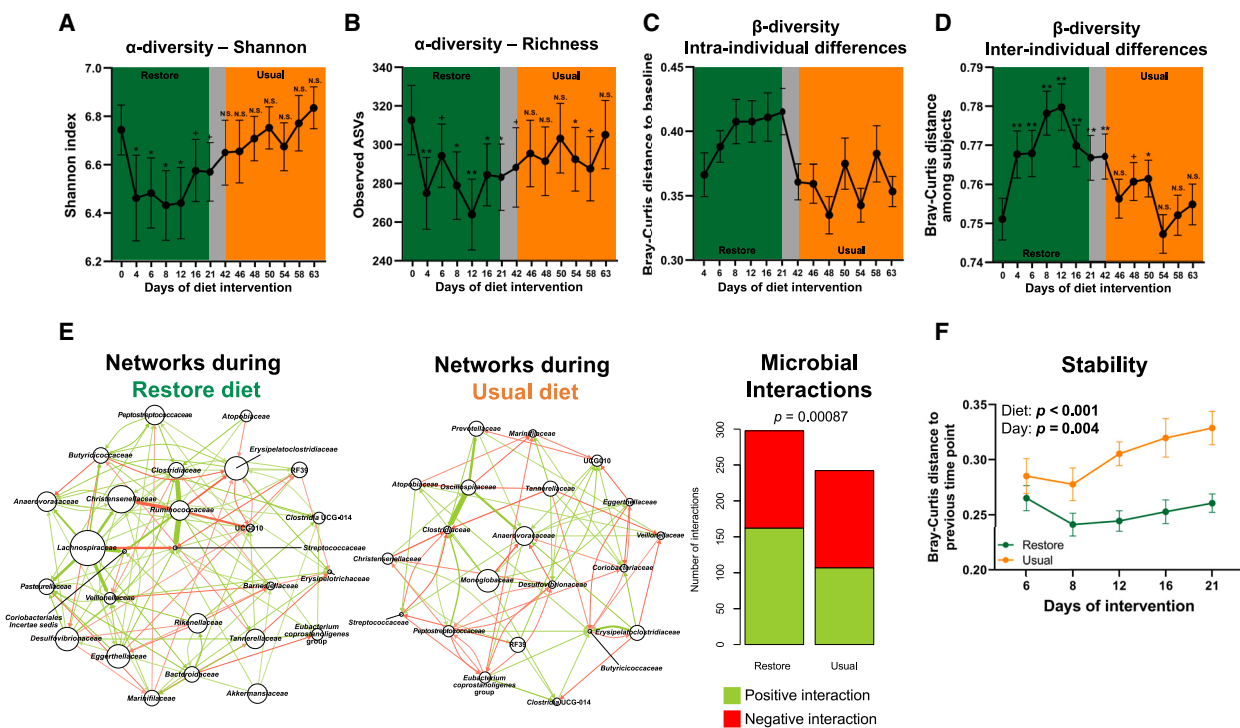
Figure 4. Resilience and stability of gut microbiota during the diet intervention and the main drivers of these ecological responses

(A–D) Temporal responses and resilience of microbiota after consuming the restore diet represented as (A) Shannon index (i.e., alpha diversity), (B) observed features (i.e., richness, based on ASVs), (C) Bray-Curtis distances of each subject's microbiota during the two diet periods compared with their baseline (i.e., beta diversity, intra-individual distance), and (D) Bray-Curtis distances among subject's microbiota (i.e., beta diversity, inter-individual distance) (paired Wilcoxon signed rank tests, $p < 0.05$). Data derived from 16 participants who were randomized to consume the restore diet first.

(E) Interaction networks of bacterial families during each diet period (linear models). Node size indicates the number of taxa that the node taxon affects, and arrow size represents the estimate or strength of the association (i.e., how strongly the abundance of the taxon is associated with the change in abundance of the other taxon). Only those taxa with >2 interactions and an estimate of ≥ 0.2 (i.e., one unit increase in the node taxon is associated with a 0.2 unit change in the abundance of the other taxon) are shown. Bar graphs indicate number of positive (green) and negative (red) interactions among microbes.

(F) Temporal variation of gut microbiota, represented by Bray-Curtis distances between two consecutive timepoints during each of the two diet periods (linear mixed models). Bray-Curtis distances are between the "day of intervention" labeled in the x axis and the previous sampling timepoint, e.g., "day 6" represents the distance between days 4 and 6 of each diet period. Data presented as mean ± SEM. $^{+}p \leq 0.1$, $^{*}p \leq 0.05$, $^{**}p \leq 0.001$. See also Figures S5–S7. ASVs, amplicon sequence variants.

Figure 3H). The largest magnitude of decrease was observed for the CAZyme family GH29 (Figure 3H), which contains alpha-fucosidases involved in mucus degradation.[57]

Temporal dynamics after diet-induced gut microbiome perturbations

We leveraged the crossover study design and, using the dataset derived from 16S rRNA gene amplicon sequencing, analyzed the participants who consumed the restore diet first ($n = 16$) to determine to what degree, and within which time window, microbiota features returned to baseline levels. These analyses showed that alpha-diversity indices (Figures 4A and 4B), intra-individual beta diversity differences (Figure 4C), and inter-individual beta diversity differences (Figure 4D) returned to baseline values either by the end of the first washout or shortly after the usual diet period began. In addition, relative abundances of the ASVs that showed the strongest increases or decreases in response to the restore diet also returned to baseline levels after the first washout

(Figure S5). Similar reversions to baseline values were observed for SGBs and WMS functional features (pathways, CAZymes, and ECs) (Figures S6A–6F). Overall, the findings establish that the effects of the restore diet on microbiome ecology are transient and reversible, and the microbiome displayed resilience toward the dietary change.

Ecological drivers of the effects of the restore diet and consequences for community characteristics

To gain insight into the ecological drivers of gut microbiome shifts, we applied multiple linear regression (MLR) models to genus-level changes (16S rRNA gene amplicon sequencing) at day 8 and included factors that may drive microbiome alterations—diet, fecal pH, stool consistency, and bowel movement frequency. This analysis showed that most genera were not only directly impacted by the restore diet (Figure S7A) but also that reductions of genera such as *Bacteroides* and *Parabacteroides* were associated with changes in fecal pH (Figure S7B), likely due to their sensitivity to acidic pH.[58] Stool consistency
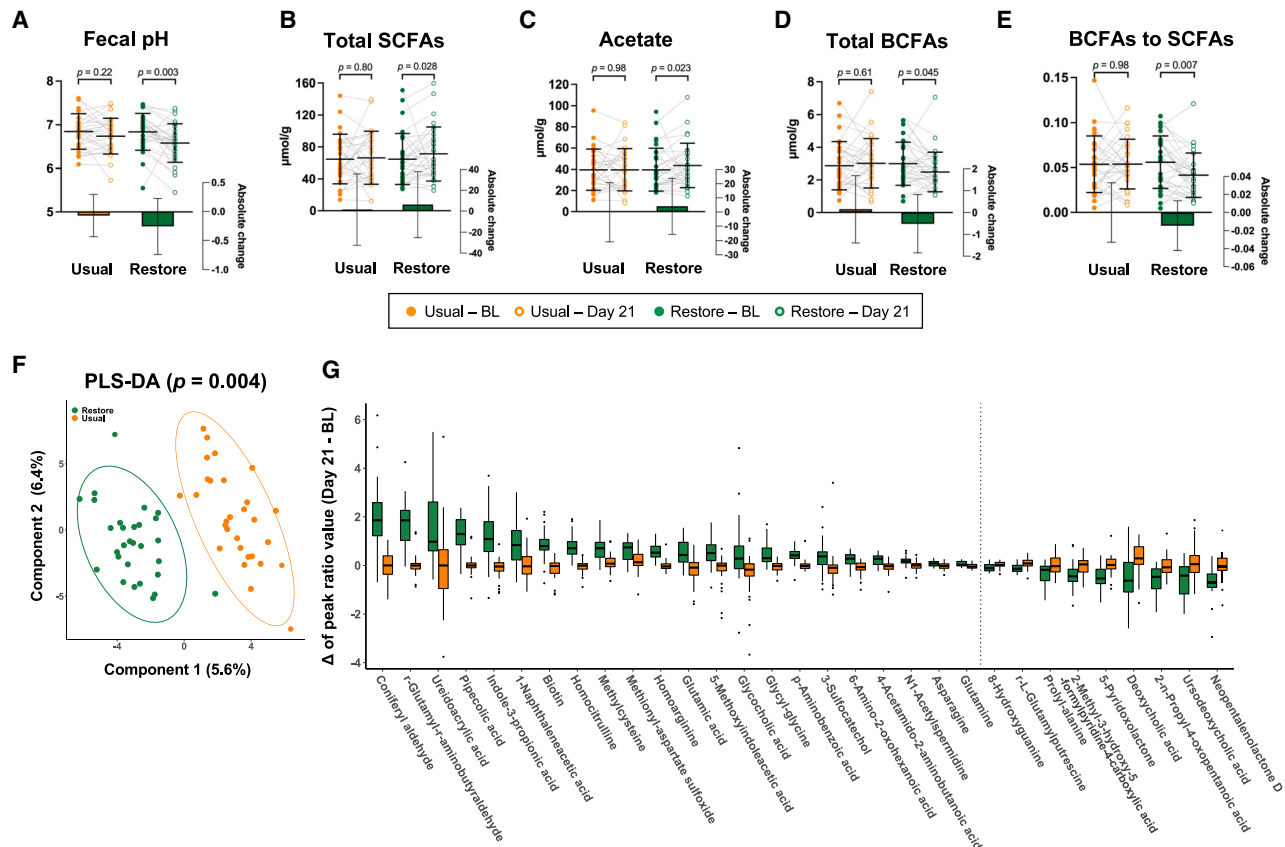
Figure 5. Effects of the restore diet on microbial fermentation and the plasma metabolome

(A–E) Changes to fecal (A) pH, (B) total SCFAs, (C) acetate, (D) totals BCFAs, and (E) ratio of BCFAs to SCFAs within each diet period (paired Wilcoxon signed rank tests, $p < 0.05$). Data presented as mean ± SD, with symbols representing individual samples. Bars (insets) represent absolute change from baseline values within each diet period.

(F) Changes in plasma metabolomic profiles from baseline to the end of each diet period (PLS-DA; p-value from 1,000 permutation validation).

(G) Shifts in metabolites from baseline to the end of each diet period (paired t tests, FDR-adjusted $p < 0.1$). Left and right panels show metabolites that increased and decreased during the restore diet period, respectively. Data presented as box plots, with dots representing outliers. See also Figures S7 and S8 and Table S6.

BCFAs, branched-chain fatty acids; BL, baseline of each diet period; PLS-DA, partial least squares-discriminant analysis; SCFAs, short-chain fatty acids.

and bowel movement frequency influenced only a few genera (Figure S7B), in agreement with their limited influence on overall microbial composition (Figure 2K).

To determine the effect of the restore diet on community interconnectedness, we compared interaction networks of bacterial families from the longitudinal 16S rRNA gene amplicon sequencing during both diet periods using linear models, where changes in relative abundances from timepoint t to $t + 1$ were predicted by abundances at time point t. This analysis revealed a higher number of positive and likely syntrophic interactions during the restore diet period, while negative interactions remained unchanged (Figures 4E and S7C). Microbial families such as *Lachnospiraceae*, *Christensenellaceae*, and *Ruminococcaceae* had strong positive influences on several other taxa and are, therefore, considered putative keystone taxa during the restore diet. Interactions of *Lachnospiraceae* and *Ruminococcaceae* with other taxa were greatly reduced on the usual diet, suggesting that they lose their apparent keystone characteristics, likely because their metabolic capac-

ities for fiber degradation are not realized. Due to the higher number of positive interactions during the restore diet period, we hypothesized that the microbiota would be more stable. Indeed, we detected smaller Bray-Curtis distances between successive timepoints during the restore diet compared with the usual diet period ($p < 0.001$, linear mixed model; Figure 4F).

Effects of the restore diet on microbial fermentation and the plasma metabolome

The restore diet decreased fecal pH from 6.82 ± 0.43 to 6.58 ± 0.44 ($p = 0.003$; paired Wilcoxon signed rank test; Figure 5A), increased total short-chain fatty acids (SCFAs) ($p = 0.028$; Figure 5B) and acetate concentrations ($p = 0.023$; Figure 5C), and reduced total branched-chain fatty acids (BCFAs) concentrations ($p = 0.045$; Figure 5D) and the ratio of BCFAs to SCFAs ($p = 0.007$; Figure 5E). Overall, these results suggest that the restore diet increased saccharolytic fermentation (SCFAs) at the expense of proteolytic metabolism (BCFAs)[59] (Table S6).
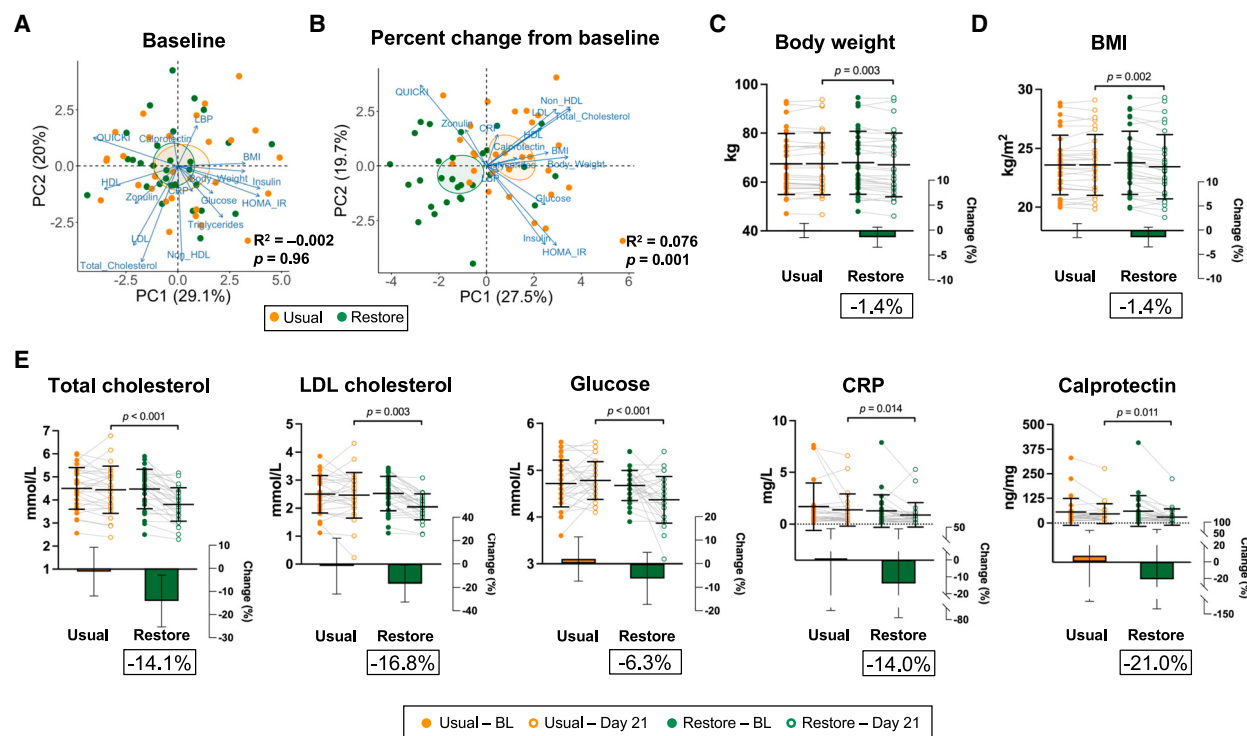
Figure 6. Effects of the restore diet on risk markers of chronic diseases
(A and B) PCA plots and results of PERMANOVA show (A) host parameters at baseline and, (B) their percent changes from baseline within each diet period.
(C–E) Differences in risk markers between each diet period (linear mixed models, FDR-adjusted $p < 0.05$). Data presented as mean ± SD, with symbols representing individual samples. Bars (insets) represent percent changes from baseline values within each diet period. Mean percent changes within the restore diet are in text boxes underneath each figure. BL, baseline of each diet period; BMI, body mass index; HDL, high-density lipoprotein; HOMA-IR, homeostatic model assessment for insulin resistance; CRP, C-reactive protein; LBP, lipopolysaccharide-binding protein; LDL, low-density lipoprotein; QUICKI, quantitative insulin sensitivity check index. See also Table S7.

We employed untargeted metabolomics to profile plasma metabolites and detected 528 metabolites with high-confidence identification. Partial least squares-discriminant analysis (PLS-DA) revealed no significant differences in metabolite shifts (4 days after administration [day 8]—baseline) between the three inoculum groups (PB-W1, DSM 20016^T, and placebo) in either the restore ($p = 0.72$, Figure S8A) or usual ($p = 0.62$, Figure S8B) diet periods. These results indicate that a single dose of *L. reuteri* did not influence plasma metabolomic profiles. By contrast, PLS-DA revealed a significant global effect of the restore diet when the shifts of each metabolite (end of diet intervention [day 21]—baseline) were compared with the usual diet ($p = 0.004$; Figure 5F).

A subset of 31 metabolites was significantly altered by the restore diet (FDR-adjusted $p < 0.10$, paired t test; Figure 5G), wherein 22 increased (e.g., indole-3-propionic acid, biotin, pipecolic acid) and nine decreased (e.g., deoxycholic acid, 8-hydroxyguanine, ursodeoxycholic acid). More than 90% of these metabolites are either produced or modified by the microbiome or co-produced by microbiome and host.[60,61] Correlation analyses revealed relationships (FDR-adjusted $p < 0.10$, Spearman's rank correlation) between metabolites and genera (Figure S8C) and ASVs (Figure S8D) that were significantly altered by the restore diet, suggesting that changes to the gut micro-

biome contributed to shifts in plasma metabolites. For example, we detected a positive correlation between *B. longum* and indole-3-propionic acid (Figure S8D), a metabolite that can be synthesized from indole-3-lactic acid that is produced by bifidobacteria.[62]

The restore diet induced major improvements in risk markers of chronic diseases
Given the links between industrialization and westernized diet and risk of NCDs,[63] we were especially interested in the effects of the microbiome restoration strategy on risk markers of NCDs. While *L. reuteri* did not influence these markers (FDR-adjusted $p > 0.05$, linear mixed models; Table S7), the restore diet had pronounced effects. Principal-component analysis (PCA) ordination of the risk markers revealed no differences between the two baselines of each diet period ($p = 0.96$, PERMANOVA; Figure 6A); however, distinct clustering was apparent based on percent changes from baseline within each diet period ($p = 0.001$; Figure 6B), suggesting the restore diet induced significant overall physiological changes.

Despite being fed to their calculated energy requirements, participants experienced a small but significant decrease in body weight (percent change from baseline to day 21 of
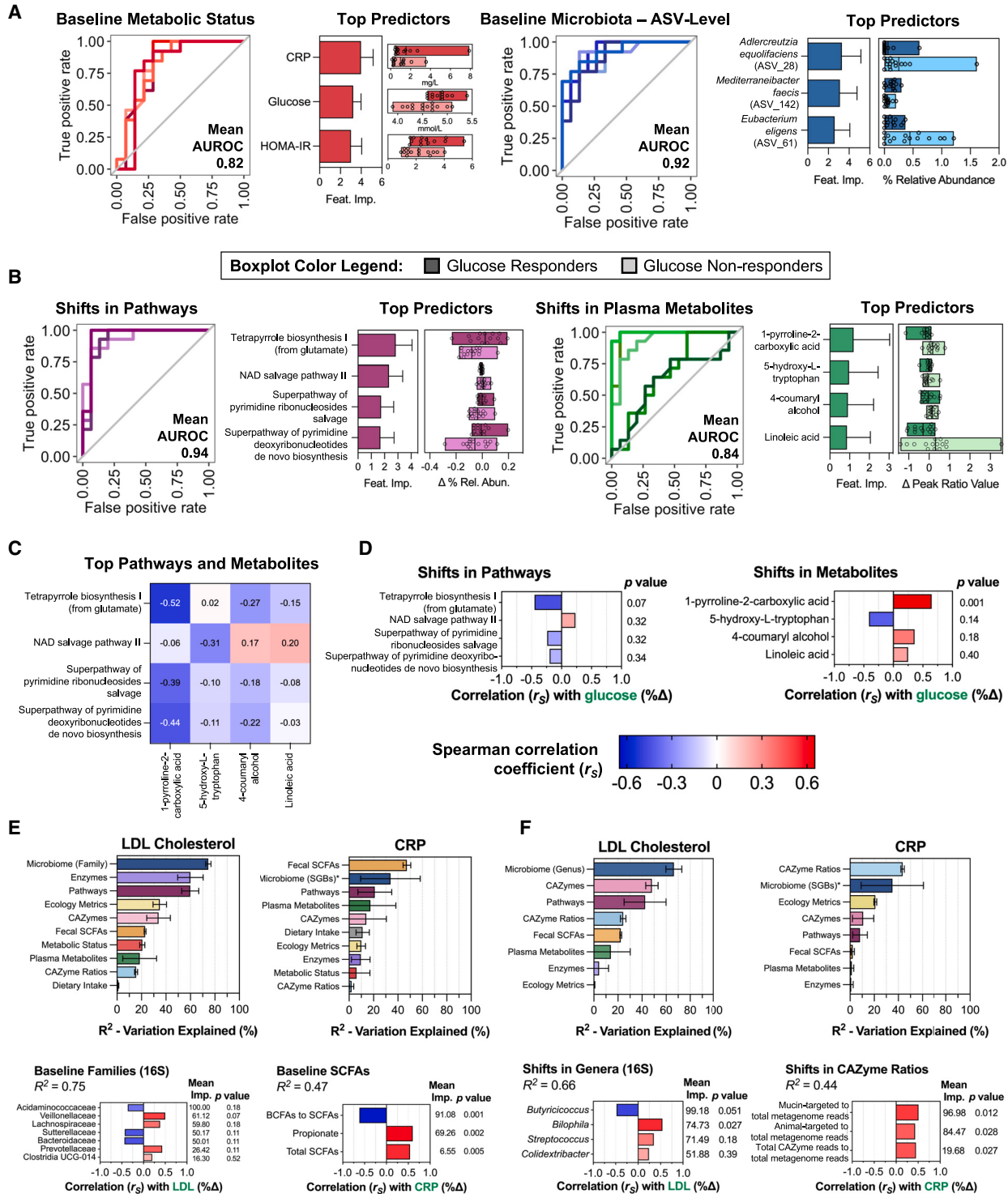
Figure 7. Data integration to determine variables that predict responses in risk markers of chronic diseases to the restore diet

(A and B) RF classification models were applied to predict responders (reduction in glucose $\geq$ 0.3 mmol/L) and non-responders (<0.3 mmol/L reduction) using (A) baseline values (best models: metabolic status and microbiota composition, ASV level) and (B) absolute changes of features (best models: pathways and plasma metabolites). Model performance is depicted as ROC curves—plots contain five individual curves, each representing the ROC of one of the 5-fold of external cross validation. Different shades of the main color were used so that overlapping lines were clearly visible, and the gray line depicts AUROC of 0.5 (i.e.,

restore diet = −1.4 ± 1.9%, mean ± SD; FDR-adjusted p = 0.003, linear mixed model; Figure 6C) and BMI (−1.4 ± 1.9%, p = 0.002; Figure 6D). This could be due to reduced bioaccessibility of macronutrients due to their encapsulation within three-dimensional cell wall structures in fiber-rich plant foods.[64,65]

The restore diet reduced fasting plasma total cholesterol (−14.1 ± 11.2%, FDR-adjusted p < 0.001), low-density lipoprotein (LDL) cholesterol (−16.8 ± 15.8%, p = 0.003), non-high-density lipoprotein (non-HDL) cholesterol (−15.2 ± 14.5%, p = 0.002), fasting plasma glucose (−6.3 ± 11.1%, p < 0.001), C-reactive protein (CRP) (−14.0 ± 58.3%, p = 0.014), and fecal calprotectin (−21.0 ± 88.3%, p = 0.011) (Figure 6E; Table S7). Insulin sensitivity (quantitative insulin sensitivity check index [QUICKI]) was increased (2.4 ± 6.4%, p = 0.036), and insulin resistance (homeostatic model assessment of insulin resistance [HOMA-IR]) was improved (−5.8 ± 40.5%, p = 0.053), which was primarily driven by the reduction in fasting glucose, as there were no effects on fasting insulin levels (p = 0.32) (Table S7). HDL cholesterol was reduced (−11.3 ± 11.2%, p = 0.001), which has been observed with other plant-rich diets,[66,67] while triglycerides remained unaffected (p = 0.59) (Table S7).

All the clinical effects of the restore diet remained statistically significant when controlled for body weight changes (data not shown), with the exception of CRP (although p value remained low at 0.058). In addition, the effects of the restore diet were not reduced when the order by which the diets were consumed was added as an additional covariate, indicating the 3-week washout between diet periods was sufficient for participants to return to their baseline metabolic status. Considering the elevated intake of fiber from the restore diet and the effects on fermentation and SCFAs, we were interested in whether markers of gut barrier function were affected. Both plasma lipopolysaccharide-binding protein (−8.1 ± 13.8%, p = 0.13) and fecal zonulin (−14.9 ± 27.6%, p = 0.052) were reduced, but effects did not reach statistical significance (Table S7).

Identification of microbiome and metabolome features linked to clinical outcomes

To gain mechanistic explanations for the physiological effects of the restore diet, we employed a set of complementary approaches using machine learning (random forest [RF]) and MLR models to integrate the clinical findings with data on the gut microbiome and plasma metabolome. We applied these analyses to the individual omics datasets (i.e., plasma metabolites, microbiome compositional profiles at multiple taxonomic levels, inferred microbiome functions, SCFAs, and diversity indices of gut microbiome) with the goal of determining the best predictors of the physiological effects of the diet, using both baseline features and diet-induced absolute shifts. Baseline dietary intake and metabolic status (i.e., baseline risk markers such as fasting glucose, insulin, lipid panel, etc.) were also included (see STAR Methods).

As a proof of concept, we first determined if diet-induced changes to the microbiome, metabolome, and metabolic status could predict whether participants were consuming their usual diet or the restore diet. RF classification models achieved almost perfect accuracy with plasma metabolites at the end of each diet period (mean area under the receiver operating characteristic curve [AUROC] = 0.99) and WMS-based microbiota compositional profiles at day 8 of each diet period (AUROC = 0.96) (Figure S9A; Table S8), as well as diet-induced shifts in plasma metabolites (AUROC = 0.99) and WMS-based microbiota compositional profiles (AUROC = 1.00) (Figure S9B; Table S8). Overall, WMS-derived functional features (i.e., CAZymes, pathways, and ECs) were also good predictors (AUROC 0.75–0.91), but SCFAs were no better than random chance (AUROC 0.48 and 0.62) (Figures S9A and S9B; Table S8). These results suggest that effects of the restore diet on the microbiome and metabolome were strong and specific enough to result in almost perfect predictions of participants' diets.

The only risk marker that showed individualized responses to the restore diet, with clear responders and non-responders, was plasma glucose (Figure 6E). Using RF classification models to predict 'responders' (reduction in glucose ≥ 0.3 mmol/L) and "non-responders" (<0.3 mmol/L reduction), baseline metabolic status accurately predicted glucose responses (AUROC = 0.82; Figure 7A; Table S9). Top predictive features were baseline CRP, glucose, and HOMA-IR levels, which were elevated in responders, suggesting that participants' baseline immunometabolic status (e.g., elevated inflammation and glycemia) determined responses to the restore diet. Although the accuracy of this model was high and the predictors biologically meaningful, RF models using baseline microbiome composition (ASV level, AUROC = 0.92; Figure 7A; Table S9), as well as shifts in microbial pathways (AUROC = 0.94) and plasma metabolites (AUROC = 0.84) were even more accurate (Figure 7B; Table S10). Interestingly, the top predictive pathway, tetrapyrrole biosynthesis I (from glutamate), and metabolite, 1-pyrroline-2-carboxylic acid, are both implicated in pyrrole metabolism.[68] Shifts in these predictors were negatively correlated with each other (r_s = −0.52, FDR-adjusted p = 0.06) (Figure 7C) and had opposing associations with percent changes in glucose (tetrapyrrole biosynthesis I [from glutamate] r_s = −0.45,

no better than random guessing). Top predictive features of best models are visualized as bar plots with mean ± SD feature importance, and boxplots show differences in these features between responders and non-responders.

(C) Heatmap showing Spearman correlation coefficients (r_s) between top predictive pathways and metabolites.

(D–F) (D) Bar plots showing correlations (r_s) between percent changes in glucose and top predictive pathways and metabolites. RF regression models were applied for LDL cholesterol and CRP using (E) baseline values and (F) absolute changes of features. Model performance depicted as R^2 (proportion of variation explained). Horizontal bars show mean R^2, and error bars are 95% confidence intervals. *Indicates microbiome composition assessed by WMS. Absence of * indicates microbiome composition assessed by 16S rRNA gene amplicon sequencing. Only the top-performing microbiome composition model is shown to avoid repetition. Top predictors of best models to predict percent changes in LDL cholesterol and CRP are shown similarly as those in (D). FDR-adjusted p < 0.05. See also Figures S9–S11 and Tables S8, S9, S10, and S11. ASVs, amplicon sequence variants; AUROC, area under the receiver operating characteristic curve; BCFAs, branched-chain fatty acids; CRP, C-reactive protein; ROC, receiver operating characteristic; SCFAs, short-chain fatty acids.

$p = 0.07$; 1-pyrroline-2-carboxylic acid $r_s = 0.65$, $p = 0.001$) (Figure 7D). 1-Pyrroline-2-carboxylic acid can be synthesized from proline, which is an amino acid that can be converted to glucose via gluconeogenesis. Therefore, microbiome-driven reductions of 1-pyrroline-2-carboxylic acid through the tetrapyrrole biosynthesis I pathway in responders might have reduced glucose concentrations by reducing proline. These findings suggest a role of microbiome-host metabolic crosstalk in the effects of the restore diet on plasma glucose concentrations. MLR confirmed plasma metabolites as predictors for changes to glucose ($R^2 = 0.23$, $p = 0.021$) (Table S11).

In contrast to fasting glucose, the effects of the restore diet on other risk markers showed remarkably little inter-subject variation (Figure 6E). We, therefore, applied RF regression models and MLR to determine to what extent clinical responses could be explained by microbiome, metabolome, or other host features and to identify the best predictors. Baseline microbiota composition (family-level) explained a substantial amount of the variation in changes to LDL (RF mean $R^2 = 0.75$; MLR $R^2 = 0.29$, $p = 0.010$) (Figure 7E; Tables S9 and S11). Baseline fecal SCFA levels were good predictors of changes in CRP levels (RF mean $R^2 = 0.47$; MLR $R^2 = 0.35$, $p = 0.012$) (Figure 7E; Tables S9 and S11), with top predictive features being the ratio of BCFAs to SCFAs as well as concentrations of propionate and total SCFAs. Interestingly, having a higher ratio of BCFAs to SCFAs ($r_s = -0.62$, $p = 0.001$) and lower levels of propionate and total SCFAs ($r_s = 0.60$ and 0.54, $p = 0.002$ and 0.005, respectively) were correlated with greater decreases in CRP (Figure 7E). This suggests that having an unfavorable fermentation profile (i.e., more protein and less fiber fermentation) at baseline allows for greater anti-inflammatory benefits of the restore diet, but causality cannot be elucidated (e.g., baseline microbiome metabolism might influence clinical response but might also be altered by an independent factor). Unlike for glucose responses, baseline host metabolic status did not explain high amounts of variation in the other risk markers (Table S9).

MLR analysis revealed that changes in total cholesterol ($R^2 = 0.31$, $p = 0.007$), LDL ($R^2 = 0.28$, $p = 0.011$), and non-HDL ($R^2 = 0.24$, $p = 0.021$) could be explained by baseline microbiome diversity metrics (Table S11), with the second principal component (PC2; representing 27.0% of total variation) exhibiting negative associations with these risk markers (data not shown). The primary variables (explaining >10% of the variation within this PC) were observed features of CAZymes (12.71%), Shannon index of SGBs (12.05%), and Pielou's evenness of SGBs (10.80%). Overall, this analysis suggests that higher diversity indices at baseline corresponded to more pronounced reductions in cholesterol markers. Although we only detected a trend between baseline microbiome diversity metrics and CRP using MLR ($p = 0.086$; Table S11), our findings align conceptually with those from a previous study that showed better immunological responses to a high-fiber diet in subjects with higher microbiome diversity.[69]

When models were constructed using diet-induced shifts, microbiota composition at the genus-level resulted in the best model for the prediction of changes to LDL (RF mean $R^2 = 0.66$), with a top predictor being Bilophila shifts that were positively correlated with changes to LDL (meaning diet-induced

decreases in Bilophila were associated with reductions in LDL) ($r_s = 0.54$, $p = 0.027$) (Figure 7F; Table S10). Shifts in CAZyme ratios produced the best predictive model for CRP (RF mean $R^2 = 0.44$; MLR $R^2 = 0.34$, $p = 0.010$), with ratios of the abundance of CAZymes that target mucin-glycans and animal-carbohydrates to total reads being the top predictors (Figure 7F; Tables S10 and S11). These two features were positively correlated with changes to CRP ($r_s = 0.51$ and 0.43, $p = 0.012$ and 0.028, respectively), indicating that greater decreases in the abundances of mucin-glycan- and animal-carbohydrate-targeted CAZymes were associated with larger decreases in CRP.

To confirm the links among microbiome features and host clinical responses using an independent approach, we built linear regression models using stepwise model reduction. This analysis revealed that clinical responses to the restore diet could be predicted with high accuracy (Figure S10A), with the greatest amount of variation in responses explained by microbiome compositional and functional changes (Figure S10B). Certain variables mirrored the top predictors identified in the RF analyses (Figures 7A and 7F), such as reductions to Bilophila and higher baseline glucose levels contributing to greater reductions in LDL and glucose, respectively (Figure S10B). The analysis identified a measurable microbiome-independent effect of the restore diet on LDL, calprotectin, and glucose. By contrast, the restore diet had only a minor direct, microbiota-independent effect on total cholesterol, CRP, and BMI, suggesting that reductions in these parameters were mostly driven by microbiome responses.

Inter-individual variation in the effects of the restore diet

Nutrition interventions often elicit variable, person-specific responses,[70] even with standardized diets,[55] which provides rationale for personalized nutrition.[71] To quantify to what degree the various effects of the restore diet were individualized, we calculated a modified coefficient of variation (mCV) of the absolute changes of the compositional and functional microbiome features, plasma metabolites, and risk markers most impacted by the diet (either positive or negative; see STAR Methods). This analysis showed very high variation in compositional changes to the microbiome (mCV = 0.87–4.45 for ASVs; mCV = 0.66–5.05 for genera; Figure S11). Variation was lower for microbiome functions (mCV = 0.58–3.40 for pathways; mCV = 0.74–3.32 for enzymes; mCV = 0.60–1.16 for CAZymes), likely due to functional redundancy of the microbiome. Responses of plasma metabolites and risk markers had much lower variability than microbiome responses (mCV = 0.27–0.73 for plasma metabolites; mCV = 0.36–1.30 for risk markers), indicative that the restore diet elicited consistent host responses despite higher variation in microbiome responses.

DISCUSSION

NCDs have increased to epidemic proportions in industrialized societies, a development that occurred in parallel with a depletion and alteration of the gut microbiome. Industrialized lifestyle and westernization of diet clearly predispose humans to NCDs, which develop slowly over a person's lifetime. A logical yet

nontrivial solution would be to restore the gut microbiome while individuals are still healthy with the goal to prevent NCDs. We, therefore, tested a microbiome restoration strategy in healthy individuals living in Canada and determined effects on gut microbiome ecology, host metabolome, and predictors of cardiometabolic disease risk.

The findings revealed important insights into our ability to restore microbiomes and the clinical implications. We were only able to stably "reintroduce" *L. reuteri* PB-W1 in one individual, and, with a one-time dose, *L. reuteri* had no detectable effects on microbiome ecology, plasma metabolome, and risk markers of chronic diseases. In addition, the restore diet reduced microbiome diversity, and effects on microbiome composition and functional features were highly variable among subjects and small compared with the high inter-individual variation at baseline. However, when assessed within individuals, the effects of the diet explained a large proportion of the temporal variation in the microbiome. In addition, significant compositional shifts were detected, including putatively health-promoting species, and interconnectedness and stability increased. The restore diet beneficially altered several plasma metabolites, mostly of microbial origin, that are implicated to play a role in NCDs. The diet had considerable cardiometabolic effects, resulting in weight loss (despite participants being fed to calculated caloric requirements), a 17% reduction in plasma fasting LDL, a 6% reduction in fasting glucose, and a 14% reduction in CRP. Most importantly, microbiome features that are adversely affected by industrialization and have well-established roles in NCD pathology (e.g., fermentation capacity, SCFAs, *Bilophila*, mucus-degrading genes) were redressed by the restore diet, and several of these effects were predictive of its substantial cardiometabolic benefits.

L. reuteri was the dominant species in rural Papua New Guineans,[13] and its prevalence is 20 times higher in hunter-gatherers when compared with industrialized societies.[14] However, prevalence (<3%) and abundance of *L. reuteri* are nevertheless low in hunter-gatherer populations,[14] and its exact ecological role as a member of the non-industrialized microbiome remains poorly understood. Lactobacilli are minority members of the human gut microbiome (and thus often remain undetected in sequencing studies) and are often allochthonous to the ecosystem,[72] and a recent phylogenomic analysis revealed that *L. reuteri* does not share a long-term evolutionary history with humans and likely requires transmission from animals.[39] This provides a potential explanation both for why *L. reuteri* is rarely detected in human gut microbiomes and why it did not stably colonize after the one-time dose applied in our trial in all but one participant. Nevertheless, the non-industrialized-derived *L. reuteri* PB-W1 established at least 10 times higher population sizes than the type strain DSM 20016[T] 2 days after oral administration and the restore diet enhanced its persistence and survival, indicating the PB-W1 strain displays better adaptations both to the human gut and a non-industrialized-type diet. Future studies are required to test if repeated doses of PB-W1 would elicit probiotic immunological effects, especially if combined with its growth substrates to increase its performance in the gut. Further, other volatile and/or associated negatively with industrialized societies of humans (VANISH) species and lost microbes should be

tested, especially those with evolutionary connections to humans,[73] in combination with non-industrialized-type diets.

Although the restore diet provided greater diversity of fermentable substrates and increased the number of positive interactions within the microbial community, it reduced diversity (i.e., richness and evenness). This finding was unexpected, but there are potential mechanistic explanations. The diet had a profound effect on the gut environment, inducing conditions (high SCFAs, low pH) that are inhibitive to some microbes.[58] Our analysis confirmed that reductions of acid-sensitive taxa[74] like *Parabacteroides* and *Bacteroides* were driven by changes in pH (Figure S7B). In addition, the diet altered host phenotypes such as inflammation and bile acid excretion that may have reduced competitive advantages of bile-resistant taxa (e.g., *Bilophila*, *Alistipes*) that are often enriched during inflammatory conditions[75,76] at the expense of inflammation-sensitive taxa, such as *Faecalibacterium*,[77] which bloomed during the restore diet period. The restore diet further removed sources of potential growth substrates (e.g., dairy- and meat-derived glycoproteins),[78] which might have reduced abundances of microbes reliant on these resources that lacked adaptations necessary to utilize the novel substrates provided by the diet.[79] In this respect, a hurdle in restoring microbiome diversity is that microbial exposure and dispersal (e.g., through sanitation) are low in industrialized settings.[13] In a multi-generational murine model that tested western diet-induced extinctions in the gut microbiota, switching from a low- to high-fiber diet without fecal exposure was not sufficient to restore lost microbial diversity.[27] Thus, although observational studies have reported positive links between diet diversity and gut microbiome diversity,[80–82] the latter might be impossible to increase beyond the baseline in the short term without administration of lost fiber degraders or VANISH species.[83]

Despite the reduction in diversity, community interconnectedness and stability increased during the restore diet, which are considered beneficial attributes of communities,[84] and the compositional shifts induced by the restore diet are generally regarded as beneficial (e.g., increases in *Bifidobacterium*, *Faecalibacterium*, and *Lachnospiraceae*). Most importantly, gut microbiome features affected by industrialization were redressed by the restore diet: fermentation capacity and SCFA production were increased, pH was reduced, abundances of pro-inflammatory microbes (e.g., *Bilophila*, *Alistipes*) were decreased, and potential for mucus degradation was reduced. Several of these diet-mediated effects were associated with the clinical benefits of the restore diet and provide potential mechanisms by which the restore diet exerts its benefits. Reduction in pH has a wide range of positive effects on microbiome metabolism.[85] In addition, *Bilophila*, which blooms during increased saturated fat intake, has been shown to aggravate metabolic and immunological dysfunctions in mice[75,86] and is associated with adenomas and colorectal cancer in epidemiological studies.[87–89] Further, mucus degradation is an important pathological factor that drives inflammation.[28,29,90] Thus, our study provides experimental evidence in humans that these well-established mechanistic links between the microbiome and host pathology can be modulated through diet. Interestingly, the restore diet increased the abundance of bacterial genera that were predictive of mild COVID-19 outcomes,

while it reduced taxa linked to poor clinical outcomes.[91,92] Therefore, although the restore diet reduced gut microbial diversity, its overall effects on host-microbiome and microbiome-immune interactions were likely beneficial.

It is of interest to compare our findings with effects of other nutritional strategies to elucidate the most likely dietary determinants of the considerable cardiometabolic benefits of the restore diet. In a study of healthy adults that, through dietary advice, increased intake of fermented foods or dietary fiber (~43 g/day), some inflammatory cytokines were reduced due to the fermented-foods intervention, but the high-fiber intervention had no effect on lipid and glycemic profiles.[69] The striking differences in the benefits of fiber observed in this study when compared with the restore diet might stem from the advantage of strictly controlling food intake. Our findings are more in line with the cardioprotective effects of other plant-rich diets, such as the Mediterranean diet and strictly plant-based (vegan) diets. In male subjects with metabolic syndrome following a Mediterranean diet (~24 g/day fiber), glucose (−3.4%), HOMA-IR (−24.3%), total cholesterol (−17.5%), LDL (−16.7%) and HDL (−15.4%) concentrations were reduced, while CRP did not change.[93] Similar findings were observed in subjects with obesity who consumed a calorically restricted Mediterranean diet for 6 months, which improved LDL (−3.5%), HDL (+5.1%), triglycerides (−13.2%), and CRP (−10.9%).[94] In an inpatient crossover study, adults without diabetes and BMI 27.8 ± 1.3 kg/m^2 were provided a strictly plant-based diet containing similar amounts of dietary fiber as in our study (31.4 g/1,000 kcal) or a low-carbohydrate diet.[66] After 2 weeks, the plant-based diet significantly reduced total cholesterol (−25.7%), LDL (−26.3%), CRP (−42.9%), glucose (−6.6%), and insulin (−26.5%). Overall, it appears the effects of the restore diet match other plant-rich diets in their metabolic and anti-inflammatory effects.[67,95,96]

Although the health effects of plant-based diets are well-established, there are still open questions related to the underlying mechanisms and the role of the gut microbiome. Our study contributes to addressing these questions. Many of the plasma metabolites impacted by the restore diet are of microbial origin or modified by microbes and have health implications. For example, indole-3-propionic acid, which is enhanced by the restore diet, is a neuroprotective antioxidant endogenously produced by the gut microbiome that has been correlated with a reduced risk of type 2 diabetes and atherosclerosis.[97–99] Other metabolites increased by the restore diet have antioxidant and anti-inflammatory properties, such as coniferyl aldehyde,[100,101] pipecolic acid,[102] and glycocholic acid.[103] The secondary bile acids deoxycholic and ursodeoxycholic acid, which were reduced by the restore diet, are established carcinogens, while 8-hydroxyguanine is a marker of mutagenesis and carcinogenesis.[104,105] Thus, our findings provide potential mechanistic explanations for the well-established benefits of plant-based diets on brain aging and cognition, cancer prevention, and longevity, and clearly implicate the gut microbiome in these effects.

Many dietary interventions show a considerable degree of inter-individual variation in their physiological effects,[70,106,107] which provides rationale for personalized nutritional approaches.[108,109] Given its highly individualized nature and importance for the effects of diet,[109] the microbiome has

been proposed to constitute an important factor in attempts to personalize diet. By conducting a controlled feeding trial, we directly established the extent of variation in microbial and physiological responses to a standardized diet. Although changes to gut microbiome composition were highly individualized, less variation was observed in the diet's effects on functional features (e.g., CAZymes), and the effects on blood metabolites and risk markers were highly consistent among individuals. Potential explanations for these findings are that functional redundancies exist among different microbial members, the complex range of nutrients in the restore diet influenced a wide variety of microbial taxa, and microbiome-independent effects of the diet. These findings are of considerable relevance for dietary recommendations, as they demonstrate that plant-rich diets exert consistent and likely population-wide benefits that require no personalization.

There has been active debate around the rationale, challenges, and limitations of gut microbiome restoration attempts and the validity of the conceptual framework on which such approaches rest.[30] Concerns have been raised about the inability to define an ancestral microbiome—or even a "healthy" microbiome[110]—and the lack of evidence that microbiome traits associated with non-industrialized populations promote health (e.g., considering the higher life expectancy in industrialized settings). In addition, phenotypic effects of the gut microbiome are context dependent—they may be beneficial or detrimental depending on environmental factors or genetic predisposition. Furthermore, an industrialized microbiome is likely well-adapted to its particular environment and difficult to change. Our study revealed important insights into the ecological constraints that apply when attempting to restore the industrialized gut microbiome. Reduced diversity, which characterizes industrialized microbiomes, was not redressed, *L. reuteri* could not be reintroduced after one dose, and microbiome changes were highly individualized. In addition, our findings suggest that at least some members of the industrialized microbiome are misadapted to fiber-rich diets. It might be impossible to increase diversity with fiber-based strategies,[79] especially without co-administration of repeated doses of VANISH species, and to restore industrialized microbiomes to more ancestral states.

Although these concerns are certainly warranted, we consider several of our findings promising, as they point to the ability to redress relevant compositional and functional characteristics of the gut microbiome with beneficial outcomes, even if a more complete restoration of diversity is not possible. Several microbiome features altered by industrialization that have well-established roles in pathology (e.g., fermentation capacity, SCFAs, *Bilophila*, mucus degradation) were redressed and predictive of the considerable clinical benefits of the diet. In addition, our findings point to functional redundancy between industrialized and non-industrialized gut microbiomes in that the industrialized gut microbiome, although depleted and devoid of VANISH species, has maintained its ability to mediate at least some of the health effects of a non-industrialized-type diet.

Limitations of the study

Non-industrialized dietary patterns are diverse, and there are uncertainties about ancestral diets,[111] making it impossible to

CellPress
OPEN ACCESS

Cell
Article

exactly replicate such diets. In addition, being comprised of food items available in Canada, the restore diet is only an approximation of a non-industrialized diet. Our focus was, therefore, to replicate key diet characteristics, such as an enrichment of plant-based, high-fiber foods and avoidance of highly processed foods. *L. reuteri* DSM 20016[T] has been propagated in laboratories much longer than the non-industrialized PB-W1 strain, which may have reduced its ecological performance in humans. Participants enrolled in our study were mainly students or university employees due to their proximity to campus and willingness to attend clinic visits, which may limit the generalizability of the results to the general population. The sample size was relatively small (*n* = 30), and although this was partially mitigated by the crossover design for the diet intervention, the number of participants randomized in the parallel-arm design to the *L. reuteri* and placebo groups (*n* = 9–11 per group) may have limited statistical power to detect effects of *L. reuteri* on the gut microbiome and/ or host physiology. The sample size is also a limitation for the machine learning approach, as we did not have a large enough *n* to create an independent test set to evaluate the predictive models; however, potential bias was partially mitigated through our use of the standard technique of external cross-validation for model evaluation. We conducted per-protocol as opposed to intention-to-treat analyses in an effort to maintain statistical power and detect meaningful microbiome changes and potential host-microbiome interactions. The controlled feeding trial was designed to determine the causal effects of the restore diet on the gut microbiome and risk markers of chronic diseases.[112] However, our study cannot determine to what degree the microbiome changes caused the clinical effects of diet. Future research is required to confirm the mechanistic underpinnings of the non-industrialized-type diet and the causal contributions of the microbiome.

RESOURCE AVAILABILITY

Lead contact
Further information and requests for resources and reagents should be directed to and will be fulfilled by the lead contact, Jens Walter (jenswalter@ucc.ie).

Materials availability
This study did not generate new unique reagents.

Data and code availability
All original sequencing data (16S rRNA gene amplicon sequencing and WMS) has been deposited at the NCBI Sequence Read Archive (SRA; accession number: SRA: PRJNA1000186). DOIs are listed in the key resources table. Any additional information required to reanalyze data reported in this paper is available from the lead contact upon request.

AUTHOR CONTRIBUTIONS

DECLARATION OF INTERESTS

STAR★METHODS

Detailed methods are provided in the online version of this paper and include the following:

- KEY RESOURCES TABLE
- EXPERIMENTAL MODEL AND STUDY PARTICIPANT DETAILS
  - Recruitment and selection of participants
  - Specimen collection
- METHOD DETAILS
  - Intervention
  - *L. reuteri* inocula and placebo preparation
  - Restore diet preparation and adherence
  - Participant-reported outcomes
  - DNA extraction and sequencing
  - Bioinformatics analysis
  - Fecal SCFAs, BCFAs, pH, and dry mass percentage

Cell
Article

CellPress
OPEN ACCESS

- ○ Plasma metabolomics
- ○ Safety-related laboratory measures
- ○ Risk markers of chronic diseases
- ○ Markers of gut barrier function
- QUANTIFICATION AND STATISTICAL ANALYSIS
  - ○ Quantification of *L. reuteri* in fecal samples
  - ○ Statistical analyses
  - ○ Machine learning models
  - ○ Linear models
- ADDITIONAL RESOURCES

REFERENCES

1. de Vos, W.M., Tilg, H., Van Hul, M., and Cani, P.D. (2022). Gut microbiome and health: mechanistic insights. Gut 71, 1020–1032. https://doi.org/10.1136/gutjnl-2021-326789.

2. Tannock, G.W. (2024). Understanding the gut microbiota by considering human evolution: a story of fire, cereals, cooking, molecular ingenuity, and functional cooperation. Microbiol. Mol. Biol. Rev. 88, e0012722. https://doi.org/10.1128/mmbr.00127-22.

3. Alcock, J., Carroll-Portillo, A., Coffman, C., and Lin, H.C. (2021). Evolution of human diet and microbiome-driven disease. Curr. Opin. Physiol. 23. https://doi.org/10.1016/j.cophys.2021.06.009.

4. Sonnenburg, E.D., and Sonnenburg, J.L. (2019). The ancestral and industrialized gut microbiota and implications for human health. Nat. Rev. Microbiol. 17, 383–390. https://doi.org/10.1038/s41579-019-0191-8.

5. Sonnenburg, J.L., and Sonnenburg, E.D. (2019). Vulnerability of the industrialized microbiota. Science 366, eaaw9255. https://doi.org/10.1126/science.aaw9255.

6. Baker, R.E., Mahmud, A.S., Miller, I.F., Rajeev, M., Rasambainarivo, F., Rice, B.L., Takahashi, S., Tatem, A.J., Wagner, C.E., Wang, L.F., et al. (2022). Infectious disease in an era of global change. Nat. Rev. Microbiol. 20, 193–205. https://doi.org/10.1038/s41579-021-00639-z.

7. Scott, F.I., Horton, D.B., Mamtani, R., Haynes, K., Goldberg, D.S., Lee, D.Y., and Lewis, J.D. (2016). Administration of antibiotics to children before age 2 years increases risk for childhood obesity. Gastroenterology 151, 120–129.e5. https://doi.org/10.1053/j.gastro.2016.03.006.

8. Chavarro, J.E., Martín-Calvo, N., Yuan, C., Arvizu, M., Rich-Edwards, J.W., Michels, K.B., and Sun, Q. (2020). Association of birth by cesarean delivery with obesity and type 2 diabetes among adult women. JAMA Netw. Open 3, e202605. https://doi.org/10.1001/jamanetworkopen.2020.2605.

9. Simin, J., Fornes, R., Liu, Q., Olsen, R.S., Callens, S., Engstrand, L., and Brusselaers, N. (2020). Antibiotic use and risk of colorectal cancer: a systematic review and dose-response meta-analysis. Br. J. Cancer 123, 1825–1832. https://doi.org/10.1038/s41416-020-01082-2.

10. GBD 2021 Diseases and Injuries Collaborators (2024). Global incidence, prevalence, years lived with disability (YLDs), disability-adjusted life-years (DALYs), and healthy life expectancy (HALE) for 371 diseases and injuries in 204 countries and territories and 811 subnational locations, 1990–2021: a systematic analysis for the Global Burden of Disease Study 2021. Lancet 403, 2133–2161. https://doi.org/10.1016/S0140-6736(24)00757-8.

11. Blaser, M.J., and Falkow, S. (2009). What are the consequences of the disappearing human microbiota? Nat. Rev. Microbiol. 7, 887–894. https://doi.org/10.1038/nrmicro2245.

12. Sonnenburg, E.D., and Sonnenburg, J.L. (2014). Starving our microbial self: the deleterious consequences of a diet deficient in microbiota-accessible carbohydrates. Cell Metab. 20, 779–786. https://doi.org/10.1016/j.cmet.2014.07.003.

13. Martínez, I., Stegen, J.C., Maldonado-Gómez, M.X., Eren, A.M., Siba, P.M., Greenhill, A.R., and Walter, J. (2015). The gut microbiota of rural Papua New Guineans: composition, diversity patterns, and ecological processes. Cell Rep. 11, 527–538. https://doi.org/10.1016/j.celrep.2015.03.049.

14. Carter, M.M., Olm, M.R., Merrill, B.D., Dahan, D., Tripathi, S., Spencer, S.P., Yu, F.B., Jain, S., Neff, N., Jha, A.R., et al. (2023). Ultra-deep sequencing of Hadza hunter-gatherers recovers vanishing gut microbes. Cell 186, 3111–3124.e13. https://doi.org/10.1016/j.cell.2023.05.046.

15. Clemente, J.C., Pehrsson, E.C., Blaser, M.J., Sandhu, K., Gao, Z., Wang, B., Magris, M., Hidalgo, G., Contreras, M., Noya-Alarcón, Ó., et al. (2015). The microbiome of uncontacted Amerindians. Sci. Adv. 1, e1500183. https://doi.org/10.1126/sciadv.1500183.

16. Pasolli, E., Asnicar, F., Manara, S., Zolfo, M., Karcher, N., Armanini, F., Beghini, F., Manghi, P., Tett, A., Ghensi, P., et al. (2019). Extensive unexplored human microbiome diversity revealed by over 150,000 genomes from metagenomes spanning age, geography, and lifestyle. Cell 176, 649–662.e20. https://doi.org/10.1016/j.cell.2019.01.001.

17. Obregon-Tito, A.J., Tito, R.Y., Metcalf, J., Sankaranarayanan, K., Clemente, J.C., Ursell, L.K., Zech Xu, Z., Van Treuren, W., Knight, R., Gaffney, P.M., et al. (2015). Subsistence strategies in traditional societies distinguish gut microbiomes. Nat. Commun. 6, 6505. https://doi.org/10.1038/ncomms7505.

18. Jha, A.R., Davenport, E.R., Gautam, Y., Bhandari, D., Tandukar, S., Ng, K.M., Fragiadakis, G.K., Holmes, S., Gautam, G.P., Leach, J., et al. (2018). Gut microbiome transition across a lifestyle gradient in Himalaya. PLoS Biol. 16, e2005396. https://doi.org/10.1371/journal.pbio.2005396.

19. Ramaboli, M.C., Ocvirk, S., Khan Mirzaei, M., Eberhart, B.L., Valdivia-Garcia, M., Metwaly, A., Neuhaus, K., Barker, G., Ru, J., Nesengani, L.T., et al. (2024). Diet changes due to urbanization in South Africa are linked to microbiome and metabolome signatures of Westernization and colorectal cancer. Nat. Commun. 15, 3379. https://doi.org/10.1038/s41467-024-46265-0.

20. Vangay, P., Johnson, A.J., Ward, T.L., Al-Ghalith, G.A., Shields-Cutler, R.R., Hillmann, B.M., Lucas, S.K., Beura, L.K., Thompson, E.A., Till, L.M., et al. (2018). US immigration westernizes the human gut microbiome. Cell 175, 962–972.e10. https://doi.org/10.1016/j.cell.2018.10.029.

21. Wibowo, M.C., Yang, Z., Borry, M., Hübner, A., Huang, K.D., Tierney, B.T., Zimmerman, S., Barajas-Olmos, F., Contreras-Cubas, C., García-Ortiz, H., et al. (2021). Reconstruction of ancient microbial genomes from the human gut. Nature 594, 234–239. https://doi.org/10.1038/s41586-021-03532-0.

22. De Filippo, C., Cavalieri, D., Di Paola, M., Ramazzotti, M., Poullet, J.B., Massart, S., Collini, S., Pieraccini, G., and Lionetti, P. (2010). Impact of diet in shaping gut microbiota revealed by a comparative study in children from Europe and rural Africa. Proc. Natl. Acad. Sci. USA. 107, 14691–14696. https://doi.org/10.1073/pnas.1005963107.

23. Moraïs, S., Winkler, S., Zorea, A., Levin, L., Nagies, F.S.P., Kapust, N., Lamed, E., Artan-Furman, A., Bolam, D.N., Yadav, M.P., et al. (2024). Cryptic diversity of cellulose-degrading gut bacteria in industrialized humans. Science 383, eadj9223. https://doi.org/10.1126/science.adj9223.

24. Blanco-Míguez, A., Gálvez, E.J.C., Pasolli, E., De Filippis, F., Amend, L., Huang, K.D., Manghi, P., Lesker, T.R., Riedel, T., Cova, L., et al. (2023). Extension of the *Segatella copri* complex to 13 species with distinct large extrachromosomal elements and associations with host conditions. Cell

Host Microbe *31*, 1804–1819.e9. https://doi.org/10.1016/j.chom.2023.09.013.

25. Tett, A., Huang, K.D., Asnicar, F., Fehlner-Peach, H., Pasolli, E., Karcher, N., Armanini, F., Manghi, P., Bonham, K., Zolfo, M., et al. (2019). The *Prevotella copri* complex comprises four distinct clades underrepresented in westernized populations. Cell Host Microbe *26*, 666–679.e7. https://doi.org/10.1016/j.chom.2019.08.018.

26. Smits, S.A., Leach, J., Sonnenburg, E.D., Gonzalez, C.G., Lichtman, J.S., Reid, G., Knight, R., Manjurano, A., Changalucha, J., Elias, J.E., et al. (2017). Seasonal cycling in the gut microbiome of the Hadza hunter-gatherers of Tanzania. Science *357*, 802–806. https://doi.org/10.1126/science.aan4834.

27. Sonnenburg, E.D., Smits, S.A., Tikhonov, M., Higginbottom, S.K., Wingreen, N.S., and Sonnenburg, J.L. (2016). Diet-induced extinctions in the gut microbiota compound over generations. Nature *529*, 212–215. https://doi.org/10.1038/nature16504.

28. Desai, M.S., Seekatz, A.M., Koropatkin, N.M., Kamada, N., Hickey, C.A., Wolter, M., Pudlo, N.A., Kitamoto, S., Terrapon, N., Muller, A., et al. (2016). A dietary fiber-deprived gut microbiota degrades the colonic mucus barrier and enhances pathogen susceptibility. Cell *167*, 1339–1353.e21. https://doi.org/10.1016/j.cell.2016.10.043.

29. Earle, K.A., Billings, G., Sigal, M., Lichtman, J.S., Hansson, G.C., Elias, J.E., Amieva, M.R., Huang, K.C., and Sonnenburg, J.L. (2015). Quantitative imaging of gut microbiota spatial organization. Cell Host Microbe *18*, 478–488. https://doi.org/10.1016/j.chom.2015.09.002.

30. Carmody, R.N., Sarkar, A., and Reese, A.T. (2021). Gut microbiota through an evolutionary lens. Science *372*, 462–463. https://doi.org/10.1126/science.abf0590.

31. Handsley-Davis, M., Anderson, M.Z., Bader, A.C., Ehau-Taumaunu, H., Fox, K., Kowal, E., and Weyrich, L.S. (2023). Microbiome ownership for Indigenous peoples. Nat. Microbiol. *8*, 1777–1786. https://doi.org/10.1038/s41564-023-01470-3.

32. Walter, J., Britton, R.A., and Roos, S. (2011). Host-microbial symbiosis in the vertebrate gastrointestinal tract and the *Lactobacillus reuteri* paradigm. Proc. Natl. Acad. Sci. USA *108*, 4645–4652. https://doi.org/10.1073/pnas.1000099107.

33. Dos Reis Buzzo Zermiani, A.P., de Paula Soares, A.L.P.P., da Silva Guedes de Moura, B.L., Miguel, E.R.A., Lopes, L.D.G., de Carvalho Scharf Santana, N., da Silva Santos, T., Demarchi, I.G., and Teixeira, J.J. (2021). Evidence of *Lactobacillus reuteri* to reduce colic in breastfed babies: systematic review and meta-analysis. Complement. Ther. Med. *63*, 102781. https://doi.org/10.1016/j.ctim.2021.102781.

34. McFarland, L.V., Evans, C.T., and Goldstein, E.J.C. (2018). Strain-specificity and disease-specificity of probiotic efficacy: A systematic review and meta-analysis. Front. Med. (Lausanne) *5*, 124. https://doi.org/10.3389/fmed.2018.00124.

35. Morgan, R.L., Preidis, G.A., Kashyap, P.C., Weizman, A.V., and Sadeghirad, B.; McMaster Probiotic, Prebiotic, and Synbiotic Work Group (2020). Probiotics reduce mortality and morbidity in preterm, low-birth-weight infants: A systematic review and network meta-analysis of randomized trials. Gastroenterology *159*, 467–480. https://doi.org/10.1053/j.gastro.2020.05.096.

36. AEProbio (2024). Clinical guide to probiotic products available in Canada. http://www.probioticchart.ca/PBCIntroduction.html?utm_source=intro_pg&utm_medium=civ&utm_campaign=CDN_CHART.

37. Archer, D., Perez-Muñoz, M.E., Tollenaar, S., Veniamin, S., Cheng, C.C., Richard, C., Barreda, D.R., Field, C.J., and Walter, J. (2023). The importance of the timing of microbial signals for perinatal immune system development. Microbiome Res. Rep. *2*, 11. https://doi.org/10.20517/mrr.2023.03.

38. Lerche, M., and Reuter, G. (1962). Das Vorkommen aerob wachsender Gram-positiver Stäbchen des Genus Lactobacillus Beijerinck im Darminhalt erwachsener Menschen. Zentralbl. Bakteriol. Parasitenkd. Infektionskr. Hyg. I Orig. *185*, 446–481.

39. Li, F., Li, X., Cheng, C.C., Bujdoš, D., Tollenaar, S., Simpson, D.J., Tasseva, G., Perez-Muñoz, M.E., Frese, S., Gänzle, M.G., et al. (2023). A phylogenomic analysis of *Limosilactobacillus reuteri* reveals ancient and stable evolutionary relationships with rodents and birds and zoonotic transmission to humans. BMC Biol. *21*, 53. https://doi.org/10.1186/s12915-023-01541-1.

40. Li, F., Cheng, C.C., Zheng, J., Liu, J., Quevedo, R.M., Li, J., Roos, S., Gänzle, M.G., and Walter, J. (2021). *Limosilactobacillus balticus* sp. nov., *Limosilactobacillus agrestis* sp. nov., *Limosilactobacillus albertensis* sp. nov., *Limosilactobacillus rudii* sp. nov. and *Limosilactobacillus fastidiosus* sp. nov., five novel *Limosilactobacillus* species isolated from the vertebrate gastrointestinal tract, and proposal of six subspecies of *Limosilactobacillus reuteri* adapted to the gastrointestinal tract of specific vertebrate hosts. Int. J. Syst. Evol. Microbiol. *71*, 004644. https://doi.org/10.1099/ijsem.0.004644.

41. Han, I.H., and Baik, B.K. (2006). Oligosaccharide content and composition of legumes and their reduction by soaking, cooking, ultrasound, and high hydrostatic pressure. Cereal Chem. *83*, 428–433. https://doi.org/10.1094/CC-83-0428.

42. Jovanovic-Malinovska, R., Kuzmanova, S., and Winkelhausen, E. (2014). Oligosaccharide profile in fruits and vegetables as sources of prebiotics and functional foods. Int. J. Food Prop. *17*, 949–965. https://doi.org/10.1080/10942912.2012.680221.

43. Rattanaprasert, M., van Pijkeren, J.P., Ramer-Tait, A.E., Quintero, M., Kok, C.R., Walter, J., and Hutkins, R.W. (2019). Genes involved in galactooligosaccharide metabolism in *Lactobacillus reuteri* and their ecological role in the gastrointestinal tract. Appl. Environ. Microbiol. *85*, e01788-19. https://doi.org/10.1128/AEM.01788-19.

44. Konner, M.J., and Eaton, S.B. (2010). Paleolithic nutrition: twenty-five years later. Nutr. Clin. Pract. *25*, 594–602. https://doi.org/10.1177/0884533610385702.

45. Institute of Medicine (2006). DRI, Dietary Reference Intakes: the Essential Guide to Nutrient Requirements (National Academies Press).

46. Burkitt, D.P., Walker, A.R., and Painter, N.S. (1972). Effect of dietary fibre on stools and transit-times, and its role in the causation of disease. Lancet *2*, 1408–1412. https://doi.org/10.1016/S0140-6736(72)92974-1.

47. de Vries, J., Birkett, A., Hulshof, T., Verbeke, K., and Gibes, K. (2016). Effects of cereal, fruit and vegetable fibers on human fecal weight and transit time: a comprehensive review of intervention trials. Nutrients *8*, 130. https://doi.org/10.3390/nu8030130.

48. McCann, K.S. (2000). The diversity–stability debate. Nature *405*, 228–233. https://doi.org/10.1038/35012234.

49. Cotillard, A., Kennedy, S.P., Kong, L.C., Prifti, E., Pons, N., Le Chatelier, E., Almeida, M., Quinquis, B., Levenez, F., Galleron, N., et al. (2013). Dietary intervention impact on gut microbial gene richness. Nature *500*, 585–588. https://doi.org/10.1038/nature12480.

50. Salonen, A., Lahti, L., Salojärvi, J., Holtrop, G., Korpela, K., Duncan, S.H., Date, P., Farquharson, F., Johnstone, A.M., Lobley, G.E., et al. (2014). Impact of diet and individual variation on intestinal microbiota composition and fermentation products in obese men. ISME J. *8*, 2218–2230. https://doi.org/10.1038/ismej.2014.63.

51. Bourdeau-Julien, I., Castonguay-Paradis, S., Rochefort, G., Perron, J., Lamarche, B., Flamand, N., Di Marzo, V., Veilleux, A., and Raymond, F. (2023). The diet rapidly and differentially affects the gut microbiota and host lipid mediators in a healthy population. Microbiome *11*, 26. https://doi.org/10.1186/s40168-023-01469-2.

52. Procházková, N., Falony, G., Dragsted, L.O., Licht, T.R., Raes, J., and Roager, H.M. (2023). Advancing human gut microbiota research by considering gut transit time. Gut *72*, 180–191. https://doi.org/10.1136/gutjnl-2022-328166.

53. Asnicar, F., Leeming, E.R., Dimidi, E., Mazidi, M., Franks, P.W., Al Khatib, H., Valdes, A.M., Davies, R., Bakker, E., Francis, L., et al. (2021). Blue poo: impact of gut transit time on the gut microbiome using a novel

Cell
Article

CellPress
OPEN ACCESS

marker. Gut *70*, 1665–1674. https://doi.org/10.1136/gutjnl-2020-323877.

54. Wu, G.D., Chen, J., Hoffmann, C., Bittinger, K., Chen, Y.-Y., Keilbaugh, S.A., Bewtra, M., Knights, D., Walters, W.A., Knight, R., et al. (2011). Linking long-term dietary patterns with gut microbial enterotypes. Science *334*, 105–108. https://doi.org/10.1126/science.1208344.

55. Guthrie, L., Spencer, S.P., Perelman, D., Van Treuren, W., Han, S., Yu, F.B., Sonnenburg, E.D., Fischbach, M.A., Meyer, T.W., and Sonnenburg, J.L. (2022). Impact of a 7-day homogeneous diet on interpersonal variation in human gut microbiomes and metabolomes. Cell Host Microbe *30*, 863–874.e4. https://doi.org/10.1016/j.chom.2022.05.003.

56. Morais, M.A.B., Coines, J., Domingues, M.N., Pirolla, R.A.S., Tonoli, C.C.C., Santos, C.R., Correa, J.B.L., Gozzo, F.C., Rovira, C., and Murakami, M.T. (2021). Two distinct catalytic pathways for GH43 xylanolytic enzymes unveiled by X-ray and QM/MM simulations. Nat. Commun. *12*, 367. https://doi.org/10.1038/s41467-020-20620-3.

57. Fang, J., Wang, H., Zhou, Y., Zhang, H., Zhou, H., and Zhang, X. (2021). Slimy partners: the mucus barrier and gut microbiome in ulcerative colitis. Exp. Mol. Med. *53*, 772–787. https://doi.org/10.1038/s12276-021-00617-8.

58. Walker, A.W., Duncan, S.H., McWilliam Leitch, E.C., Child, M.W., and Flint, H.J. (2005). pH and peptide supply can radically alter bacterial populations and short-chain fatty acid ratios within microbial communities from the human colon. Appl. Environ. Microbiol. *71*, 3692–3700. https://doi.org/10.1128/AEM.71.7.3692-3700.2005.

59. Korpela, K. (2018). Diet, microbiota, and metabolic health: trade-off between saccharolytic and proteolytic fermentation. Annu. Rev. Food Sci. Technol. *9*, 65–84. https://doi.org/10.1146/annurev-food-030117-012830.

60. Wishart, D.S., Oler, E., Peters, H., Guo, A., Girod, S., Han, S., Saha, S., Lui, V.W., LeVatte, M., Gautam, V., et al. (2023). MiMeDB: the Human Microbial Metabolome Database. Nucleic Acids Res. *51*, D611–D620. https://doi.org/10.1093/nar/gkac868.

61. Diener, C., Dai, C.L., Wilmanski, T., Baloni, P., Smith, B., Rappaport, N., Hood, L., Magis, A.T., and Gibbons, S.M. (2022). Genome-microbiome interplay provides insight into the determinants of the human blood metabolome. Nat. Metab. *4*, 1560–1572. https://doi.org/10.1038/s42255-022-00670-1.

62. Yong, C.C., Sakurai, T., Kaneko, H., Horigome, A., Mitsuyama, E., Nakajima, A., Katoh, T., Sakanaka, M., Abe, T., Xiao, J.Z., et al. (2024). Human gut-associated *Bifidobacterium* species salvage exogenous indole, a uremic toxin precursor, to synthesize indole-3-lactic acid via tryptophan. Gut Microbes *16*, 2347728. https://doi.org/10.1080/19490976.2024.2347728.

63. Adolph, T.E., and Tilg, H. (2024). Western diets and chronic diseases. Nat. Med. *30*, 2133–2147. https://doi.org/10.1038/s41591-024-03165-6.

64. Grundy, M.M.L., Edwards, C.H., Mackie, A.R., Gidley, M.J., Butterworth, P.J., and Ellis, P.R. (2016). Re-evaluation of the mechanisms of dietary fibre and implications for macronutrient bioaccessibility, digestion and postprandial metabolism. Br. J. Nutr. *116*, 816–833. https://doi.org/10.1017/S0007114516002610.

65. Corbin, K.D., Carnero, E.A., Dirks, B., Igudesman, D., Yi, F., Marcus, A., Davis, T.L., Pratley, R.E., Rittmann, B.E., Krajmalnik-Brown, R., et al. (2023). Host-diet-gut microbiome interactions influence human energy balance: a randomized clinical trial. Nat. Commun. *14*, 3161. https://doi.org/10.1038/s41467-023-38778-x.

66. Hall, K.D., Guo, J., Courville, A.B., Boring, J., Brychta, R., Chen, K.Y., Darcey, V., Forde, C.G., Gharib, A.M., Gallagher, I., et al. (2021). Effect of a plant-based, low-fat diet versus an animal-based, ketogenic diet on ad libitum energy intake. Nat. Med. *27*, 344–353. https://doi.org/10.1038/s41591-020-01209-1.

67. Landry, M.J., Ward, C.P., Cunanan, K.M., Durand, L.R., Perelman, D., Robinson, J.L., Hennings, T., Koh, L., Dant, C., Zeitlin, A., et al. (2023). Cardiometabolic effects of omnivorous vs vegan diets in identical twins:

68. Bellina, F., and Rossi, R. (2006). Synthesis and biological activity of pyrrole, pyrroline and pyrrolidine derivatives with two aryl groups on adjacent positions. Tetrahedron *62*, 7213–7256. https://doi.org/10.1016/j.tet.2006.05.024.

69. Wastyk, H.C., Fragiadakis, G.K., Perelman, D., Dahan, D., Merrill, B.D., Yu, F.B., Topf, M., Gonzalez, C.G., Van Treuren, W., Han, S., et al. (2021). Gut-microbiota-targeted diets modulate human immune status. Cell *184*, 4137–4153.e14. https://doi.org/10.1016/j.cell.2021.06.019.

70. Gardner, C.D., Trepanowski, J.F., Del Gobbo, L.C., Hauser, M.E., Rigdon, J., Ioannidis, J.P.A., Desai, M., and King, A.C. (2018). Effect of low-fat vs low-carbohydrate diet on 12-month weight loss in overweight adults and the association with genotype pattern or insulin secretion: the DIETFITS randomized clinical trial. JAMA *319*, 667–679. https://doi.org/10.1001/jama.2018.0245.

71. Leshem, A., Segal, E., and Elinav, E. (2020). The gut microbiome and individual-specific responses to diet. mSystems *5*, e00665-20. https://doi.org/10.1128/mSystems.00665-20.

72. Walter, J. (2008). Ecological role of lactobacilli in the gastrointestinal tract: implications for fundamental and biomedical research. Appl. Environ. Microbiol. *74*, 4985–4996. https://doi.org/10.1128/AEM.00753-08.

73. Sanders, J.G., Sprockett, D.D., Li, Y., Mjungu, D., Lonsdorf, E.V., Ndjango, J.N., Georgiev, A.V., Hart, J.A., Sanz, C.M., Morgan, D.B., et al. (2023). Widespread extinctions of co-diversified primate gut bacterial symbionts from humans. Nat. Microbiol. *8*, 1039–1050. https://doi.org/10.1038/s41564-023-01388-w.

74. Duncan, S.H., Louis, P., Thomson, J.M., and Flint, H.J. (2009). The role of pH in determining the species composition of the human colonic microbiota. Environ. Microbiol. *11*, 2112–2122. https://doi.org/10.1111/j.1462-2920.2009.01931.x.

75. Devkota, S., Wang, Y., Musch, M.W., Leone, V., Fehlner-Peach, H., Nadimpalli, A., Antonopoulos, D.A., Jabri, B., and Chang, E.B. (2012). Dietary-fat-induced taurocholic acid promotes pathobiont expansion and colitis in *Il10-/-* mice. Nature *487*, 104–108. https://doi.org/10.1038/nature11225.

76. Parker, B.J., Wearsch, P.A., Veloo, A.C.M., and Rodriguez-Palacios, A. (2020). The genus *Alistipes*: gut bacteria with emerging implications to inflammation, cancer, and mental health. Front. Immunol. *11*, 906. https://doi.org/10.3389/fimmu.2020.00906.

77. Martín, R., Rios-Covian, D., Huillet, E., Auger, S., Khazaal, S., Bermúdez-Humarán, L.G., Sokol, H., Chatel, J.M., and Langella, P. (2023). *Faecalibacterium*: a bacterial genus with promising human health applications. FEMS Microbiol. Rev. *47*, fuad039. https://doi.org/10.1093/femsre/fuad039.

78. Peled, S., and Livney, Y.D. (2021). The role of dietary proteins and carbohydrates in gut microbiome composition and activity: a review. Food Hydrocoll. *120*, 106911. https://doi.org/10.1016/j.foodhyd.2021.106911.

79. Cantu-Jungles, T.M., and Hamaker, B.R. (2023). Tuning expectations to reality: don't expect increased gut microbiota diversity with dietary fiber. J. Nutr. *153*, 3156–3163. https://doi.org/10.1016/j.tjnut.2023.09.001.

80. McDonald, D., Hyde, E., Debelius, J.W., Morton, J.T., Gonzalez, A., Ackermann, G., Aksenov, A.A., Behsaz, B., Brennan, C., Chen, Y., et al. (2018). American Gut: an open platform for citizen science microbiome research. mSystems *3*, e00031-18. https://doi.org/10.1128/mSystems.00060-18.

81. Yu, D., Nguyen, S.M., Yang, Y., Xu, W., Cai, H., Wu, J., Cai, Q., Long, J., Zheng, W., and Shu, X.O. (2021). Long-term diet quality is associated with gut microbiome diversity and composition among urban Chinese adults. Am. J. Clin. Nutr. *113*, 684–694. https://doi.org/10.1093/ajcn/nqaa350.

82. Asnicar, F., Berry, S.E., Valdes, A.M., Nguyen, L.H., Piccinno, G., Drew, D.A., Leeming, E., Gibson, R., Le Roy, C., Khatib, H.A., et al. (2021).

Microbiome connections with host metabolism and habitual diet from 1,098 deeply phenotyped individuals. Nat. Med. *27*, 321–332. https://doi.org/10.1038/s41591-020-01183-8.

83. Fragiadakis, G.K., Smits, S.A., Sonnenburg, E.D., Van Treuren, W., Reid, G., Knight, R., Manjurano, A., Changalucha, J., Dominguez-Bello, M.G., Leach, J., et al. (2019). Links between environment, diet, and the hunter-gatherer microbiome. Gut Microbes *10*, 216–227. https://doi.org/10.1080/19490976.2018.1494103.

84. Philippot, L., Griffiths, B.S., and Langenheder, S. (2021). Microbial community resilience across ecosystems and multiple disturbances. Microbiol. Mol. Biol. Rev. *85*, e00026-20. https://doi.org/10.1128/MMBR.00026-20.

85. Yamamura, R., Inoue, K.Y., Nishino, K., and Yamasaki, S. (2023). Intestinal and fecal pH in human health. Front. Microbiomes *2*. https://doi.org/10.3389/frmbi.2023.1192316.

86. Natividad, J.M., Lamas, B., Pham, H.P., Michel, M.L., Rainteau, D., Bridonneau, C., da Costa, G., van Hylckama Vlieg, J., Sovran, B., Chamignon, C., et al. (2018). *Bilophila wadsworthia* aggravates high fat diet induced metabolic dysfunctions in mice. Nat. Commun. *9*, 2802. https://doi.org/10.1038/s41467-018-05249-7.

87. Wolf, P.G., Cowley, E.S., Breister, A., Matatov, S., Lucio, L., Polak, P., Ridlon, J.M., Gaskins, H.R., and Anantharaman, K. (2022). Diversity and distribution of sulfur metabolic genes in the human gut microbiome and their association with colorectal cancer. Microbiome *10*, 64. https://doi.org/10.1186/s40168-022-01242-x.

88. Hale, V.L., Chen, J., Johnson, S., Harrington, S.C., Yab, T.C., Smyrk, T.C., Nelson, H., Boardman, L.A., Druliner, B.R., Levin, T.R., et al. (2017). Shifts in the fecal microbiota associated with adenomatous polyps. Cancer Epidemiol. Biomarkers Prev. *26*, 85–94. https://doi.org/10.1158/1055-9965.EPI-16-0337.

89. Ai, D., Pan, H., Li, X., Gao, Y., Liu, G., and Xia, L.C. (2019). Identifying gut microbiota associated with colorectal cancer using a zero-inflated lognormal model. Front. Microbiol. *10*, 826. https://doi.org/10.3389/fmicb.2019.00826.

90. Johansson, M.E.V., and Hansson, G.C. (2016). Immunological aspects of intestinal mucus and mucins. Nat. Rev. Immunol. *16*, 639–649. https://doi.org/10.1038/nri.2016.88.

91. Albrich, W.C., Ghosh, T.S., Ahearn-Ford, S., Mikaeloff, F., Lunjani, N., Forde, B., Suh, N., Kleger, G.R., Pietsch, U., Frischknecht, M., et al. (2022). A high-risk gut microbiota configuration associates with fatal hyperinflammatory immune and metabolic responses to SARS-CoV-2. Gut Microbes *14*, 2073131. https://doi.org/10.1080/19490976.2022.2073131.

92. Wolff, D., Nee, S., Hickey, N.S., and Marschollek, M. (2021). Risk factors for Covid-19 severity and fatality: a structured literature review. Infection *49*, 15–28. https://doi.org/10.1007/s15010-020-01509-1.

93. Koopen, A.M., Almeida, E.L., Attaye, I., Witjes, J.J., Rampanelli, E., Majait, S., Kemper, M., Levels, J.H.M., Schimmel, A.W.M., Herrema, H., et al. (2021). Effect of fecal microbiota transplantation combined with Mediterranean diet on insulin sensitivity in subjects with metabolic syndrome. Front. Microbiol. *12*, 662159. https://doi.org/10.3389/fmicb.2021.662159.

94. Shai, I., Schwarzfuchs, D., Henkin, Y., Shahar, D.R., Witkow, S., Greenberg, I., Golan, R., Fraser, D., Bolotin, A., Vardi, H., et al. (2008). Weight loss with a low-carbohydrate, Mediterranean, or low-fat diet. N. Engl. J. Med. *359*, 229–241. https://doi.org/10.1056/NEJMoa0708681.

95. Eichelmann, F., Schwingshackl, L., Fedirko, V., and Aleksandrova, K. (2016). Effect of plant-based diets on obesity-related inflammatory profiles: a systematic review and meta-analysis of intervention trials. Obes. Rev. *17*, 1067–1079. https://doi.org/10.1111/obr.12439.

96. Termannsen, A.D., Clemmensen, K.K.B., Thomsen, J.M., Nørgaard, O., Díaz, L.J., Torekov, S.S., Quist, J.S., and Faerch, K. (2022). Effects of vegan diets on cardiometabolic health: a systematic review and meta-

analysis of randomized controlled trials. Obes. Rev. *23*, e13462. https://doi.org/10.1111/obr.13462.

97. Abildgaard, A., Elfving, B., Hokland, M., Wegener, G., and Lund, S. (2018). The microbial metabolite indole-3-propionic acid improves glucose metabolism in rats, but does not affect behaviour. Arch. Physiol. Biochem. *124*, 306–312. https://doi.org/10.1080/13813455.2017.1398262.

98. de Mello, V.D., Paananen, J., Lindström, J., Lankinen, M.A., Shi, L., Kuusisto, J., Pihlajamäki, J., Auriola, S., Lehtonen, M., Rolandsson, O., et al. (2017). Indolepropionic acid and novel lipid metabolites are associated with a lower risk of type 2 diabetes in the Finnish Diabetes Prevention Study. Sci. Rep. *7*, 46337. https://doi.org/10.1038/srep46337.

99. Cason, C.A., Dolan, K.T., Sharma, G., Tao, M., Kulkarni, R., Helenowski, I.B., Doane, B.M., Avram, M.J., McDermott, M.M., Chang, E.B., et al. (2018). Plasma microbiome-modulated indole- and phenyl-derived metabolites associate with advanced atherosclerosis and postoperative outcomes. J. Vasc. Surg. *68*, 1552–1562.e7. https://doi.org/10.1016/j.jvs.2017.09.029.

100. Jeong, Y.J., Jung, M.G., Son, Y., Jang, J.H., Lee, Y.J., Kim, S.H., Ko, Y.G., Lee, Y.S., and Lee, H.J. (2015). Coniferyl aldehyde attenuates radiation enteropathy by inhibiting cell death and promoting endothelial cell function. PLoS One *10*, e0128552. https://doi.org/10.1371/journal.pone.0128552.

101. Karamać, M., Koleva, L., Kancheva, V.D., and Amarowicz, R. (2017). The structure-antioxidant activity relationship of ferulates. Molecules *22*, 527. https://doi.org/10.3390/molecules22040527.

102. Natarajan, S.K., Muthukrishnan, E., Khalimonchuk, O., Mott, J.L., and Becker, D.F. (2017). Evidence for pipecolate oxidase in mediating protection against hydrogen peroxide stress. J. Cell. Biochem. *118*, 1678–1688. https://doi.org/10.1002/jcb.25825.

103. Warden, C., and Brantley, M.A., Jr. (2021). Glycine-conjugated bile acids protect RPE tight junctions against oxidative stress and inhibit choroidal endothelial cell angiogenesis in vitro. Biomolecules *11*, 626. https://doi.org/10.3390/biom11050626.

104. Louis, P., Hold, G.L., and Flint, H.J. (2014). The gut microbiota, bacterial metabolites and colorectal cancer. Nat. Rev. Microbiol. *12*, 661–672. https://doi.org/10.1038/nrmicro3344.

105. Suzuki, T., and Kamiya, H. (2017). Mutations induced by 8-hydroxyguanine (8-oxo-7,8-dihydroguanine), a representative oxidized base, in mammalian cells. Genes Environ. *39*, 2. https://doi.org/10.1186/s41021-016-0051-y.

106. Manach, C., Milenkovic, D., Van de Wiele, T., Rodriguez-Mateos, A., de Roos, B., Garcia-Conesa, M.T., Landberg, R., Gibney, E.R., Heinonen, M., Tomás-Barberan, F., et al. (2017). Addressing the inter-individual variation in response to consumption of plant food bioactives: towards a better understanding of their role in healthy aging and cardiometabolic risk reduction. Mol. Nutr. Food Res. *61*, 1600557. https://doi.org/10.1002/mnfr.201600557.

107. Nguyen, N.K., Deehan, E.C., Zhang, Z., Jin, M., Baskota, N., Perez-Muñoz, M.E., Cole, J., Tuncil, Y.E., Seethaler, B., Wang, T., et al. (2020). Gut microbiota modulation with long-chain corn bran arabinoxylan in adults with overweight and obesity is linked to an individualized temporal increase in fecal propionate. Microbiome *8*, 118. https://doi.org/10.1186/s40168-020-00887-w.

108. Rodgers, G.P., and Collins, F.S. (2020). Precision nutrition-the answer to "what to eat to stay healthy". JAMA *324*, 735–736. https://doi.org/10.1001/jama.2020.13601.

109. Kolodziejczyk, A.A., Zheng, D., and Elinav, E. (2019). Diet-microbiota interactions and personalized nutrition. Nat. Rev. Microbiol. *17*, 742–753. https://doi.org/10.1038/s41579-019-0256-8.

110. McBurney, M.I., Davis, C., Fraser, C.M., Schneeman, B.O., Huttenhower, C., Verbeke, K., Walter, J., and Latulippe, M.E. (2019). Establishing what constitutes a healthy human gut microbiome: state of the science,

Cell
Article

CellPress
OPEN ACCESS

regulatory considerations, and future directions. J. Nutr. *149*, 1882–1895. https://doi.org/10.1093/jn/nxz154.

111. Eaton, S.B., and Konner, M. (1985). Paleolithic nutrition — a consideration of its nature and current implications. N. Engl. J. Med. *312*, 283–289. https://doi.org/10.1056/NEJM198501313120505.

112. Johnson, A.J., Zheng, J.J., Kang, J.W., Saboe, A., Knights, D., and Zivkovic, A.M. (2020). A guide to diet-microbiome study design. Front. Nutr. *7*, 79. https://doi.org/10.3389/fnut.2020.00079.

113. Li, F., Liu, J., Maldonado-Gómez, M.X., Frese, S.A., Gänzle, M.G., and Walter, J. (2024). Highly accurate and sensitive absolute quantification of bacterial strains in human fecal samples. Microbiome *12*, 168. https://doi.org/10.1186/s40168-024-01881-2.

114. Bolyen, E., Rideout, J.R., Dillon, M.R., Bokulich, N.A., Abnet, C.C., Al-Ghalith, G.A., Alexander, H., Alm, E.J., Arumugam, M., Asnicar, F., et al. (2019). Reproducible, interactive, scalable and extensible microbiome data science using QIIME 2. Nat. Biotechnol. *37*, 852–857. https://doi.org/10.1038/s41587-019-0209-9.

115. Chen, I.A., Chu, K., Palaniappan, K., Pillay, M., Ratner, A., Huang, J., Huntemann, M., Varghese, N., White, J.R., Seshadri, R., et al. (2019). IMG/M v.5.0: an integrated data management and comparative analysis system for microbial genomes and microbiomes. Nucleic Acids Res. *47*, D666–D677. https://doi.org/10.1093/nar/gky901.

116. Bolger, A.M., Lohse, M., and Usadel, B. (2014). Trimmomatic: a flexible trimmer for Illumina sequence data. Bioinformatics *30*, 2114–2120. https://doi.org/10.1093/bioinformatics/btu170.

117. Langmead, B., and Salzberg, S.L. (2012). Fast gapped-read alignment with Bowtie 2. Nat. Methods *9*, 357–359. https://doi.org/10.1038/nmeth.1923.

118. Beghini, F., McIver, L.J., Blanco-Míguez, A., Dubois, L., Asnicar, F., Maharjan, S., Mailyan, A., Manghi, P., Scholz, M., Thomas, A.M., et al. (2021). Integrating taxonomic, functional, and strain-level profiling of diverse microbial communities with bioBakery 3. eLife *10*, e65088. https://doi.org/10.7554/eLife.65088.

119. Buchfink, B., Reuter, K., and Drost, H.G. (2021). Sensitive protein alignments at tree-of-life scale using DIAMOND. Nat. Methods *18*, 366–368. https://doi.org/10.1038/s41592-021-01101-x.

120. Smith, D.P. (2021). rbiom: Read/Write, Transform, and Summarize 'BIOM' Data. https://cran.r-project.org/web/packages/rbiom/rbiom.pdf.

121. van Buuren, S., and Groothuis-Oudshoorn, K. (2011). mice: Multivariate Imputation by Chained Equations in R. J. Stat. Softw. *45*, 1–67. https://doi.org/10.18637/jss.v045.i03.

122. Kassambara, A., and Mundt, F. (2020). factoextra: Extract and Visualize the Results of Multivariate Data Analyses. https://CRAN.R-project.org/package=factoextra.

123. Husson, F., Josse, J., Le, S., and Mazet, J. (2023). FactoMineR: Multivariate Exploratory Data Analysis and Data Mining. https://cran.r-project.org/web/packages/FactoMineR/FactoMineR.pdf.

124. Oksanen, J., Blanchet, F.G., Kindt, R., Legendre, P., Minchin, P., O'Hara, B., Simpson, G., Solymos, P., Stevens, H., and Wagner, H. (2015). vegan: Community Ecology Package. https://cran.r-project.org/web/packages/vegan/vegan.pdf.

125. Pinheiro, J., Bates, D., DebRoy, S., Sarkar, D., and Team, R.C. (2022). nlme: Linear and nonlinear mixed effects models. http://CRAN.R-project.org/package=nlme.

126. Barton, K. (2024). MuMIn: Multi-Model Inference. https://cran.r-project.org/web/packages/MuMIn/MuMIn.pdf.

127. Halekoh, U., Højsgaard, S., and Yan, J. (2006). The R package geepack for generalized estimating equations. J. Stat. Softw. *15*, 1–11. https://doi.org/10.18637/jss.v015.i02.

128. Lenth, R., Singmann, H., Love, J., Buerkner, P., and Herve, M. (2022). emmeans: Estimated marginal means, aka least-squares means. https://cran.r-project.org/web/packages/emmeans/emmeans.pdf.

129. Beigy, M. (2019). cvcqv: Coefficient of Variation (CV) with Confidence Intervals (CI) (GitHub). https://github.com/MaaniBeigy/cvcqv.

130. Kuhn, M. (2022). caret: Classification and Regression Training. https://cran.r-project.org/web/packages/caret/caret.pdf.

131. Fox, J., and Weisberg, S. (2019). car: An R Companion to Applied Regression, Third Edition (Sage).

132. Mallick, H., Rahnavard, A., McIver, L.J., Ma, S., Zhang, Y., Nguyen, L.H., Tickle, T.L., Weingart, G., Ren, B., Schwager, E.H., et al. (2021). Multivariable association discovery in population-scale meta-omics studies. PLoS Comput. Biol. *17*, e1009442. https://doi.org/10.1371/journal.pcbi.1009442.

133. Chong, J., Wishart, D.S., and Xia, J. (2019). Using MetaboAnalyst 4.0 for comprehensive and integrative metabolomics data analysis. Curr. Protoc. Bioinformatics *68*, e86. https://doi.org/10.1002/cpbi.86.

134. Duar, R.M., Frese, S.A., Lin, X.B., Fernando, S.C., Burkey, T.E., Tasseva, G., Peterson, D.A., Blom, J., Wenzel, C.Q., Szymanski, C.M., et al. (2017). Experimental evaluation of host adaptation of *Lactobacillus reuteri* to different vertebrate species. Appl. Environ. Microbiol. *83*, e00132-17. https://doi.org/10.1128/AEM.00132-17.

135. Harris, P.A., Taylor, R., Thielke, R., Payne, J., Gonzalez, N., and Conde, J.G. (2009). Research electronic data capture (REDCap) — A metadata-driven methodology and workflow process for providing translational research informatics support. J. Biomed. Inform. *42*, 377–381. https://doi.org/10.1016/j.jbi.2008.08.010.

136. Deehan, E.C., Yang, C., Perez-Muñoz, M.E., Nguyen, N.K., Cheng, C.C., Triador, L., Zhang, Z., Bakal, J.A., and Walter, J. (2020). Precision microbiome modulation with discrete dietary fiber structures directs short-chain fatty acid production. Cell Host Microbe *27*, 389–404.e6. https://doi.org/10.1016/j.chom.2020.01.006.

137. Mifflin, M.D., St Jeor, S.T., Hill, L.A., Scott, B.J., Daugherty, S.A., and Koh, Y.O. (1990). A new predictive equation for resting energy expenditure in healthy individuals. Am. J. Clin. Nutr. *51*, 241–247. https://doi.org/10.1093/ajcn/51.2.241.

138. Mäder, U., Martin, B.W., Schutz, Y., and Marti, B. (2006). Validity of four short physical activity questionnaires in middle-aged persons. Med. Sci. Sports Exerc. *38*, 1255–1266. https://doi.org/10.1249/01.mss.0000227310.18902.28.

139. Cohen, S. (1988). Perceived stress in a probability sample of the United States. In The Social Psychology of Health (Sage Publications, Inc), pp. 31–67.

140. McNair, D.M., Lon, M., and Droppelman, L.F. (1971). Manual for the Profile of Mood States (Educational and Industrial Testing Service), pp. 1–27.

141. Jessri, M., Ng, A.P., and L'Abbé, M.R. (2017). Adapting the Healthy Eating Index 2010 for the Canadian population: Evidence from the Canadian National Nutrition Survey. Nutrients *9*, 910. https://doi.org/10.3390/nu9080910.

142. Blanco-Míguez, A., Beghini, F., Cumbo, F., McIver, L.J., Thompson, K.N., Zolfo, M., Manghi, P., Dubois, L., Huang, K.D., Thomas, A.M., et al. (2023). Extending and improving metagenomic taxonomic profiling with uncharacterized species using MetaPhlAn 4. Nat. Biotechnol. *41*, 1633–1644. https://doi.org/10.1038/s41587-023-01688-w.

143. Zhang, H., Yohe, T., Huang, L., Entwistle, S., Wu, P., Yang, Z., Busk, P.K., Xu, Y., and Yin, Y. (2018). dbCAN2: a meta server for automated carbohydrate-active enzyme annotation. Nucleic Acids Res. *46*, W95–W101. https://doi.org/10.1093/nar/gky418.

144. Jin, M., Kalainy, S., Baskota, N., Chiang, D., Deehan, E.C., McDougall, C., Tandon, P., Martínez, I., Cervera, C., Walter, J., et al. (2019). Faecal microbiota from patients with cirrhosis has a low capacity to ferment non-digestible carbohydrates into short-chain fatty acids. Liver Int. *39*, 1437–1447. https://doi.org/10.1111/liv.14106.

145. Zhao, S., and Li, L. (2020). Chemical derivatization in LC-MS-based metabolomics study. TrAC Trends Anal. Chem. *131*, 115988. https://doi.org/10.1016/j.trac.2020.115988.

146. Knopfholz, J., Disserol, C.C.D., Pierin, A.J., Schirr, F.L., Streisky, L., Takito, L.L., Massucheto Ledesma, P., Faria-Neto, J.R., Olandoski, M., da Cunha, C.L.P., et al. (2014). Validation of the friedewald formula in patients with metabolic syndrome. Cholesterol *2014*, 261878. https://doi.org/10.1155/2014/261878.

147. Matthews, D.R., Hosker, J.P., Rudenski, A.S., Naylor, B.A., Treacher, D.F., and Turner, R.C. (1985). Homeostasis model assessment: insulin resistance and beta-cell function from fasting plasma glucose and insulin concentrations in man. Diabetologia *28*, 412–419. https://doi.org/10.1007/BF00280883.

148. Katz, A., Nambi, S.S., Mather, K., Baron, A.D., Follmann, D.A., Sullivan, G., and Quon, M.J. (2000). Quantitative insulin sensitivity check index: a simple, accurate method for assessing insulin sensitivity in humans. J. Clin. Endocrinol. Metab. *85*, 2402–2410. https://doi.org/10.1210/jcem.85.7.6661.

149. Tannock, G.W., Munro, K., Harmsen, H.J., Welling, G.W., Smart, J., and Gopal, P.K. (2000). Analysis of the fecal microflora of human subjects consuming a probiotic product containing *Lactobacillus rhamnosus* DR20. Appl. Environ. Microbiol. *66*, 2578–2588. https://doi.org/10.1128/aem.66.6.2578-2588.2000.

150. Depommier, C., Everard, A., Druart, C., Plovier, H., Van Hul, M., Vieira-Silva, S., Falony, G., Raes, J., Maiter, D., Delzenne, N.M., et al. (2019). Supplementation with *Akkermansia muciniphila* in overweight and obese human volunteers: a proof-of-concept exploratory study. Nat. Med. *25*, 1096–1103. https://doi.org/10.1038/s41591-019-0495-2.

151. Holscher, H.D., Bauer, L.L., Gourineni, V., Pelkman, C.L., Fahey, G.C., Jr., and Swanson, K.S. (2015). Agave inulin supplementation affects the fecal microbiota of healthy adults participating in a randomized, double-blind, placebo-controlled, crossover trial. J. Nutr. *145*, 2025–2032. https://doi.org/10.3945/jn.115.217331.

152. Wang, D.D., Nguyen, L.H., Li, Y., Yan, Y., Ma, W., Rinott, E., Ivey, K.L., Shai, I., Willett, W.C., Hu, F.B., et al. (2021). The gut microbiome modulates the protective association between a Mediterranean diet and cardiometabolic disease risk. Nat. Med. *27*, 333–343. https://doi.org/10.1038/s41591-020-01223-3.

153. Berrar, D. (2024). Cross-validation. In Encyclopedia of Bioinformatics and Computational Biology, Second Edition (Elsevier), pp. 1–13.

STAR★METHODS

KEY RESOURCES TABLE

REAGENT or RESOURCE	SOURCE	IDENTIFIER
Bacterial and virus strains		
Limosilactobacillus reuteri PB-W1	Archer et al.[37]	PMID: 38047281
Limosilactobacillus reuteri DSM 20016[T]	Lerche and Reuter[38]	N/A
Chemicals, peptides, and recombinant proteins		
DmPA-labeling kit	Nova Medical Testing Inc.	NMT-4167-KT
Dansyl-labeling kit	Nova Medical Testing Inc.	NMT-4101-KT
Critical commercial assays		
QIAamp Fast DNA Stool Mini Kit	Qiagen	Cat# 51604
U-PLEX Human Insulin Assay	MesoScale Discovery	Cat# K1516HK-1
V-PLEX Human CRP Kit	MesoScale Discovery	Cat# K151STD-2
IDK® Calprotectin (MRP 8/14) (Stool) ELISA	Immundiagnostik AG	Cat# K6927
Lipopolysacharid bindendes Protein (LBP) ELISA	Immundiagnostik AG	Cat# KR6813
IDK® Zonulin (Stool) ELISA	Immundiagnostik AG	Cat# K5600
Deposited data		
Original data of 16S rRNA gene amplicon sequencing and whole metagenome sequencing	This paper	https://www.ncbi.nlm.nih.gov/bioproject/PRJNA1000186
Oligonucleotides		
Primer pair: 784F (Forward: 5′-RGGATTAGATACCC-3′); 1064R (Reverse: 5′-CGACRRCCATGCANCACCT-3′)	Martínez et al.[13]	PMID: 25892234
Strain- and lineage-specific qPCR primers for *L. reuteri* PB-W1 and DSM 20016[T]	Li et al.[113]	PMID: 39244633
Software and algorithms		
QIIME2 (v2020.11)	Bolyen et al.[114]	https://qiime2.org/
IMG/MER	Chen et al.[115]	https://img.jgi.doe.gov/
NCBI Web BLAST	N/A	https://blast.ncbi.nlm.nih.gov/Blast.cgi
FastQC (v0.11.8)	N/A	https://github.com/s-andrews/FastQC
Trimmomatic (v0.39)	Bolger et al.[116]	http://www.usadellab.org/cms/?page=trimmomatic
Bowtie2 (v2.3.5.1)	Langmead and Salzberg[117]	https://bowtie-bio.sourceforge.net/bowtie2/index.shtml
MetaPhlAn 4.0	Blanco-Míguez et al.[24]	https://huttenhower.sph.harvard.edu/metaphlan/
HUMAanN 3.0	Beghini et al.[118]	https://huttenhower.sph.harvard.edu/humann/
DIAMOND (v0.9.32)	Buchfink et al.[119]	https://github.com/bbuchfink/diamond
R (v4.2.1)	R Core Team	https://cran.r-project.org/
rbiom (v.1.0.3)	Smith[120]	https://cmmr.github.io/rbiom/index.html
mice (v4.2.1)	van Buuren and Groothuis-Oudshoorn[121]	https://github.com/amices/mice
Factoextra (v1.0.7)	Kassambara and Mundt[122]	https://rpkgs.datanovia.com/factoextra/index.html
FactoMineR (v2.8)	Husson et al.[123]	http://factominer.free.fr/
vegan (v2.6.4)	Oksanen et al.[124]	https://github.com/vegandevs/vegan
nlme (v3.1.157)	Pinheiro et al.[125]	https://cran.r-project.org/web/packages/nlme/index.html

(Continued on next page)

Continued

REAGENT or RESOURCE	SOURCE	IDENTIFIER
MuMIn (v1.48.4)	Barton[126]	https://cran.r-project.org/web/packages/MuMIn/index.html
geepack (v1.3.9)	Halekoh et al.[127]	https://cran.r-project.org/web/packages/geepack/index.html
emmeans (v1.8.3)	Lenth et al.[128]	https://github.com/rvlenth/emmeans
cvcqv (v1.0.0)	Beigy[129]	https://github.com/MaaniBeigy/cvcqv
caret (v6.0.93)	Kuhn[130]	https://topepo.github.io/caret/
car (v3.1.1)	Fox and Weisberg[131]	https://cran.r-project.org/web/packages/car/index.html
MaAsLin2	Mallick et al.[132]	https://github.com/biobakery/Maaslin2
DataAnalysis (v4.4)	Bruker Corporation	https://www.bruker.com/en/products-and-solutions/mass-spectrometry/ms-software.html
IsoMS Pro (v1.2.7)	Nova Medical Testing Inc.	NMT-5101-SW
MetaboAnalyst 4.0	Chong et al.[133]	https://www.metaboanalyst.ca/
Prism (v10.2.2)	GraphPad	https://www.graphpad.com/
Other		
Globe® 10DE Maltodextrin, Non-GMO	Ingredion Canada Corporation, Mississauga, Ontario, Canada	https://www.ingredion.com/na/en-us.html
Food-grade media for *L. reuteri*	This paper	Table S12 of this paper
L. reuteri isolation media (LRIM)	Duar et al.[134]	PMID: 28389535
100% Complete Multi For Adults	Jamieson	https://www.jamiesonvitamins.com/

EXPERIMENTAL MODEL AND STUDY PARTICIPANT DETAILS

Recruitment and selection of participants

This proof-of-concept study was approved by the University of Alberta's Health Research Ethics Board (Pro00077565) and Health Canada (file number 237696) and was prospectively registered on ClinicalTrials.gov (NCT03501082). The study adhered to all relevant institutional and national regulatory body requirements. Safety monitoring was independently conducted by the University of Alberta's Quality Management in Clinical Research Department. Study data was collected and managed using REDCap electronic data capture tools hosted and supported by the Women and Children's Health Research Institute at the University of Alberta.[135]

Healthy individuals aged 18-45 years with BMI 20.0-29.9 kg/m² were recruited between January 2019 and January 2020. Exclusion criteria were: history of long-term gastrointestinal disorders (*e.g.,* inflammatory bowel diseases, Celiac disease), diabetes, cardiovascular disease, cancer, or other inflammatory conditions; chronic use of laxatives, anti-diabetic, anti-hypertensive, lipid-lowering, or anti-inflammatory medications; positive pregnancy test (as determined by urine sample at screening visit) or self-reported lactating or menopausal women; bowel movement frequency <1 per day; >7 drinks of alcohol per week, tobacco (smoking or chewing), or use of illicit drugs or marijuana; vigorous exercise of >5 hours per week; allergy or intolerance to any foods or ingredients of the restore diet; vegetarian or vegan; antibiotic use ≤3 months prior to enrollment; use of probiotic, prebiotic, fiber, omega-3 fatty acid, or herbal supplements (if subjects used any of these supplements but were otherwise eligible, they could elect to undergo a four-week washout period before participating in the study); presence of *L. reuteri* above 10^4 cells/gram of feces (assessed only in individuals who met all of the above criteria; $n = 42$). As requested by the Health Research Ethics Board of the University of Alberta, information on participants' ancestry, race, or ethnicity was not collected as these factors were not pertinent to the objectives of this study.

Specimen collection

Fecal samples were collected on Days 0, 4, 6, 8, 12, 16, 21, 42, 46, 48, 50, 54, 58, 63, and 84 (*i.e.,* Days 0, 4, 6, 8, 12, 16, and 21 of each diet period, as well as the last day of the last washout; Figure 1A). Participants were provided stool collection kits consisting of a stool specimen container (Fisher, Canada) and an airtight plastic bag. Once received, within four hours of collection, stool samples were processed in an anaerobic environment (5% CO_2, 5% H_2, 90% N_2). Raw fecal material was aliquoted for downstream analyses, and was also diluted in sterile 1:5 phosphoric acid (5%) for SCFA quantification as well as sterile 1:10 phosphate buffered saline (PBS) with 10% glycerol for the quantitative culture of *L. reuteri*; all aliquots were immediately stored at -80°C after processing.[136] Fecal samples were stored without undergoing DNA extraction, SCFA quantification, quantitative culture of *L. reuteri*, or other measurements until the completion of the human trial to avoid any potential batch effects.

Cell
Article

On Days 0 and 21 of each diet period (*i.e.*, Days 0, 21, 42 and 63), after participants fasted for 12 hours overnight, blood was collected via venipuncture using K_2-ethylenediaminetetraacetic acid-coated and lithium heparin tubes. Whole blood was sent within 90 minutes of collection to Alberta Precision Laboratories (Edmonton, AB, Canada) for downstream analyses. Blood for plasma was centrifuged, aliquoted, and stored immediately at -80°C for downstream analyses. Additional blood samples were collected for plasma metabolomics (detailed below) on Day 8 of each diet period (4 days post-supplementation of *L. reuteri*; Days 8 and 50).

METHOD DETAILS

Intervention
We designed a randomized controlled feeding trial (Figure 1A) to allow for the simultaneous assessment of the effects of: 1) a single dose of *L. reuteri* supplementation and if it could be re-established in the gut microbiome, 2) the restore diet, independent of *L. reuteri*, and 3) potential interactions between *L. reuteri* and diet. Given the extreme nature and stark contrast of the restore diet (trademarked as NiMe™ diet by A.M.A. and J.W.) compared to typical Canadian diets, we chose to provide it in a strictly controlled and standardized fashion. Using a crossover design, participants were randomized to either the restore diet or remained on their usual diet for three weeks and then, after a three-week washout, switched to the other diet period for three weeks. Using a parallel-arm design, participants were further randomized to either the *L. reuteri* strain derived from rural Papua New Guinea (PB-W1™; trademark of PrecisionBiotics Group Ltd.), the type-strain (DSM 20016^T), or a placebo (maltodextrin). On the fourth day of each diet period, participants received a single dose of either *L. reuteri* or placebo. The study concluded with a final three-week washout to assess potential long-term persistence of *L. reuteri*.

The random allocation sequence was computer-generated and concealed by a researcher not involved in subject allocation. Random allocation considered both designs (*i.e.*, six groups in total): participants were assigned to a starting diet period (restore or usual) and inoculum (either *L. reuteri* strain or placebo). If a participant withdrew from the study, an additional subject was recruited to replace them and were assigned using the same random allocation methods. The randomization scheme was not revealed to participants or study investigators/staff, and double-blinding was maintained for *L. reuteri* assignment until after data analysis was completed. Due to the nature of the dietary intervention, blinding to diet assignment was not possible.

L. reuteri inocula and placebo preparation
L. reuteri inocula were prepared at the food-grade laboratory of the Department of Agricultural, Food & Nutritional Science at the University of Alberta, following our Standard Operating Procedure developed previously that assured highly standardized viable *L. reuteri* cell counts.[134] Briefly, *L. reuteri* strains were cultured overnight twice in MRS broth, washed twice using sterile mQ H_2O, and then transferred to sterile food-grade media (see Table S12 for recipe) for one overnight culture and one 16 h culture to generate cultures for the inocula. Cells were harvested and suspended in bottled spring water immediately prior to participant consumption, and samples were plated quantitatively on MRS agar for quantification of *L. reuteri* and on BHI agar to check for contamination. Maltodextrin placebo (2 g of GLOBE® 10DE Maltodextrin, Non-GMO, Ingredion, IL, USA) was also dissolved in bottled spring water.

L. reuteri inocula and placebo were prepared in opaque cups fitted with lids by a researcher not involved in subject allocation or data analysis. The cups were labelled 'A', 'B', or 'C' to ensure double-blinding was maintained. Based on the culture results before consumption, cell numbers of PB-W1 and DSM 20016^T provided to the participants throughout the human trial were 10.44 ± 0.02 and 10.23 ± 0.04 Log_{10} of viable cells (mean ± SEM), respectively.

Restore diet preparation and adherence
All meals and snacks of the restore diet were prepared in the metabolic kitchen of the Human Nutrition Research Unit (Edmonton, AB, Canada), with ingredients and foods weighed to the nearest 0.1 g. All participants were provided identical meals and snacks during the restore diet period. Caloric requirements were calculated based on the Mifflin St. Jeor predictive equation[137] multiplied by an appropriate physical activity coefficient, and participants were fed to the nearest 100 kcal of their requirements in an attempt to maintain body weight. Drinks were not provided as part of the restore diet, but rather caloric assignments were adjusted based on self-reported daily calorie-containing beverage consumption at the screening visit. Participants were encouraged to only consume the provided study foods but were allowed one daily snack of approximately 100 kcal if all study foods were eaten. Participants picked up their study foods every three to five days and were instructed to bring back all containers so that study investigators could weigh any remaining food to assess adherence. If participants consumed less than 80% of the provided study foods during the intervention, they were removed from the study (*n* = 2). Of the participants who completed the study, adherence to the restore diet protocol was $94.4 \pm 6.4\%$ (mean ± SD). Finally, to account for potential differences in micronutrient intake between the restore diet and participants' usual diets, they were provided a multivitamin (100% Complete Multi For Adults, Jamieson, Canada) and instructed to consume it daily throughout the twelve-week study.

Participant-reported outcomes
A gastrointestinal symptom questionnaire was used to determine the intensity of stomach aches, abdominal tension, and flatulence using a 5-point hedonic scale with no symptoms (0) and severe symptoms (4) on either end.[136] On the same questionnaire, markers of stool transit time were assessed[136]: stool consistency was assessed using the Bristol Stool Scale, with "hard or fragmented" (0) and

"entirely liquid" (6) on either end, and "sausage or snake-shaped, smooth, and soft" in the center (3); bowel movement frequency was assessed using a 5-point hedonic scale, with "every third day or less often" (0) and "three times a day or more often" (4) on either end and "once a day" in the center (2). The questionnaire was administered weekly in both diet periods (*i.e.* at baseline, Week 1, Week 2, and Week 3).

Physical activity levels were assessed using the validated International Physical Activity Questionnaire.[138] A validated perceived stress questionnaire was used to assess stress experienced within the previous month.[139] To assess mood states, the validated Profile of Mood States questionnaire was used.[140] These questionnaires were administered on Days 0, 21, 42, and 63.

To assess participants' usual dietary intake, the Canadian version of the Automated Self-Administered 24-hour Dietary Assessment Tool (ASA24-Canada 2016) was used to administer 24-hour dietary recalls (National Cancer Institute, MD, USA). Participants completed two 24-hour dietary recalls (one on a weekday and another on a weekend day) at baseline and Week 3 of the usual diet period, as well as at baseline of the restore diet period. This was to confirm no significant dietary changes were made during the usual diet period, and also to compare participants' usual dietary intake to the composition of the restore diet. Pooled values for the usual diet were calculated as the averages of all of the dietary recalls (*i.e.,* baseline and week 3 of the usual diet, baseline of the restore diet). These values were used to test for differences between the two diet periods (i.e., pooled usual diet vs Week 3 restore diet). An HEI score adapted to Canada's Food Guide (2007) was also calculated based on the procedure outlined in Jessri et al.[141] to quantify baseline diet quality.

DNA extraction and sequencing

Microbial DNA was extracted from fecal samples using a modified protocol based on QIAamp Fast DNA Stool Mini Kit as described previously.[113] Briefly, 0.1 g of fecal material was washed three times with ice-cold PBS buffer. Then, 100 μl of lysis buffer was added to cell pellets and the mixtures were incubated at 37°C for 30 min. Samples were then mixed with 1 mL of buffer InhibitEX, and homogenized through vortexing and bead-beating. The remaining steps of the manufacturer's protocol for DNA isolation were followed. The V5-V6 hypervariable region of bacterial 16S rRNA gene was chosen as it provides greater resolution not only for *bifidobacteria* and *lactobacilli* but also the entire microbial community of human fecal samples. This targeted region was amplified using the primer pair 784F (5′-RGGATTAGATACCC-3′) and 1064R (5′-CGACRRCCATGCANCACCT-3′). The amplicons were paired-end sequenced (2 x 300 bp) using Illumina MiSeq PE300 at the University of Minnesota Genomics Center (Minneapolis, MN, USA). To ensure sufficient sequencing depth and prevent batch effects, amplicons from all samples were pooled together, and the same pool was repeatedly sequenced using two sequencing lanes; following this, data generated from the two lanes were integrated into a singular dataset. DNA extracted from samples of Days 0, 8, 42, and 50 (*i.e.,* Days 0 and 8 of each diet period) were also subjected to WMS. WMS libraries of each DNA sample were generated using the NEBNext Ultra II DNA Library Prep Kit for Illumina (New England Biolabs, Whitby, ON, Canada). The libraries were pooled and sequenced using NovaSeq 6000 S4 PE150 platform (2 x 150 bp paired-end sequencing) at the Génome Québec Innovation Centre (Montréal, QC, Canada). The WMS data for all samples were generated using a single lane concurrently to avoid batch effects.

Bioinformatics analysis

16S rRNA gene amplicon sequencing data were processed using QIIME2.[114] Briefly, the plugin *cutadapt trim-paired* was used to trim the residual primers and adapters. The *dada2 denoise-paired* pipeline was applied to truncate low-quality bases, join paired-end reads, remove chimeras, generate an ASV table, and obtain representative sequences of ASVs. The hypervariable V5-V6 region of 16S sequences of the SILVA database (version 138) was extracted using the *feature-classifier extract-reads* function, then used to train the Naive Bayes classifier using *feature-classifier fit-classifier-naive-bayes* that assigned the taxonomy of the sequences. The representative sequence of each ASV was further assigned taxonomy at the species-level, if possible, using the IMG/MER system[115] and/or the NCBI Web BLAST (https://blast.ncbi.nlm.nih.gov/Blast.cgi). While the NCBI Taxonomy database has appended a list of 42 names of prokaryote phyla (*e.g.*, *Bacillota* [formerly *Firmicutes*], *Bacteroidota* [formerly *Bacteroidetes*], *Actinomycetota* [formerly *Actinobacteria*], and *Pseudomonadota* [formerly *Proteobacteria*]), the majority of the publications referenced in this study adhere to the former nomenclature for these microorganisms. Therefore, we have maintained the use of their previous nomenclature in the current study.

Singleton and doubleton ASVs were removed for downstream analyses. To estimate alpha-diversity indices (*i.e.*, observed features, Pielou's evenness, and Shannon index) and the Bray-Curtis dissimilarity matrix among samples, the number of bacterial sequences was rarefied to 4,200 reads per sample, and samples with read numbers <4,200 were removed for further analyses. Alpha- and beta-diversity indices were then calculated for ASVs with the function *diversity core-metrics-phylogenetic*. Microbial taxa with relative abundance >0.1% in at least 20% of the samples (*i.e.*, 6, 9, 19, 34, 74, 124, and 205 at the phylum, class, order, family, genus, species, and ASV level, respectively) were used for downstream analyses.

The quality of WMS dataset was examined using FastQC (https://github.com/s-andrews/FastQC), the residual adapter sequences were filtered, and the bases with average quality scores <20 were trimmed using Trimmomatic v0.39.[116] Trimmed reads with lengths lower than 100 bp were then discarded for downstream analyses. Sequences of bacteriophage phiX174 (Illumina spike-in of WMS libraries) and human DNA reads were eliminated through mapping WMS dataset to phiX174 genome reference (NCBI accession: NC_001422.1) and human genome reference GRCh38 using Bowtie2 (version 2.3.5.1),[117] with -N 1 and

otherwise default settings. The compositional profile of WMS dataset was generated using MetaPhlAn 4.0 with default parameters.[142] The functional profile of gut microbiome (*i.e.,* pathways and ECs) was predicted using HUMAanN 3.0 with default settings.[118] To identify CAZymes, DIAMOND (version 0.9.32.133)[119] was used to align post-QC WMS reads to the dbCAN2 database (version 9.0)[143] with an E value <1e-10 as the cut-off. For each mapped read, the best hit with the lowest E-value was used for downstream analyses. CAZymes related to the utilization of various carbohydrate categories were grouped as suggested previously[26] with further updates by adding more CAZyme families to each category (Table S13). Bioinformatic analyses for the WMS data were conducted on the computing platform provided by the Digital Research Alliance of Canada. Singleton and doubleton microbial features were removed for downstream analyses. Compositional and functional features with relative abundance >0.005% in at least 20% of the samples were included in downstream analyses. The alpha-diversity indices of WMS features were computed using the plugin *diversity alpha* of QIIME2. The Bray-Curtis dissimilarity matrix of samples based on WMS features (*i.e.,* SGBs, pathways, CAZymes, and ECs) was generated using R package rbiom[120] and PCoA was then visualized via the plugin *diversity pcoa* and *emperor plot* of QIIME2.

Fecal SCFAs, BCFAs, pH, and dry mass percentage

SCFAs and BCFAs were quantified using gas chromatography at the Agricultural, Food & Nutritional Science Chromatography Facility (University of Alberta, Edmonton, Canada) in fecal samples from Days 0, 8, 21, 42, 50, and 63 (*i.e.,* Days 0, 8, and 21 of each diet period), as previously described.[144] Total SCFA concentrations were determined as the sum of acetate, propionate, butyrate, and valerate, and the relative proportions of each SCFA were determined by dividing these individual SCFA by total SCFAs. Total BCFAs were the sum of isobutyrate and isovalerate concentrations. Fecal dry mass percentage was determined by drying raw fecal material overnight in an oven at 103°C.[107] Fecal pH was analyzed using an Accumet™ AB150 pH meter (Fisher, Canada) by diluting raw fecal material 1:4 in distilled water, as previously described.[107]

Plasma metabolomics

The metabolome of plasma samples was profiled using high-performance chemical isotope labeling liquid chromatography-mass spectrometry (CIL LC-MS) platform for carboxyl and amine/phenol submetabolome.[145] Briefly, two aliquots (30 μL) of each sample were labelled using DmPA-labeling kit (for carboxyl submetabolome) and Dansyl-labeling kit (for amine and phenol submetabolome), respectively. To measure the relative concentration of each metabolite, individual samples were separately labelled by $^{12}C_2$-reagent (light labeling), and the pooled sample containing aliquots from all the samples (serving as an internal standard) was labelled by $^{13}C_2$-reagent (heavy labeling). The equal volume of $^{13}C_2$-labeled reference pool was mixed with each $^{12}C_2$-individual sample, and the LC-MS analysis of the mixtures was carried out within a single run to prevent any batch effects. The resulting data was interpreted using software IsoMS Pro 1.2.7 (Nova Medical Testing Inc., Edmonton, AB, Canada) and applied to extract peak pairs and calculate the intensity ratio of each peak pair. For metabolite identification, based on multiple metabolite identifiers, peak pairs were searched against the CIL-labeled metabolite library and linked identity library.

Safety-related laboratory measures

Complete blood count differential analysis was performed on a Sysmex XN-10™ Automated Hematology Analyzer (Lincolnshire, IL, USA) to determine red blood cells, hemoglobin, hematocrit, mean corpuscular volume, mean corpuscular hemoglobin concentration, red cell distribution width, platelets, white blood cells, neutrophils, and lymphocytes. Albumin, sodium, potassium, chloride, urea, creatinine, estimated glomerular filtration rate, total protein, immunoglobulin (Ig) G, IgA, and IgM were quantified on a Beckman Coulter UniCel DxC-800 (Mississauga, ON, Canada).

Risk markers of chronic diseases

Glucose, total cholesterol, HDL, non-HDL, and triglycerides were quantified on a Beckman Coulter UniCel DxC-800 (Mississauga, ON, Canada). LDL was calculated using the Friedewald equation.[146] Insulin and CRP were measured in aliquoted plasma using the U-PLEX Human Insulin Assay (intra-assay CV 5.2%) and the V-PLEX Human CRP Kit (CV 5.0%), respectively, which were analyzed using the SECTOR® Imager 6000 according to the manufacturer's protocols (Meso Scale Discovery®; Rockville, MD, USA). Glucose and insulin data were used to calculate HOMA-IR[147] and QUICKI.[148] Fecal calprotectin was measured using an enzyme-linked immunosorbent assay (Catalog Number K6927, Immundiagnostik AG, Hessen, Germany; CV 4.8%), following the manufacturer's protocol.

Weight was measured using a calibrated digital scale to the nearest 0.1 kg (Health o meter® Professional 752KL, Pelstar LLC; McCook, IL, USA) on Days 0, 8, 21, 42, 50, and 63. Height was measured to the nearest 0.01 cm (Digi-kit digital stadiometer, Measurement Concepts, Quick Medical®; Issaquah, WA, USA) on Day 0. Height and weight were measured with participants wearing light clothing, having empty pockets, and shoes removed, and were then used to calculate BMI (kg/m^2).

Markers of gut barrier function

Lipopolysaccharide-binding protein was measured in plasma, while zonulin was measured in raw fecal material. Both markers were measured using enzyme-linked immunosorbent assays (Catalog Numbers KR6813 and K5600, CV 4.2% and 4.7%, respectively; Immundiagnostik AG, Hessen, Germany) following the manufacturer's protocols.

QUANTIFICATION AND STATISTICAL ANALYSIS

Quantification of *L. reuteri* in fecal samples

The abundance of *L. reuteri* strains in fecal samples was determined by both quantitative culture and qPCR. Quantitative culture was performed on *L. reuteri* isolation medium (LRIM), which is sufficiently selective to quantitatively isolate *L. reuteri* from human fecal samples of most subjects.[134] Quantification of PB-W1 and DSM 20016^T by qPCR was performed as previously described[113] using strain- or lineage-specific primers, respectively. Given that qPCR captures DNA from both live and dead cells, while quantitative culture estimates the number of live cells, the ratio of cell numbers estimated using quantitative culture to qPCR in fecal samples was used to assess the survival of *L. reuteri* as suggested previously.[113]

Quantitative culture data were obtained for 26 participants without background bacterial colonies growing on LRIM selective medium ($n = 9$ for PB-W1, $n = 10$ for DSM 20016^T, and $n = 7$ for placebo); *i.e.*, four participants ($n = 1$ from the DSM 20016^T group, and $n = 3$ from the placebo group) with bacteria species other than *L. reuteri* (confirmed by 16S Sanger sequencing) growing on LRIM were excluded from the culture analysis. Strain-specific qPCR data were obtained for 20 subjects ($n = 9$ for PB-W1, and $n = 11$ for DSM 20016^T), while the placebo group was not included due to confirmed absence of *L. reuteri* by selective culture on LRIM. Since *L. reuteri* PB-W1 stably engrafted in one subject (RW-16) throughout the entire trial (Figure S3B), their culture and qPCR data were excluded from subsequent analyses on persistence.

Statistical analyses

For this proof-of-concept study, we could not conduct a power calculation as our primary outcome had not been explored previously. However, we aimed to enroll ten participants in each *L. reuteri* arm (previously used to test persistence of a probiotic[149]), and a total of 30 individuals based on similar intervention trials.[150,151] Statistical analyses were performed using R and/or GraphPad Prism unless otherwise specified. Only participants who completed the entire trial were included in the final analyses ($n = 30$). One participant could not provide a blood sample at the end of both diet periods; therefore, for all analyses of plasma samples, $n = 29$ was included. Data were assessed for normality using visual inspection of histograms and QQ-plots, and homogeneity of variances was confirmed using Levene's test. The statistical tests used in each analysis as well as the types of center and dispersion measures are described in the main text and figure legends. When box plots were utilized, the center line denotes the median, the box encapsulates the interquartile range (IQR) from the 25th to 75th percentiles, and the black whiskers indicate the minimum and maximum values of the data, unless outliers were identified. Missing data was imputed for statistical analyses using multivariate imputation using the R package mice.[121]

Baseline data of risk markers of chronic diseases and gut barrier function markers as well as percent changes for each marker within each diet period were ordinated by PCA using factoextra[122] and FactoMineR[123] packages. Between-group differences (restore diet *vs.* usual diet) were assessed by PERMANOVA using the R package vegan.[124] PERMANOVA was also conducted to evaluate effects of various factors (*i.e.*, individuality, diet, bowel movement frequency, stool consistency) on the overall structure of microbiome (with 1000 permutations).

For linear mixed models, participant ID was included as the random factor, and diet period and *L. reuteri* inoculum were included as fixed factors. For data derived from 16S rRNA gene amplicon sequencing, day of intervention was included as an additional fixed factor. Baseline values of each diet period were included as covariates for each outcome variable for safety-related laboratory measures, risk markers of chronic diseases, and markers of gut barrier function using the R package nlme,[125] as well as in per-feature testing conducted for data derived from 16S rRNA gene amplicon sequencing and WMS adapted in MaAsLin2.[132] The relative abundance of each microbial feature was log-transformed before inputting into the model, as suggested previously.[152] FDR-adjusted two-tailed $p < 0.05$ was considered significant after Benjamini-Hochberg correction for multiple comparisons.

Data derived from the gastrointestinal symptoms, perceived stress, physical activity, and mood questionnaires were either ordinal or derived from ordinal data (*i.e.*, sum or mean) and were non-normally distributed. The R package geepack[127] was used for GEE with repeated-measures models to assess the overall effect of diet and *L. reuteri*. When a significant effect was observed, within-group pairwise comparisons were applied using estimated marginal means and the emmeans package.[128]

MetaboAnalyst (https://www.metaboanalyst.ca/) was used for statistical analyses and data visualization of the plasma metabolome dataset.[133] To estimate the overall effects of the restore diet, PLS-DA was conducted based on shifts from baseline to the end of each diet period (Day 21), and the p value was obtained from 1000 permutation validation. To detect the influence of *L. reuteri*, PLS-DA was conducted based on shifts ([Day 8; 4 days after *L. reuteri* inoculum] – baseline) in each diet period.

Correlations between microbial taxa and plasma metabolites that significantly responded to the restore diet were investigated using Spearman's rank correlation. According to the beta-coefficients obtained from the linear mixed models described above, the top 30 (*i.e.*, those with the highest absolute beta-coefficient values) genera and ASVs (from 16S rRNA gene amplicon sequencing dataset) increased or decreased by the restore diet were identified and included in analyses. Relative abundance shifts of these taxa were correlated with shifts of metabolites driven by the restore diet, and possible outliers (those falling outside the range of mean ± 3SD) were removed before analysis.

To quantify variation in responses of the gut microbiome and host to the restore diet, modified coefficients of variation (mCVs) were calculated by first adding the absolute value of the minimum to all values (*i.e.*, to make them non-negative) then calculating the CV as the ratio of the standard deviation to the mean. This was calculated for: ASVs and genera (16S rRNA gene amplicon sequencing);

pathways, enzymes, and CAZymes (WMS); plasma metabolites; and risk markers of chronic diseases. The R package cvcqv[129] was used to calculate mCVs and 95% confidence intervals of the absolute changes in the features within each dataset that had the greatest (positive and negative) effect sizes.

Machine learning models

RF classification and regression models were developed using the default settings in the R package caret.[130] Recursive feature selection was used to determine the optimal number of features included in each model, as many datasets had several hundred features. Due to the small sample size of the participant cohort, the lack of an independent test set, and to maximize the number of samples used to identify the most informative set of features, internal leave-one-out cross-validation was used for feature selection. The identified set of features was then used to train the model to predict the outcome of interest. Leave-one-out cross-validation was implemented again to maximize the number of samples used to train the model. Using a standard machine learning approach to reduce the risk of bias,[153] this entire process (feature selection and model training) was performed five separate times using external 5-fold cross-validation, and the average AUROC (classification) or R^2 (regression) across these five folds was reported. Other model performance metrics, such as sensitivity and specificity for classification tasks and root mean squared error (RMSE) and mean absolute error (MAE) for regression tasks are reported in supplementary tables (Tables S8, S9, and S10). Separate models were trained using microbial compositional profiles (ASV/SGBs, genus, family, phylum, and all taxonomic levels combined), microbiome functional features (SCFAs, pathways, CAZymes, ECs), and host features (risk markers of chronic diseases, plasma metabolome, dietary intake). Ecology metrics (including alpha-diversity indices and Bray-Curtis distances calculated for ASVs, SGBs, pathways, CAZymes, and ECs, as well as the Prevotella/Bacteroides ratio derived from 16S rRNA gene amplicon sequencing and WMS) and Average Influencer (a variable derived from our interaction network analysis, reflecting the average relative abundance of *Streptococcaceae*, *Bacteroidaceae*, *Erysipelatoclostridiaceae*, *Rikenellaceae*, *Pasteurellaceae*, *Akkermansiaceae*, *Clostridiaceae*, and *Desulfovibrionaceae*, which exhibited increasing positive effects on others during the restore diet phase) were also evaluated for their predictive value. Scaled top predictive features of the models were identified based on importance values in the models and were averaged across the five folds to give mean importance scores. For the best-performing regression models (*i.e.,* $R^2 > 0.30$), Spearman's correlation coefficients were calculated between top predictive features and percent changes in risk markers, as described above.

The same input variables employed in the RF models were used in MLR models; however, to decrease data dimensionality, PCA was applied to obtain the top three PCs that explained the most variation in dietary intake, risk markers of chronic diseases, ecology metrics, microbial compositional profiles (at each taxonomic level separately), functional profiles (at each function category separately and combined together), SCFAs, and plasma metabolomic profiles. Sample outliers of PCs were identified as more than five median absolute deviations away from the median, and removed from downstream analyses. For CAZyme categories for utilizing different carbohydrate sources, variance inflation factors (VIF) were calculated using the R package car[131] before running analyses, and high multi-collinearity was considered with VIF > 10. PCs and variables with $p < 0.05$ were considered significant, and adjusted R^2 values were used to evaluate the models.

Linear models

The combined effects of different types of variables on host responses were analysed with linear models using the package nlme,[125] with participant ID as the random factor. Explanatory variables, including changes in microbiome features such as taxonomic composition, diversity indices, CAZyme ratios, and SCFAs, their changes between time points, as well as baseline levels of risk markers and baseline diet were selected for the model based on their association with the outcome variable. The most strongly associated variables were included in a single model, which was reduced using stepwise AIC-based model selection with the penalty parameter *k* set to 4. The final model contained as explanatory variables both microbiota features and the diet (usual or restore diet), thus effectively adjusting for microbiota changes and enabling the assessment of microbiota-independent effects of the restore diet on each risk marker. The variance explained by each variable in the final model was calculated using the package MuMIn.[126] Interactions between microbes and effects of changes in pH, stool consistency, and bowel movement frequency were assessed using a similar stepwise model reduction protocol with the changes in microbial relative abundances between time points as the response variables and the relative abundances of microbes at the previous time point as the predictor variables.

ADDITIONAL RESOURCES

Clinical trial registry #NCT03501082: https://www.clinicaltrials.gov/study/NCT03501082

Supplemental figures

Figure S1. Example of food provided to participants during restore diet period, related to Figure 1

One-days' worth of food consumed by a participant assigned to the 2000 kcal increment based on calculated caloric requirements. Photo depicts menu items from day 4 of the 4-day rotating menu of the restore diet (approximately 46 g dietary fiber): (A) sweet potato and black bean hash and (B) mandarin oranges (breakfast); (C) quinoa tabbouleh salad and (D) canned pears (lunch); (E) baked pork tenderloin, roasted Jerusalem artichokes and potatoes, and coleslaw (dinner); and (F) dried apricots and almonds (snack). See also Table S1. Photo by: A.M.A.
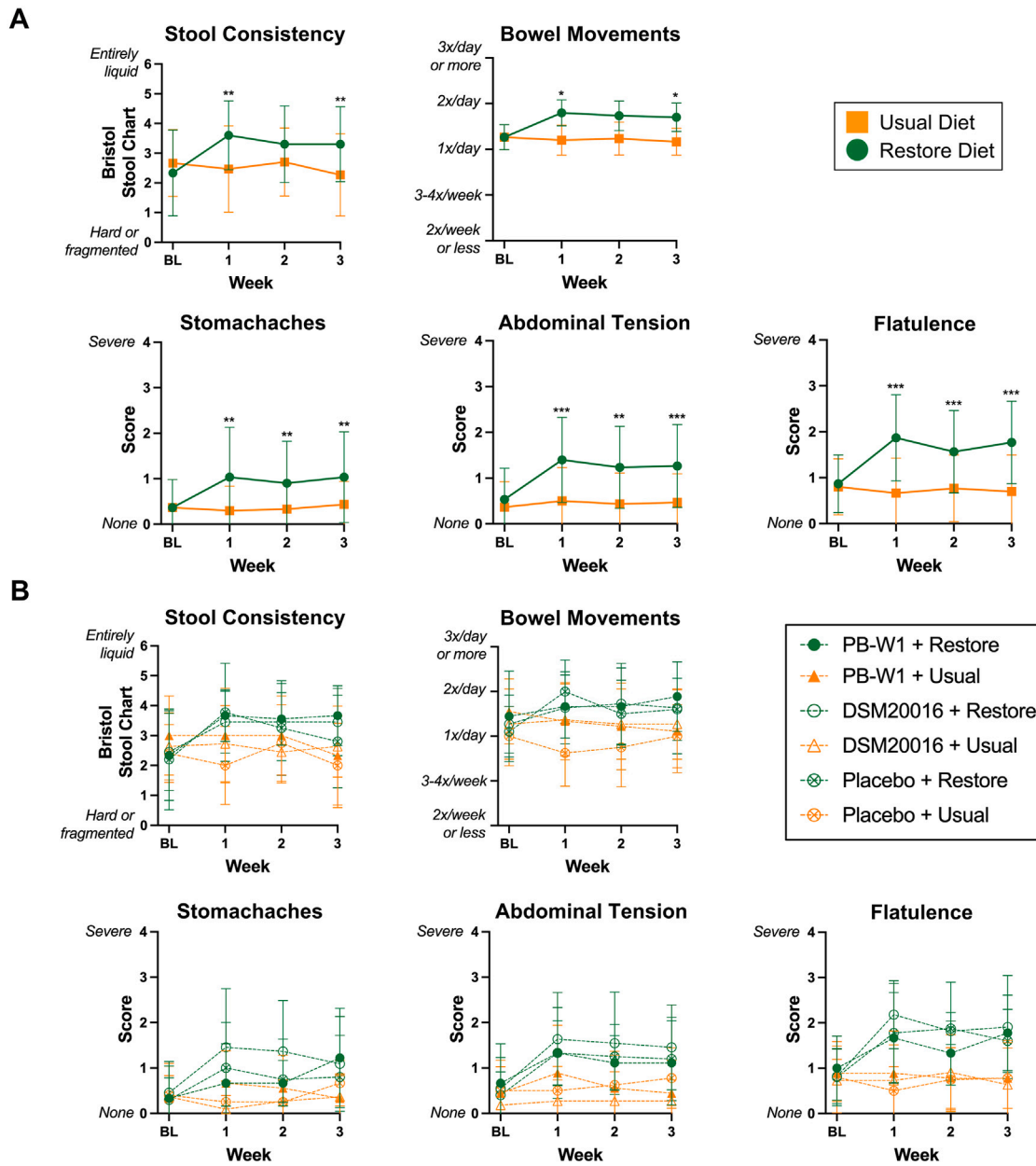
Figure S2. Effects of microbiome restoration strategy on markers of transit time and gastrointestinal tolerance, related to Figure 2
Self-reported stool consistency, bowel movement frequency, and gastrointestinal symptoms assessed via weekly questionnaire. (A) Effect of diet alone, and (B) effect of *L. reuteri* supplementation within each diet period. GEE with repeated-measures models; FDR-adjusted $p < 0.05$. Data presented as mean ± SD. *$p < 0.05$; **$p < 0.01$; ***$p < 0.001$. BL, baseline of each diet period; DSM 20016[T], *L. reuteri*-type strain; PB-W1, *L. reuteri* strain from rural Papua New Guinea.
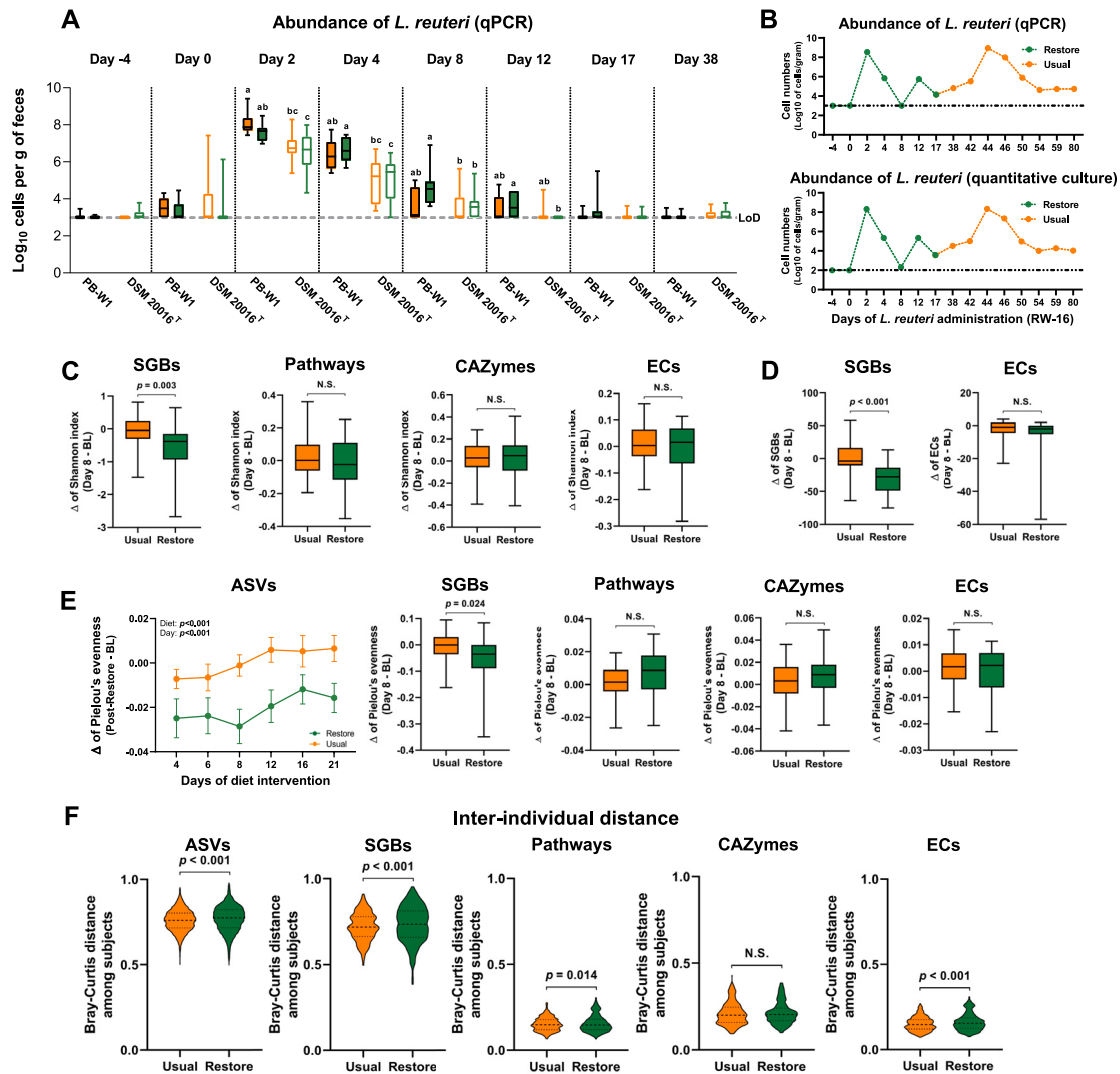
Figure S3. Effects of the restore diet on the microbiome and persistence of *Limosilactobacillus reuteri*, related to Figure 2

(A) Cell numbers of *L. reuteri* in fecal samples determined by quantitative PCR (qPCR). Data presented as Log$_{10}$ of cells per g of feces, and within each day of the intervention, different letters indicate significant differences based on repeated-measures two-way ANOVA with $p < 0.05$.

(B–E) (B) *L. reuteri* PB-W1 stably engrafted for the entirety of the trial in one subject (RW-16), confirmed by both qPCR and quantitative culture. Changes in alpha-diversity indices between each subject's gut microbiome at baseline and during the dietary intervention, specifically (C) Shannon index, (D) richness, displayed as observed features, and (E) evenness, displayed as Pielou's evenness (linear mixed models or repeated-measures two-way ANOVA).

(F) Bray-Curtis distance among different subjects (inter-individual distance) calculated based on ASVs and WMS features; paired Wilcoxon signed rank test was performed, with $p < 0.05$ considered significant. Data presented as box plots, violin plots, or mean ± SEM. ASVs, amplicon sequencing variants; BL, baseline of each diet period; CAZymes, carbohydrate-active enzymes; ECs, level-4 enzyme commission categories; LoD, limit of detection; N.S., not significant; SGBs, species-level genome bins; WMS, whole metagenome sequencing.
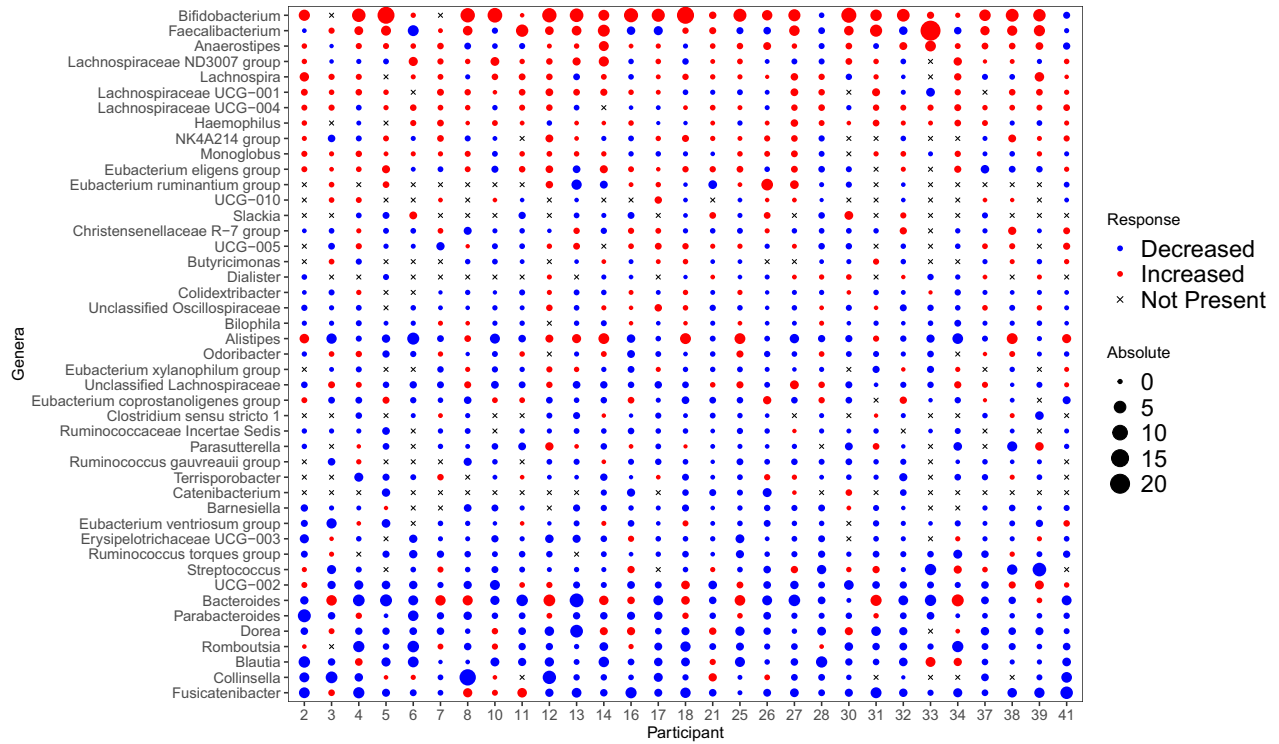
Figure S4. Individualized response of microbial genera to the restore diet, related to Figure 3

Bubble graph shows absolute change (day 8—baseline) in relative abundance of genera that were significantly altered in the restore diet period. Each column represents one participant. Red indicates an increase, blue indicates a decrease, and an X indicates the taxa were not detected in that participant. Bubble size represents the magnitude of the shift. See also Table S5.
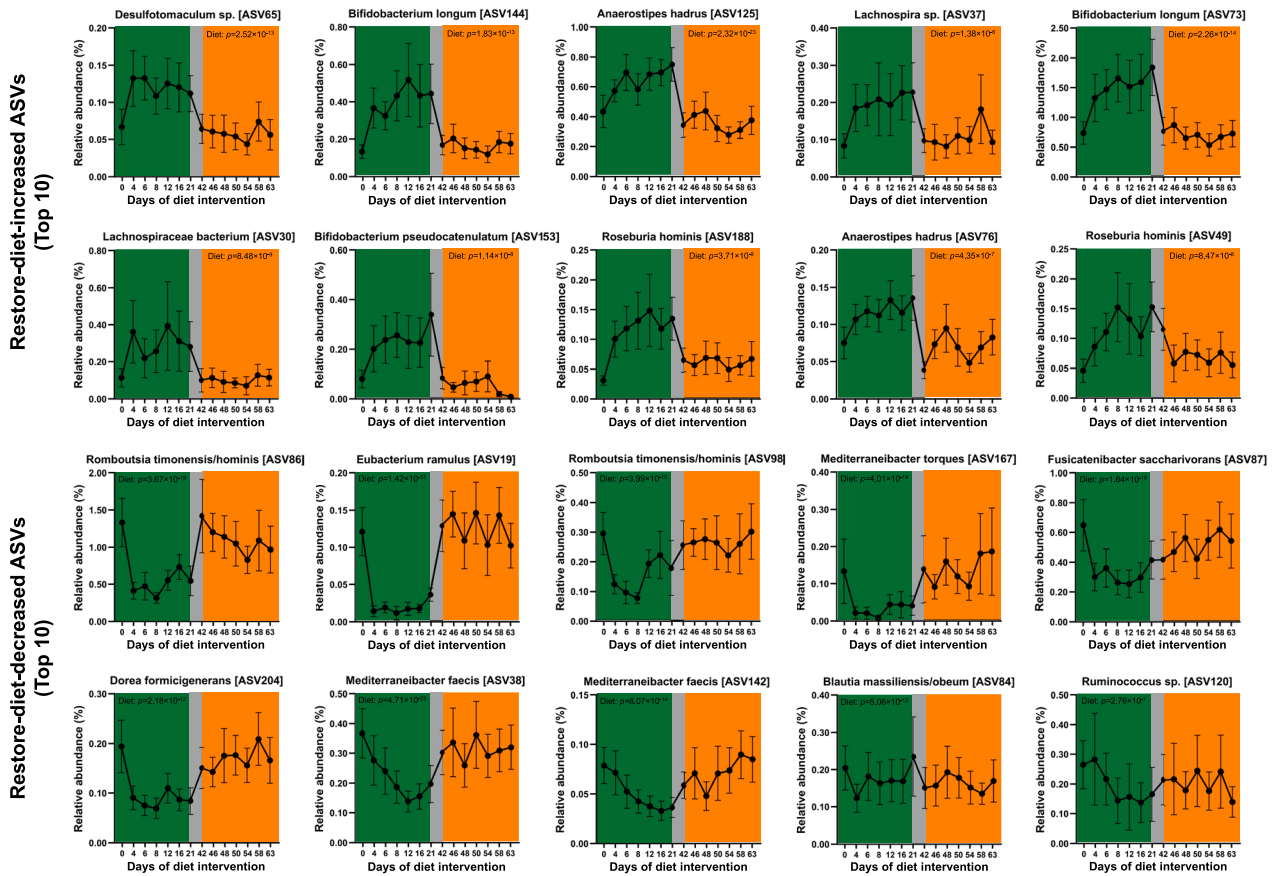
Figure S5. Temporal response and resilience of gut microbiota to the restore diet, related to Figure 4

Microbiota dynamics in participants (*n* = 16) who were randomized to the restore diet in the first period. Fluctuation of top 10 ASVs that increased (top) or decreased (bottom) in response to the restore diet (identified through linear mixed models). Data presented as mean ± SEM. Green column is the restore diet period, orange is the usual diet period, and gray is the washout.
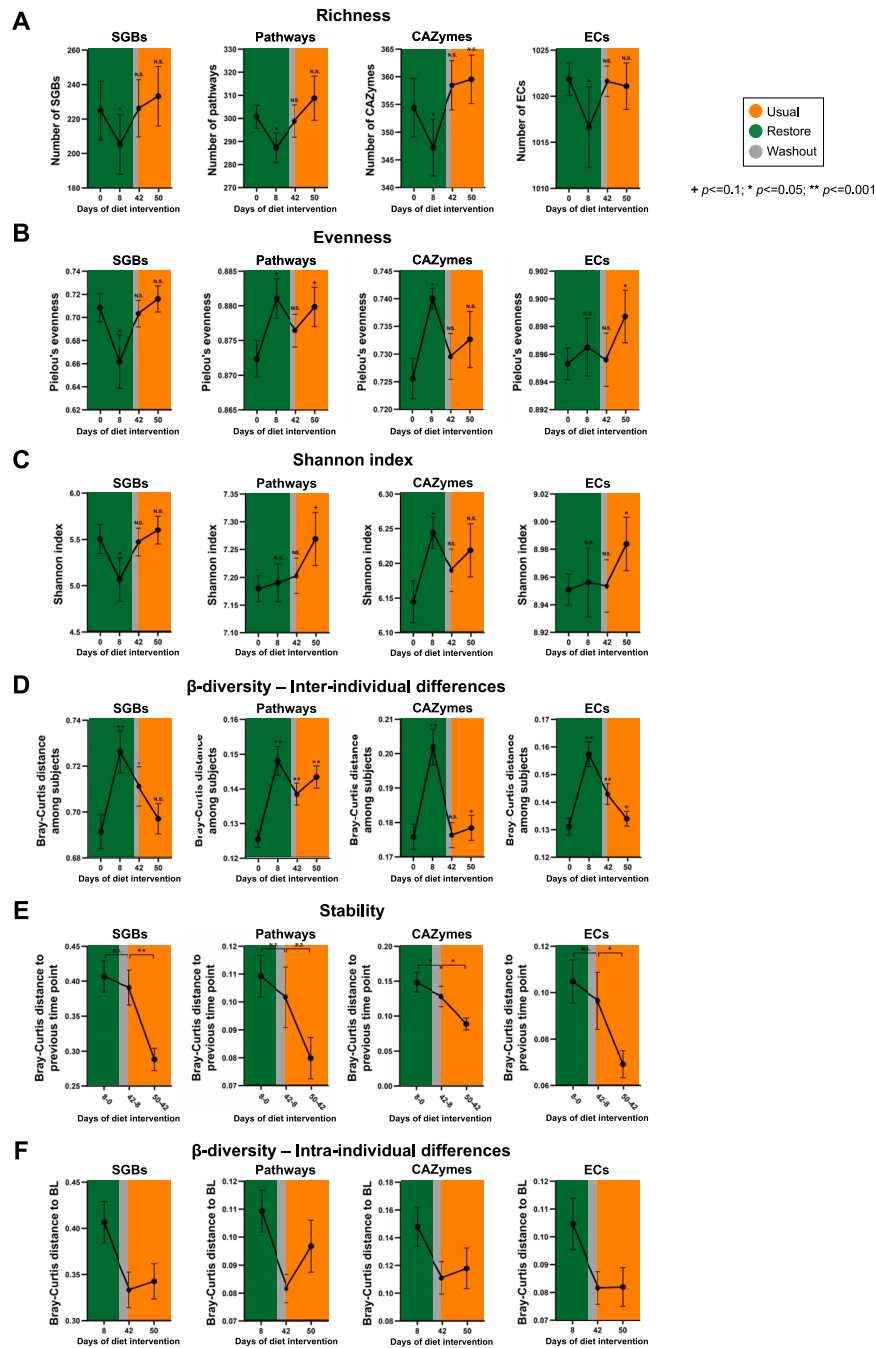
Figure S6. Temporal response and resilience of predicted WMS features, related to Figure 4

Microbiome dynamics in participants (n = 16) who were randomized to the restore diet in the first period, specifically: (A) observed features (richness), (B) Pielou's evenness, (C) Shannon index, (D) Bray-Curtis distance among different subjects within the same day (inter-individual distance), (E) Bray-Curtis distance of each subject's gut microbiome to the previous timepoint (stability, rate of distance change), and (F) Bray-Curtis distance of each subject's gut microbiome at different timepoints compared with the baseline (beta diversity; intra-individual distance). Data presented as mean ± SEM. Paired Wilcoxon signed rank tests; $^+p \leq 0.1$, $^*p \leq 0.05$, $^{**}p \leq 0.001$. BL, baseline of each diet period; CAZymes, carbohydrate-active enzymes; ECs, level-4 enzyme commission categories; N.S., not significant; SGBs, species-level genome bins; WMS, whole metagenome sequencing. Green column is the restore diet period, orange is the usual diet period, and gray is the washout.

Figure S7. Ecological drivers of the effects of the restore diet, related to Figures 4 and 5

(A) Direct effect of the diet intervention on absolute shifts (day 8 - baseline) at the genus-level (16S rRNA gene amplicon sequencing).

(B) Effects of changes to fecal pH, stool consistency, and bowel movements on microbial taxa at day 8 of the restore diet period. Legend represents which taxonomic classes to which the genera belong. Negative values indicate a negative effect, positive values indicate positive effect (R^2).

(C) Number of interactions each microbial family had during the restore and usual diet periods. Positive indicates that a high abundance of that taxon is associated with a subsequent increase in other taxa, and negative indicates that a high abundance of that taxon is associated with a subsequent decrease in other taxa.
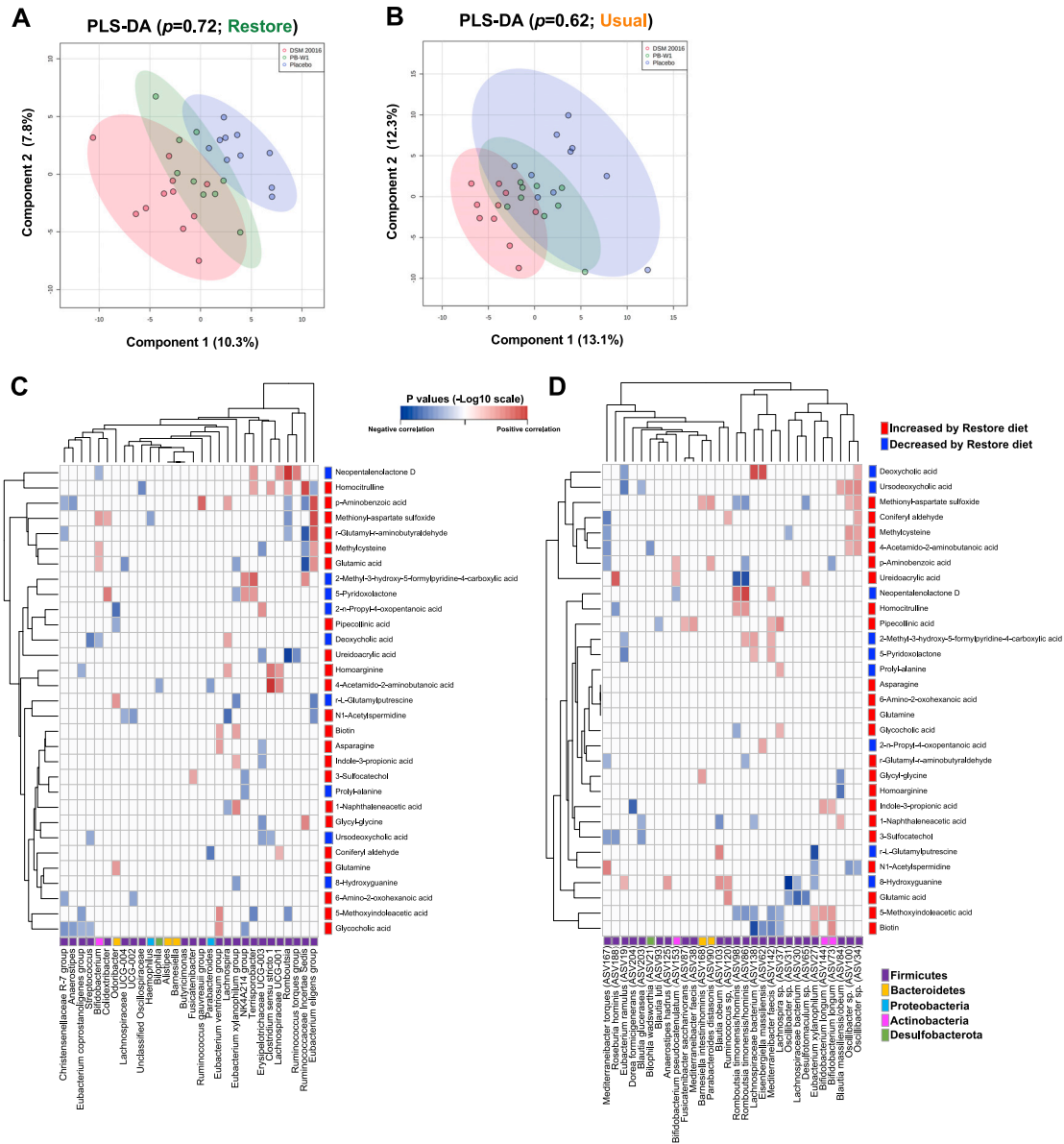
Figure S8. Effects of *L. reuteri* on the plasma metabolomic profiles, related to Figure 5
PLS-DA based on shifts (from baseline to 4 days after *L. reuteri* treatment [day 8]) of metabolites during the (A) restore diet and (B) usual diet periods (*p*-value from 1,000 permutation validation). Correlation matrices of Spearman's rank correlations between plasma metabolites and the top 30 (C) genera and (D) ASVs that were significantly altered by the restore diet (16S rRNA gene amplicon sequencing). Only correlations with FDR-adjusted *p* < 0.10 were displayed. Taxa colored based on phyla, and metabolites colored based on whether they were increased (red) or decreased (blue) by the restore diet. ASVs, amplicon sequencing variants; PLS-DA, partial least squares-discriminant analysis.
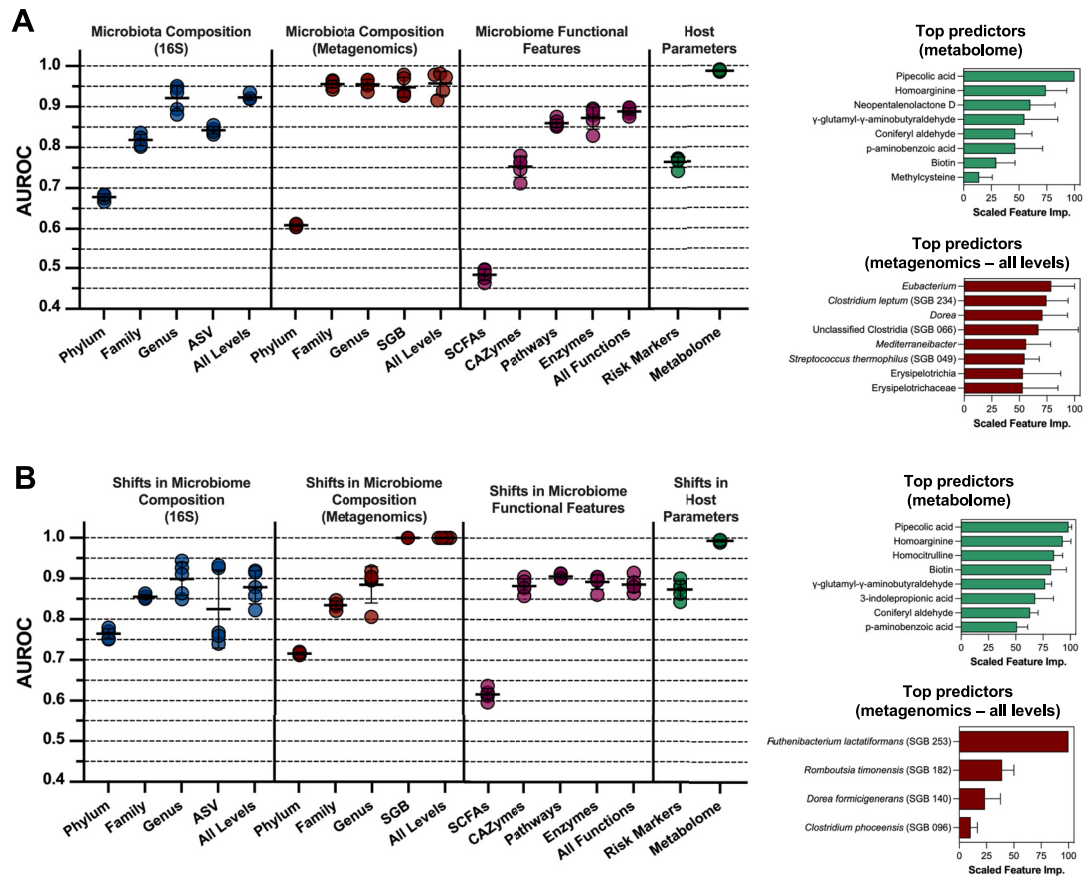
Figure S9. Prediction of diet period (restore versus usual) based on gut microbiome and host features, related to Figure 7
RF classification models were built, with input features based on individual omics datasets (plasma metabolites, microbiome compositional profiles at multiple taxonomic levels from both 16S rRNA gene amplicon sequencing and WMS, inferred microbiome functions, SCFAs, and risk markers of chronic diseases), using (A) features measured during each diet period (day 8 for microbiome taxonomic and functional features; day 21 for SCFAs, plasma metabolites, and risk markers) and (B) absolute shifts of these features within each diet period. Model performance was based on AUROC, and individual dots represent AUROC for each of the 5-fold with the black line representing the mean AUROC. Bar plots show scaled feature importance (mean ± SD) for the top predictive features of the two best-performing models based on (A) endpoint data or (B) absolute shifts. See also Table S8. ASVs, amplicon sequence variants; AUROC, area under the receiver operating characteristic curve; CAZymes, carbohydrate-active enzymes; SCFAs, short-chain fatty acids; SGBs, species-level genome bins.
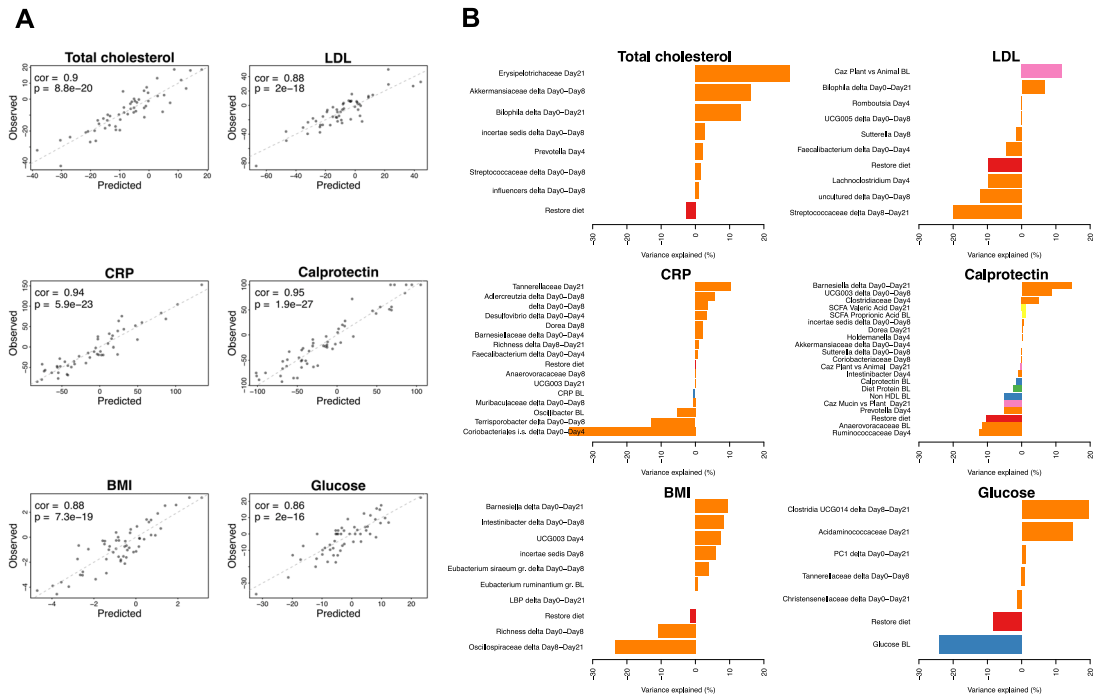
Figure S10. Contribution of different host and microbiome factors to clinical responses to the restore diet based on linear regression models using stepwise model reduction, related to Figure 7

(A) Correlations between predicted and actual changes to risk markers of chronic diseases.

(B) Percent variation explained by different variables for percent changes to risk markers of chronic diseases. Taxonomic and functional microbiota changes included either as change from baseline to days 4, 8, or 21 or relative abundance on days 4, 8, or 21 of the restore diet period. "Restore diet" variable indicates microbiome-independent effect of restore diet on markers. BMI, body mass index; CRP, C-reactive protein; LDL, low-density lipoprotein.
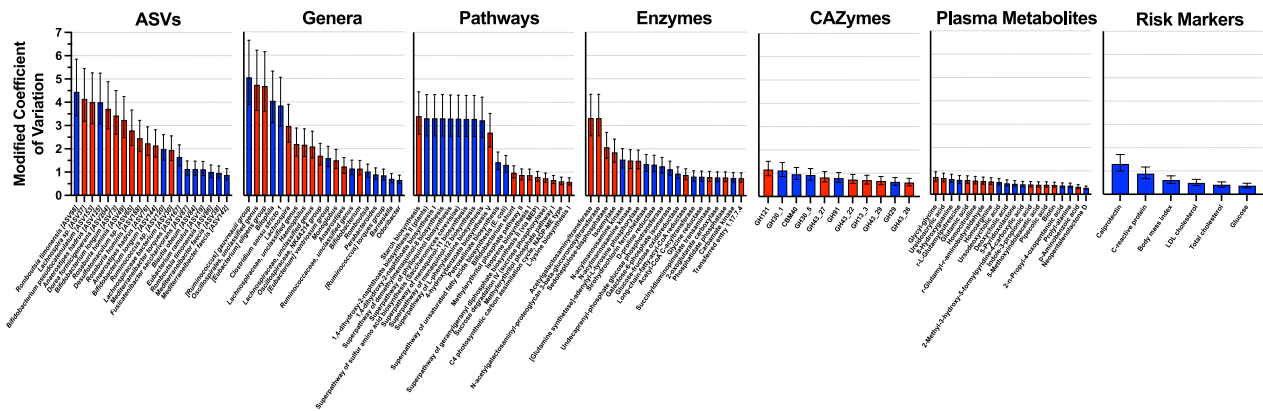
Figure S11. Variability in responses of the gut microbiome and host to the restore diet, related to Figure 7

Modified Coefficient of Variation (mCV) and 95% confidence intervals of the absolute changes in each feature within the restore diet period are depicted as bar graphs. The parameters within each dataset that had the greatest (positive and negative, identified by linear mixed models) effect sizes were included. Bars are colored based on coefficients—red indicates positive, and blue indicates negative. ASVs, amplicon sequence variants; CAZymes, carbohydrate-active enzymes.